

## Design and performance evaluation of a simplified dynamic model for combined sewer overflows in pumped sewer systems

van Daal-Rombouts, Petra; Sun, Siao; Langeveld, Jeroen; Bertrand-Krajewski, J.-L.; Clemens, Francois

**DOI**

[10.1016/j.jhydrol.2016.04.056](https://doi.org/10.1016/j.jhydrol.2016.04.056)

**Publication date**

2016

**Document Version**

Accepted author manuscript

**Published in**

Journal of Hydrology

**Citation (APA)**

van Daal-Rombouts, P., Sun, S., Langeveld, J., Bertrand-Krajewski, J.-L., & Clemens, F. (2016). Design and performance evaluation of a simplified dynamic model for combined sewer overflows in pumped sewer systems. *Journal of Hydrology*, 538(July), 609-624. <https://doi.org/10.1016/j.jhydrol.2016.04.056>

**Important note**

To cite this publication, please use the final published version (if applicable). Please check the document version above.

**Copyright**

Other than for strictly personal use, it is not permitted to download, forward or distribute the text or part of it, without the consent of the author(s) and/or copyright holder(s), unless the work is under an open content license such as Creative Commons.

**Takedown policy**

Please contact us and provide details if you believe this document breaches copyrights. We will remove access to the work immediately and investigate your claim.

1    **DESIGN AND PERFORMANCE EVALUATION OF A SIMPLIFIED DYNAMIC MODEL FOR**  
2    **COMBINED SEWER OVERFLOWS IN PUMPED SEWER SYSTEMS**

3

4    Petra VAN DAAL-ROMBOUITS<sup>1,2,\*</sup>, Siao SUN<sup>3</sup>, Jeroen LANGEVELD<sup>1,4</sup>, Jean-Luc BERTRAND-  
5    KRAJEWSKI<sup>5</sup>, François CLEMENS<sup>1,6</sup>

6

7    <sup>1</sup> Delft University of Technology, P.O. Box 5048, 2600 GA Delft, the Netherlands

8    <sup>2</sup> Witteveen+Bos, P.O. Box 233, 7400 AE Deventer, the Netherlands

9    <sup>3</sup> Key laboratory of Regional Sustainable Development Modeling, Institute of Geographical Sciences and  
10    Natural Resource Research, Chinese Academy of Sciences, Beijing, 100101, People's Republic of China

11   <sup>4</sup> Partners4UrbanWater, Javastraat 104A, 6524 MJ Nijmegen, the Netherlands

12   <sup>5</sup> University of Lyon, INSA Lyon, DEEP – EA 7429, F-69621 Villeurbanne Cedex, France

13   <sup>6</sup> Deltares, P.O. Box 177, 2600 MH Delft, the Netherlands

14

15   \*Corresponding author's e-mail: p.m.m.vandaal-rombouts@tudelft.nl

16

17

18    **Abstract**

19    Optimisation or real time control (RTC) studies in wastewater systems increasingly require  
20    rapid simulations of sewer systems in extensive catchments. To reduce the simulation time  
21    calibrated simplified models are applied, with the performance generally based on the  
22    goodness of fit of the calibration. In this research the performance of three simplified and a full  
23    hydrodynamic (FH) model for two catchments are compared based on the correct  
24    determination of CSO event occurrences and of the total discharged volumes to the surface  
25    water. Simplified model M1 consists of a rainfall runoff outflow (RRO) model only. M2  
26    combines the RRO model with a static reservoir model for the sewer behaviour. M3 comprises

27 the RRO model and a dynamic reservoir model. The dynamic reservoir characteristics were  
28 derived from FH model simulations. It was found that M2 and M3 are able to describe the  
29 sewer behaviour of the catchments, contrary to M1. The preferred model structure depends  
30 on the quality of the information (geometrical database and monitoring data) available for the  
31 design and calibration of the model. Finally, calibrated simplified models are shown to be  
32 preferable to uncalibrated FH models when performing optimisation or RTC studies.

33

34

35 **Keywords**

36 calibration, conceptual models, full hydrodynamic models, integrated modelling, monitoring,  
37 urban drainage systems

38

39 **1. Introduction**

40 Optimisation studies in wastewater management are increasingly common (Bach et al., 2014;  
41 Benedetti et al., 2013), requiring model simulations for the wastewater system as a whole, i.e.  
42 the contributing sewer systems, wastewater treatment plants (WWTP) and receiving surface  
43 waters. These model simulations are performed by coupling models for each sub system into  
44 an integrated model. In integrated modelling studies and real time control (RTC) applications  
45 two properties are of main importance: accuracy of the results and the required simulation  
46 time. Accurate results are essential for any modelling study. When working with integrated  
47 models this is especially true since faulty results from one sub model serve as input for the  
48 next sub model. As the simulation time increases with the model size, integrated model  
49 simulations take much time to perform. For example, simulating the full hydrodynamic sewer  
50 model for the Eindhoven case study (4,000 ha) as described in (Langeveld et al., 2013) for a  
51 period of 24 hours takes approximately 45 minutes on a regular laptop (4 cores of 2.8 GHz  
52 each). As optimisation studies generally consist of scenario analysis or the application of RTC,  
53 making evaluation of alternative scenarios beforehand or in real time necessary, the need for  
54 rapid simulation is evident.

55

56 To reduce the simulation time, simplified models, also commonly referred to as conceptual or  
57 surrogate models, are applied. Simplified models consist in many representations, see e.g.  
58 (Coutu et al., 2012; Mannina and Viviani, 2010; Motiee et al., 1997; Vaes et al., 1999; Wolfs  
59 and Willems, 2014), but all aim to compress the complexity of the real system in only a few  
60 characteristics and/or relationships. To ensure their representativeness, the simplified models  
61 are calibrated against field measurements. The model structure and parameter set that lead to  
62 the best overall fit with the measurements is accepted as the best simplified model. Attempts

63 to find appropriate calibration algorithms are described in e.g. (Krebs et al., 2014; Mair et al.,  
64 2012; Vrugt et al., 2009; Wolfs et al., 2013).

65

66 Previous research, see e.g. (Del Giudice et al., 2015; Dotto et al., 2014; Kleidorfer et al., 2009;  
67 Sun and Bertrand-Krajewski, 2013a, 2012; Vaes et al., 2001), made clear that the model input  
68 can have a major impact on the simplified models performance. When constructing simplified  
69 models for sewer systems in practice, however, usually only a few measurements are available  
70 for model calibration. Sewer systems that are not specifically monitored for research purposes  
71 will likely have water level measurements at the systems edges, at the discharges to the  
72 WWTP and surface water and flow measurements if sewerage is pumped to the WWTP. No  
73 flow measurements are generally available at free flow discharges to the WWTP and at  
74 combined sewer overflow (CSO) locations. Simplified models are therefore, in the majority of  
75 cases, calibrated based on the available water level measurements. The best performing  
76 model is obtained by adjusting model parameters to reproduce the measurements based on  
77 criteria such as Nash-Sutcliffe or root mean squared errors (RMSE).

78

79 The outputs of a (simplified) sewer model applied in integrated modelling are the discharges to  
80 the other sub systems: the WWTP and surface water. Although the quality of the calibration is  
81 a measure for the capability of the simplified sewer model to reproduce observations, it does  
82 not necessarily imply a sufficiently accurate determination of the discharges. Therefore, in the  
83 study presented here, simplified sewer models are calibrated with the established DREAM  
84 algorithm (Vrugt et al., 2008 and 2009), while the performance is evaluated on the correct  
85 determination of the occurrence of CSO events and the best estimation of the total volumes  
86 discharged to the surface water.

87

88 Three simplified models are used in this paper to represent the processes in sewer systems:  
89 i) rainfall runoff outflow (RRO) model, ii) static reservoir model (SR) and iii) dynamic reservoir  
90 model (DR). RRO models simulate the surface runoff generation process and the discharges at  
91 the outlet of small catchments equipped with sloped sewer systems. Among RRO models, (Sun  
92 and Bertrand-Krajewski, 2013b) have demonstrated the effectiveness of the standard linear  
93 reservoir model for such cases. However, the simple linear relation between the discharge and  
94 the storage in the fictitious reservoir of the model is likely not to be effective for looped sewer  
95 systems equipped with pumping stations and CSO structures. Other process descriptions are  
96 needed in order to characterize the flow behaviour in these more complicated systems. In this  
97 study, a standard RRO model is thus complemented with either the SR model or the more  
98 elaborate DR model to represent looped, pumped, systems. For the derivation of the SR  
99 models geometrical information and pumping station settings are taken from a full  
100 hydrodynamic (FH) model, i.e. a 1D model taking into account hydrodynamic processes in the  
101 sewer system. For the DR models additional key relationships between variables are obtained  
102 through FH model simulations. In the development of SR and DR models, simplicity was  
103 constantly balanced against physical representativeness. Simplicity, and by that reproducibility  
104 and applicability in practical RTC situations, was pursued.

105

106 This paper thus presents a comparison of three simplified models: i) a single RRO model, ii) a  
107 combination RRO + SR models and iii) a combination RRO + DR models for the simulation of  
108 CSO events and volumes. Finally, the performances of the simplified and FH models are  
109 compared. This study has been conducted for two catchment areas in the Netherlands: Loenen  
110 and Waalre. Both catchments consist of pumped, combined sewer systems, but differ in size,  
111 structure and average ground level slope.

112

113 **2. Materials and method**

114 **2.1. Catchment areas**

115 Two combined sewer systems have been selected to test the simplified models: Loenen and  
116 Waalre. Loenen is located in the central east of the Netherlands in a mildly sloping area. This  
117 system has a partly looped and partly branched character. It is equipped with one pumping  
118 station and two CSOs. One CSO, referred to as primary, is located downstream in the sewer  
119 system and discharges much more and more often than the upstream, secondary, CSO. At the  
120 location of the pumping station an additional inflow from a small neighbouring sewer system is  
121 incorporated. Sewer system characteristics and layout can be found in table 1 and figure 1  
122 (left).

123

124 Waalre is located in the south of the Netherlands. The sewer system is looped with one  
125 pumping station, a primary CSO equipped with a settling tank and a secondary CSO that rarely  
126 discharges. Additionally Waalre is connected to a neighbouring catchment in the east.

127 Although water can flow both ways, it serves as a discharge for Waalre. Characteristics of the  
128 sewer systems are listed in table 1, while figure 1 (right) displays the sewer system layout.

129 **2.2. Monitoring data**

130 For Loenen monitoring data is available at a one minute interval from June 2001 to January  
131 2002, collected as part of a dedicated research project. Flow measurements are available at  
132 the pumping station and an inflow into the pumping station from a neighbouring catchment.  
133 Level measurements are available in the pumping chamber and at the CSO locations, as  
134 displayed in figure 1 (left). Additionally, two rain gauges were installed in the catchment. Due  
135 to various reasons no continuous data set is available for the measuring period.

136

137 For Waalre monitoring data at the sewer system edges is available at a one minute interval.

138 Flow is measured at the pumping station. Level measurements are available in the pumping

139 chamber, inside the settling tank and at the secondary CSO location. The measuring locations

140 are indicated in figure 1 (right). Additional one minute interval rain gauge measurements are

141 performed at several locations approximately 10 km around Waalre. All measurements are

142 recorded permanently. Data validation was performed applying the algorithms described in

143 (Van Bijnen and Korving, 2008). Rain radar data with a five minute interval and pixel size of one

144 square kilometre are available from the Royal Netherlands Meteorological Institute (KNMI).

145 The radar data is calibrated against the rain gauge measurements using a procedure based on

146 conditional merging as described in (De Niet et al., 2013). The rain radar calibration was

147 performed only during wet weather days and when the rain gauges functioned in the period of

148 April 2011 to January 2012.

149

### 150 **Dry Weather Flow (DWF)**

151 Daily dry weather flow (DWF) profiles have been derived from the monitoring data for both

152 catchments. For Waalre it was based on the pump flow measurements in 2011. The mean

153 hourly pumped discharge at DWF days was used to represent a typical daily DWF profile. DWF

154 days are defined as having received less than 0.05 mm of precipitation after exponential

155 smoothing (80% accounted to the current day and 20% to the following day) to prevent false

156 detection of DWF days due to the absence of rain gauges inside the catchment. Unrealistic

157 measurements and periods with snowfall have been manually discarded. The DWF profile for

158 Loenen was previously derived by (Langeveld, 2004) based on the pump flow measurements

159 using a similar strategy. The resulting profiles can be found in figure 2.

### 160 **2.3. Full hydrodynamic (FH) models**



161 FH models for both catchments are available in InfoWorks ICM ([www.innovyze.com](http://www.innovyze.com)). The FH  
162 model for Loenen was calibrated by (Langeveld, 2004), following the procedure described by  
163 (Clemens, 2001). The calibration involved a detailed check of the geometrical database and  
164 tuning of several parameters to match measured and modelled water levels at up to ten  
165 locations. As the calibration resulted in very close resemblance between the modelled and  
166 measured water levels (deviations < 5 cm), it was concluded that the geometrical database  
167 was virtually without errors. The FH model for Waalre was validated following the procedure  
168 described in (Langeveld et al., 2013). It involved the comparison of measured and modelled  
169 water levels as a function of time at the three monitoring locations. No parameter  
170 optimisation was performed. As mentioned in the report (Liefing, 2012) the measured and  
171 modelled water levels resembled one another in general and it was concluded that no large  
172 errors in the geometrical database existed. Nevertheless, occasional deviations in measured  
173 and modelled water levels of up to 50 cm occurred.

174

175 The FH models are applied in this study for three purposes: i) properties of the geometrical  
176 database and pumping station settings are utilized in the design of the SR and DR models,  
177 ii) key relationships between variables are obtained by means of FH model simulations and  
178 applied in the DR model, and iii) the performance of the simplified models is compared to the  
179 performance of the FH models. For all simulations with the FH models for any of the above  
180 purposes, a standard (uncalibrated) parameter set is employed as (Korving and Clemens, 2005)  
181 showed that the portability of event specific parameter sets for FH models is low. The main  
182 distinction between the calibrated FH model for Loenen and validated FH model for Waalre  
183 lies therefore in the trustworthiness of the underlying geometrical database.

184

185 The simulations performed with the FH model for the second purpose, application in the  
186 design of the DR model, are based on ten years (1955-1964) of 15 minute interval rainfall  
187 measurements in De Bilt in the Netherlands. The simulations were executed with a one minute  
188 time step, recording for every time step the volume, water level and flows in all manholes,  
189 conduits, pumps, CSOs etc. The derivation of the required relationships is described in detail in  
190 section 2.4.3.

## 191 **2.4. Model structures**

192 The general structure of the three simplified models tested in this paper is shown in figure 3.  
193 Model M1 includes only a RRO model. Model M2 combines a RRO model and a SR model,  
194 while model M3 combines a RRO model and a DR model. Rainfall, DWF and optional additional  
195 flows are model inputs, while flows to the surface water ( $Q_{SW}$ ) and to the WWTP ( $Q_{WWTP}$ ) are  
196 model outputs. In the following sections, all models are explained in more detail.

### 197 **2.4.1. Rainfall runoff outflow (RRO) model**

198 The standard linear reservoir model is a typical RRO model, see e.g. (Sun and Bertrand-  
199 Krajewski, 2013b). It comprises of a rainfall loss model followed by a linear reservoir. The  
200 rainfall loss model consists of initial ( $I_{ini}$  [mm]) and proportional ( $P_{cons}$  [-]) rainfall losses, i.e.  
201 depression losses and ratio of contributing and total area. The resulting net rainfall ( $I_{net}$  [mm])  
202 occurs with a time lag ( $T_{lag}$  [min]) and feeds the linear reservoir with a reservoir constant ( $K$   
203 [min]). The outflow of the standard linear reservoir ( $Q_{out}$ ) is derived from the inputs using:

204

$$205 \quad Q_{out}(t) = \exp\left(-\frac{\Delta t}{K}\right) Q_{out}(t - \Delta t) + \left[1 - \exp\left(-\frac{\Delta t}{K}\right)\right] I_{net}(t - T_{lag})A, \quad (1)$$

206

207 with A the catchment area [ha]. For more details on the standard linear reservoir model the  
208 reader is referred to (Sun and Bertrand-Krajewski, 2013b).

209

210 To determine the total inflow into the sewer models ( $Q_{in}$  in figure 3) for models M2 and M3,  
211  $Q_{DWF}$  and  $Q_{optional}$  are simply added to  $Q_{out}$ . For model M1,  $Q_{out}$  together with  $Q_{DWF}$  and  $Q_{optional}$   
212 represent both the surface runoff and the subsequent flow routing within the sewer system. It  
213 is split in the two sewer discharges  $Q_{SW}$  and  $Q_{WWTP}$  on the assumption that as much water is  
214 pumped to the WWTP as possible, i.e. all discharges up to the maximum pumping capacity is  
215 accounted to  $Q_{WWTP}$  as illustrated in figure 4 for Loenen. For Waalre,  $Q_{WWTP}$  is determined using  
216 the same method. From the remainder the discharge through the connection to the  
217 neighbouring catchment (determined from FH model simulations as it is not monitored) is  
218 subtracted before accounting it to  $Q_{SW}$ .

#### 219 **2.4.2. Static reservoir (SR) model**

220 The SR model aims to represent processes within the sewer system that the basic RRO model  
221 cannot explicitly simulate. FH model properties of the geometrical database and pumping  
222 station settings are applied in its design. A schematic representation of the SR model for  
223 Loenen is shown in figure 5. It consists of a single basin for the sewer system which is filled by  
224  $Q_{in}$  as described in the previous section. It empties through a pump resulting in  $Q_{WWTP}$ , and a  
225 single CSO resulting in  $Q_{SW}$ .

226

227 Several characteristics or relationships are applied in the SR model, numbered S SR1-SR3 in  
228 figure 5. Their representation and derivation were performed as follows:

229 SR1. Static storage-level curve

230 The static storage-level curve is used to convert the sewer volume ( $V_s$ ) into the water  
231 level in the sewer ( $H_s$ ). It is derived from the geometrical database of the FH model as  
232 the cumulative volume of all manholes, conduits, etc. of the sewer system under each  
233 possible water level.

234 SR2. Discharge through pump

235 The discharge through the pump ( $Q_{s,p}$ ) is calculated through  $H_s$  and the pump  
236 characteristic. The pump characteristic is taken from the FH model. The DWF and  
237 maximum capacity are 115 and 209  $m^3/h$  respectively. The switch on level is 15.00 m,  
238 and the switch off level 14.05 m above Normal Amsterdam Water Level (m AD).

239 SR3. Discharge through CSO

240 The discharge through the CSO ( $Q_{CSO}$ ) is taken to be only caused by the primary CSO.

241 The discharge is calculated through  $H_s$  and the standard weir equations for frontal  
242 weirs:

243

$$244 \quad Q_{free} = c_1 h^{c_2} \quad (2)$$

245

246 for free outflow, with flow  $Q_{free}$  [ $m^3/s$ ],  $h$  [m] water level above the weir crest,  $c_1$   
247 [ $m^{3-c_2}/s$ ] taken to be 1.36 times the weir width [m] and  $c_2$  [-] taken to be 1.5. Or

248

$$249 \quad Q_{sub} = c_3 h_{DS} \sqrt{2g(h_{US} - h_{DS})} \quad (3)$$

250

251 for submerged outflow, with flow  $Q_{sub}$  [ $m^3/s$ ],  $h_{US}$  and  $h_{DS}$  [m] the upstream and  
252 downstream water level above the weir crest,  $c_3$  [m] taken to be 0.8 times the weir  
253 width [m] and  $g$  the standard acceleration due to gravity [ $9.81 m/s^2$ ]. Submerged

254 outflow is assumed to occur when  $2/3 \cdot h_{US} < h_{DS}$ . For Loenen only free outflow is  
255 assumed.

256

257 A schematic representation of the SR model for Waalre is depicted in figure 6. It consists of a  
258 basin for the sewer system and a basin for the settling tank. The sewer basin is filled by  $Q_{in}$  and  
259 has three discharges: one through the pump resulting in  $Q_{WWTP}$ , one through the connection  
260 with the neighbouring catchment and one through a single CSO to the settling tank. The  
261 discharge through the CSO fills the settling tank that is emptied either through a pump back  
262 into the sewer basin, or through a CSO to the surface water resulting in  $Q_{SW}$ .

263

264 Again several characteristics or relationships have been applied in the model, numbered SR4-  
265 SR10 in figure 6. Their representation and derivation were performed as follows:

266 SR4. Static storage-level curve sewer

267 See SR1, and excluding the settling tank.

268 SR5. Discharge sewer through pump

269 The discharge through the pump ( $Q_{S,p}$ ) is calculated through the water level in the  
270 sewer ( $H_s$ ) and the pump characteristic. The pump characteristic is derived from  
271 analysis of the water level and flow measurements at the pumping station, and (Van  
272 Daal-Rombouts, 2012). The DWF and maximum capacity are 85 and 400 m<sup>3</sup>/h  
273 respectively. The switch on level is 17.15 m AD, the switch off level 16.30 m AD.

274 SR6. Discharge sewer through connection

275 From simulations with the FH model it was found that water only flows from Waalre to  
276 the neighbouring catchment. The discharge through the connection ( $Q_{CONN}$ ) is  
277 calculated through  $H_s$  and the standard equation for a free outflow over a V-notch  
278 weir,

279

280 
$$Q = c_1 \tan (\theta/2) h^{5/2}, \quad (4)$$

281

282 as the connecting sewer is egg shaped. Here Q is the flow [ $\text{m}^3/\text{s}$ ],  $c_1$  a constant [ $\text{m}^{1/2}/\text{s}$ ]  
283 taken to be 1.4,  $\theta$  the notch angle taken to be  $67^\circ$ , and h [m] the water level over the  
284 weir crest. Free outflow is assumed at all times and the bottom of the notch is taken to  
285 be the highest invert of the connecting conduit.

286 SR7. Discharge sewer through CSO

287 The discharge through the CSO ( $Q_{\text{CSO}}$ ) is taken to be caused only by the primary CSO  
288 and is calculated through  $H_5$  and equations 2 and 3. Both free and submerged outflow  
289 are allowed (only free outflow is displayed).

290 SR8. Static storage-level curve settling tank

291 The static storage-level curve is used to convert the settling tank volume ( $V_T$ ) into the  
292 water level in the tank ( $H_T$ ). It is derived from the FH model, similar to SR1.

293 SR9. Discharge settling tank through pump

294 The discharge of the settling tank through the pump ( $Q_{T,p}$ ) is based on  $H_T$  and the pump  
295 characteristic. The pump characteristic was taken from the FH model, where the  
296 pumping capacity was adjusted to match the monitoring data.

297 SR10. Discharge settling tank

298 The discharge of the settling tank ( $Q_T$ ) is calculated through  $H_T$  and equation 2.

### 299 **2.4.3. Dynamic reservoir (DR) model**

300 The DR models for the sewer systems are similar to the SR models, but contain additional  
301 relationships derived from FH model simulations to better account for the dynamic behaviour  
302 of a sewer system. A schematic representation of the DR model for Loenen is shown in figure 7

303 and can be compared to the SR model in figure 5. Differences are expressed in the storage-  
304 level curve applied (SR1 - DR1) and the water level applied in the CSO discharge (DR2 - no  
305 equivalent in the SR model).

306

307 The characteristics or relationships applied in the DR model are numbered DR1-DR4 in figure 7.

308 Their representation and derivation are explained below:

309 DR1. Hybrid storage-level curve

310 A so called hybrid storage-level curve is used to convert the sewer volume ( $V_s$ ) into the  
311 water level in the sewer ( $H_s$ ). The hybrid curve follows the static storage-level curve  
312 (see SR1) for low water levels to correctly model DWF circumstances and pumping  
313 behaviour, and gradually turns to the dynamic storage-level curve for high water levels  
314 (with possibly pressurised flow conditions) to take the dynamic properties of the sewer  
315 system under wet weather flow (WWF) conditions and CSO discharges into account.

316 Figure 8 (left) displays the static, dynamic, and hybrid storage curves for Loenen.

317 The dynamic storage-level curve was derived from simulations performed with the FH  
318 model as described in section 2.3. The resulting water volumes in the entire sewer  
319 system (every minute for 10 years) were grouped in one cm intervals of the  
320 corresponding water level at the pumping station. The grouped volumes were  
321 averaged and smoothed to obtain the dynamic storage-level curve, as displayed in  
322 figure 8 (right). Note that the dynamic storage-level curve converges towards the static  
323 storage-level curve for DWF conditions or low rain intensities as the water level in the  
324 sewer system levels off.

325 DR2. Level at CSO

326  $H_s$  is converted into the water level at the primary CSO location ( $H_{CSO}$ ). The relationship  
327 is based on FH model simulations, where a linear relation is fitted through the

328 simulated water levels at the pumping station and the CSO location. Only elevated  
329 water levels (WWF conditions) are taken into account.

330 DR3. Discharge through pump

331 See SR2.

332 DR4. Discharge through CSO

333 See SR3, only now  $H_{CSO}$  is applied.

334

335 A schematic representation of the DR model for Waalre is shown in figure 9 and can be  
336 compared to the SR model in figure 6. Differences are expressed in the storage-level curve  
337 applied (DR5-SR4), the water level applied in the CSO discharge (DR6-no equivalent in the SR  
338 model) and the water level applied in and the calculation of the flow through the connection  
339 (DR7-no equivalent in SR model, DR9-SR6).

340

341 The characteristics or relationships applied in the DR for Waalre are numbered DR5-DR13 in  
342 figure 9. Their representation and derivation are explained as follows:

343 DR5. Hybrid storage-level curve sewer

344 A hybrid storage-level curve is used to convert  $V_S$  into  $H_S$ . The derivation follows DR1.

345 The resulting curves for Waalre are displayed in Figure 10: (left) the static, dynamic,  
346 and hybrid storage curves, (right) the derivation of the dynamic storage-level curve  
347 from the FH model simulation results.

348 DR6. Level sewer at CSO

349 Similar to DR2, a relationship has been derived between  $H_{CSO}$  and  $H_S$ . As Waalre is  
350 equipped with the settling tank two linear segments that connect at the highest weir  
351 crest level of the settling tank have been applied. Only elevated water levels (WWF  
352 conditions) are taken into account.



353 DR7. Level sewer at connection  
354 Similar to  $H_{CSO}$  in DR6, a relationship between the water level at the connection to the  
355 neighbouring catchment ( $H_{CONN}$ ) and  $H_s$  is derived from the FH model simulations. A  
356 linear relation was fitted, taking only elevated water levels (WWF conditions) into  
357 account.

358 DR8. Discharge sewer through pump  
359 See SR5.

360 DR9. Discharge sewer through connection  
361 The discharge of the sewer through the connection to the neighbouring catchment  
362 ( $Q_{CONN}$ ) is based on  $H_{CONN}$  and a relationship derived from the FH model simulations.  
363 The simulated water levels at the connection and the corresponding flow through the  
364 connection were fitted with a third order polynomial equation. To prevent unrealistic  
365 (negative) output a maximum value is set for  $H_{CONN}$ .

366 DR10. Discharge sewer through CSO  
367 See SR7, where  $H_{CSO}$  is applied in the calculation of the discharge from the sewer.

368 DR11. Static storage-level curve settling tank  
369 See SR8.

370 DR12. Discharge settling tank through pump  
371 See SR9.

372 DR13. Discharge settling tank  
373 See SR10.

## 374 **2.5. Calibration procedure**

### 375 **2.5.1. DREAM algorithm**

376 Calibration, which adjusts model parameters by minimizing the difference between model  
377 outputs and measurements, is an important step before applying simplified models. The  
378 research on calibration methods in the area of rainfall-runoff modelling is comprehensive,  
379 leading to the application of automatic calibration methods instead of traditional manual  
380 calibration mainly based on trial and error approaches. In this study an automatic calibration  
381 method (the differential evolution adaptive metropolis (DREAM) method (Vrugt et al., 2008,  
382 2009)) was applied for the calibration of the RRO models. The DREAM method is based on the  
383 Bayesian theorem, which considers model parameters as probabilistic variables revealing the  
384 probabilistic belief on the parameters according to observed model outputs. In DREAM the  
385 probability distribution function of parameters is derived using an iterative approximation  
386 method (the Markov chain Monte Carlo (MCMC) method) coupled with multiple chains in  
387 parallel in order to provide a robust exploration of the search space. In addition to an optimal  
388 model parameter set, DREAM also results in an evaluation of model parameter uncertainty,  
389 which provides important information on model reliability. The effectiveness of DREAM in  
390 water related model calibration has been demonstrated in many previous studies, e.g. (Keating  
391 et al., 2010; Leonhardt et al., 2014).

### 392 **2.5.2. Parameter optimisation**

393 The DREAM algorithm is applied to calibrate the parameters of the RRO model to find the  
394 minimal difference between the simplified model output and the measurements. Table 2  
395 shows the parameters, units and the searching range for the calibration procedure.

396

397 The algorithm minimises the sum of squared errors (SSE) between the model output and  
398 measurements. Water level measurements are applied in the calibration as they are the actual  
399 monitoring data available, containing all information on the sewer systems behaviour. For

400 Loenen the water level measurement at the primary CSO location is used to calibrate M2 and  
401 M3. For Waalre the water level measurements at the pumping station and inside the settling  
402 tank are applied, by minimising the sum of the SSEs for each model output-measurement  
403 combination. Only periods with elevated water levels are considered in the calibration, as the  
404 RRO model parameters are connected to rainfall only. Since water levels do not have  
405 significance in M1, it's calibration is based on the total outflow from the sewer system, i.e. the  
406 sum of the measured pump flow and the calculated outflow at the CSO locations (determined  
407 with the measured water levels and equation 2) for Loenen and Waalre. For Waalre the  
408 outflow through the connection with the neighbouring catchment is added. As this flow is not  
409 monitored, it is based on FH model simulations for the respective rain events.

410

411 The information content on which the models are calibrated is similar, especially for the  
412 elevated water levels relevant for CSO discharges. M2 and M3 are calibrated on measured  
413 water levels at the CSO locations. The discharge to the surface water in M2 and M3 is  
414 calculated using the modelled water level and equation 2. The same equation with the  
415 measured water levels is applied to determine the outflow for the calibration of M1.  
416 Additionally, the pumped outflow supplies information during low intensity rainfall, as  
417 contained in the level measurements at the pumping station (in case of Waalre) or the primary  
418 CSO location (for Loenen) when it is not yet discharging.

419

420 The calibration is performed using 10,000 iterations in DREAM, as it was found from test runs  
421 that the cumulative density functions of the parameters do not change (within the parameter  
422 stability) after several thousand iterations. The last 5,000 iterations are used for further  
423 analysis: the optimal parameter set and model output are derived, and the model is run with

424 all 5,000 parameter sets to determine the 95% confidence intervals for the water levels and  
425 discharges.

### 426 **2.5.3. Events**

427 For each catchment six rain events are available for the parameter optimisation, e.g. they led  
428 to a significant rise in water level in the sewer system, with or without discharge to the surface  
429 water, no external influences were known and monitoring data was available and judged  
430 reliable after data validation. The selected events and their characteristics are summarised in  
431 table 3.

432

433 (Korving and Clemens, 2005) showed that the portability of event specific parameter sets for  
434 FH models is low. (Sun and Bertrand-Krajewski, 2012) investigated the impact of calibration  
435 data selection on the model performance of regression models. Given the limited dataset, full  
436 consideration of this aspect is considered beyond the scope of this paper. It is clear, however,  
437 that comparison of the model structures on single event calibration is insufficient. Therefore  
438 three scenarios have been explored:

- 439 1. Calibration of single rain events,
- 440 2. Calibration on all events together,
- 441 3. Calibration on any set of 3 events and verification with the remaining 3 events.

### 442 **2.6. Performance evaluation**

443 The performance of the calibrated simplified model structures should be evaluated on the  
444 capability to correctly represent the sewer systems functioning at the edges of the system. As  
445 argued in the introduction this is not obtained by comparing the best fits between the  
446 measured and modelled water levels but by comparing the discharges from the system, i.e. to

447 the WWTP and the surface water. As the RRO models are calibrated, i.e. all calibration  
448 parameters are related to rainfall, the focus of the performance evaluation will be on the CSO  
449 discharges to the surface water. As the discharge to the WWTP is also relevant for integrated  
450 studies it will be reported for completeness.

451

452 Common sense dictates that the impact of CSO events depends foremost on the occurrence of  
453 such events, with the absolute discharged flows of secondary consequence. This is supported  
454 by literature stating that impact based RTC can influence the systems performance for small  
455 and moderate events, contrary to large events on which it has no influence (Langeveld et al.,  
456 2013), and that up to a certain point overflow frequency is a good indicator of receiving water  
457 impact (Lau et al., 2002). Therefore the first evaluation criterion for the simplified sewer  
458 models is the correct determination of CSO event occurrences. The second evaluation criterion  
459 is the correct determination of the total discharged volume.

460

461 Based on the monitored water levels at the CSO locations in the sewer systems and settling  
462 tank, for each event and catchment the discharge to the surface water ( $Q_{SW}$ ) is calculated  
463 through application of equation 2. Additionally the total discharge to the WWTP ( $Q_{WWTP}$ ) is  
464 calculated from the pump flow measurements. For each model structure and scenario the  
465 modelled the total discharged volumes ( $V_{SW}$  and  $V_{WWTP}$ ) are determined as the integral of the  
466 model outputs  $Q_{SW}$  and  $Q_{WWTP}$ .

467

468 CSO event occurrences are analysed through false positives (FP) and false negatives (FN). A FP  
469 is defined as a CSO event occurrence ( $V_{SW} > 0$ ) in the model output but not in the  
470 measurements, a FN as a CSO event occurrence in the measurements but not in the model  
471 output. For the comparison of discharged volumes, differences in  $V_{SW}$  (and  $V_{WWTP}$ ) between the

472 model output and the measurements are calculated and listed for each event and scenario.

473 Cumulative results for each scenario are determined by taking the root mean squared errors

474 (RMSE) over all events.

475

476 For comparison purposes the selected rain events have also been simulated using the FH

477 models. The comparison between simplified models with calibrated inflow parameters and FH

478 models with uncalibrated inflow parameters is relevant since the FH models simulate the

479 sewer systems behaviour in greatest detail and hence are deemed to be most accurate (Ferreri

480 et al., 2010; Meirlaen et al., 2001; Rubinato et al., 2013). This might hold true for calibrated FH

481 models but not for the much more commonly applied uncalibrated models, as proper

482 calibration of FH models is very time consuming and requires a very large monitoring data set.

483

484 Finally, the simulation time needed by different simplified model structures and the FH model

485 will be compared.

486

487 **3. Results and discussion**

488 **3.1. Calibration**

489 As described in the previous section the performance of the simplified model structures will be  
490 evaluated based upon the correct determination of CSO occurrences and the total discharge to  
491 the surface water. The calibration results, however, provide useful insight into the models  
492 functioning. Therefore, a typical calibration result for each catchment will be presented. Nash-  
493 Sutcliffe efficiency indexes (NS) (Nash and Sutcliffe, 1970) are supplied for easy comparison of  
494 the calibration results. Optimal parameter sets will be given for all events and scenarios.

495

496 The results for the individual calibration of rain events 2001-08-27 (Loenen) and 2011-08-14  
497 (Waalre) for all model structures are displayed in figures 11 and 12 respectively. From top to  
498 bottom the applied rainfall is shown, followed by the model results for M1 (based on the total  
499 sewer outflow), and M2 and M3 (based on the water level in the sewer system). For Waalre  
500 additional water level measurements in the settling tank were applied, the results of which  
501 have been added to the bottom of figure 12. For each model structure the optimal results are  
502 displayed together with their 95% confidence bands.

503

504 Figures 11 and 12 show that M2 and M3 are in general well able to describe the sewer systems  
505 behaviour: the measurements applied in the calibration are closely followed during the filling  
506 of the basins, once they are full and during emptying, resulting in NS values  $> 0.95$  for Loenen  
507 and  $> 0.75$  for Waalre. Small differences occur between these models especially during filling  
508 and in the response to temporal changes in the rainfall. M1 cannot describe the sewer systems  
509 behaviour in detail as it has only the reservoir constant K to account for surface storage and in-

510 sewer storage. The response to rainfall is therefore more smoothed, which is best  
511 demonstrated in figure 11. NS values  $< 0.4$  are found.  
512  
513 For both catchments and all model structures the 95% confidence bands are mostly  $< 1\%$ .  
514 Logically, the influence of the (inflow) calibration parameters on water levels in sewer systems  
515 is most apparent at the onset of a rain event or during temporal changes, resulting in  
516 confidence bands up to 10% for M2 and M3, while they stay  $< 1\%$  for M1.  
517  
518 For all scenarios for Loenen NS values for M2 and M3  $> 0.90$ . For M1, values differ strongly  
519 from -8.52 to 0.44. For Waalre for M2 and M3 in scenario 1, NS values range between 0.61 and  
520 0.96, with one event around zero. In scenario 2 the values drop to 0.5 to 0.6. The NS values for  
521 M1 again differ strongly between events and scenarios from -9.42 to 0.82.  
522  
523 Figure 13 shows the optimal parameter values for Loenen (left) and Waalre (right) for all  
524 model structures. In asterisks the results for scenario 1 (calibration on single rain events) are  
525 given, the line indicates the parameter values for scenario 2 (all events together). Results for  
526 all twenty possible combinations of three calibration events in scenario 3 can be found in  
527 figure 14. The optimal parameter values reflect the results for the water levels and NS values:  
528 the parameters for M2 and M3 show much resemblance within a catchment, while M1  
529 deviates. Especially the difference in K stands out, as the RRO model in M1 has to account for  
530 the surface and in-sewer storage, while in M2 and M3 only for the surface storage. The  
531 optimal parameter values between scenarios 2 (line in figure 13) and 3 (figure 14) are  
532 consistent, indicating that the exact split in a calibration and verification set does not have a  
533 major impact on the outcome.

### 534 **3.2. Performance evaluation**



535 **3.2.1. Model discharge**

536 As the calibration of the simplified models is performed on rainfall related parameters, the  
537 focus of the performance evaluation will be on the discharge to the surface water ( $Q_{SW}$ ) while  
538 the discharge to the WWTP ( $Q_{WWTP}$ ) is included for completeness.

539

540 Optimal  $Q_{SW}$  and  $Q_{WWTP}$  for all model structures for the calibration of the single events of 2001-  
541 08-27 (Loenen) and 2011-08-14 (Waalre) are displayed in figures 15 and 16 as well as the  
542 discharges determined from the measurements. The difference between M1 and M2/M3  
543 observed in the calibration results are also clear from these figures, as  $Q_{SW}$  for M1 tends to be  
544 more smoothed because of the higher value for K.

545 **3.2.2. Determination of CSO events**

546 FPs and FNs for all events for each model structure and scenario, based on the optimal  
547 parameter sets, are given in table 4. For scenarios 1 and 2 the total number is reported, for  
548 scenario 3 the results have been averaged over all combinations and multiplied by two for easy  
549 comparison. Additionally, results for the FH model have been added.

550

551 Based on the FPs and FNs in table 4, M1 can be immediately discarded for these catchments.  
552 For each scenario and catchment two FPs were recorded, the exact number of rain events that  
553 did not lead to a CSO event. This is easily explained since a rain event leading to a significant  
554 rise in water level in a pumped sewer system will likely contain rain intensities higher than the  
555 pumping capacity of the sewer system reserved for WWF (design guideline in the Netherlands:  
556 0.7 mm/h). In M1 all rainfall in excess of this capacity has to be discharged to the surface  
557 water, leading to a CSO event. The calibration algorithm unsuccessfully tries to overcome this

558 inadequacy in the model structure by delaying the rainfall (high  $T_{lag}$ ) and smoothing the  
559 response (high  $K$ ), as can be found from the optimal parameter values in figure 13.  
560  
561 For M2 and M3 the results are less conclusive. Single FPs or FNs occur depending on the  
562 catchment and scenario applied. The floating point values for scenario 3 for Waalre (due to  
563 averaging over all possible combinations) and the optimal parameter values in figure 13  
564 further indicate that the inflow parameters are calibrated differently depending on the  
565 selection of calibration/verification events. Only for M3 for Loenen no FPs or FNs occur in any  
566 scenario signalling that the M3, combining the RRO and DR models, is likely the best  
567 performing model for Loenen.

### 568 **3.2.3. Determination of discharged volumes**

569 The total volumes discharged to the surface water ( $V_{sw}$ ) for each model structure and  
570 scenarios 1 and 2 are displayed in figure 17 for Loenen and 18 for Waalre.  $V_{sw}$  is the integrated  
571 model output  $Q_{sw}$ , for which the optimal values and 95% confidence bands are determined as  
572 described in section 2.5.2. The calculation of the 95% confidence intervals for the  
573 measurements is based on an uncertainty in the standard weir equation of 25%. This  
574 percentage is estimated on previous work by (Van Daal-Rombouts et al., 2014) on scale models  
575 and (Fach et al., 2009) on computational fluid dynamics. Both studies indicate deviations  
576 between the actual (measured or calculated) CSO discharge and the discharge determined  
577 with the standard weir equation of up to 50%. They also indicate that this strongly depends on  
578 the water level over the weir crest leading to under and over estimations of the flow.  
579 Therefore an intermediate value was chosen. For the FH model an uncertainty of 50% was  
580 applied based on the possibility to calibrate FH models up to 5 cm difference in water levels  
581 and equation 2.

582

583 The cumulative results for  $V_{SW}$  and  $V_{WWTP}$ , given in table 5, were determined by taking the  
584 RMSE of the results from the optimal parameter sets over all events. The RMSE for scenario 3  
585 have been averaged over all possible combinations and values for the FH model have been  
586 added.

587

588 The results for  $V_{SW}$  in figures 17 and 18 and table 5 support the preliminary conclusion that M3  
589 outperforms M2 for Loenen. For all scenarios the RMSE and the uncertainty bands for M3 are  
590 smaller than for M2. Despite the inability of M1 to correctly determine CSO event occurrences,  
591 it outperforms M2 based on  $V_{WS}$ . For Waalre the performance of M2 and M3 are similar,  
592 corresponding to the determination of the CSO events. Nevertheless, M2 consistently  
593 performs better than M3. Similar to Loenen, M1 generally performs well based on  $V_{SW}$ . The  
594 difference in the performance of M2 and M3 between the catchments is also reflected in the  
595 optimal parameter values (figure 13). The parameter values for Waalre are close resulting in  
596 similar RMSE values in table 5, while for Loenen there is more variety between the model  
597 structures especially for  $I_{ini}$  and  $K$ .

598

599 These results can be explained by the information available for the simplified model design  
600 and calibration as described in sections 2.2 and 2.3. All information is better known or of  
601 higher quality for Loenen: i) The monitoring data for Loenen was gathered for research  
602 purposes, while the monitoring campaign for Waalre received less dedicated attention. ii) For  
603 Loenen two rain gauges were installed in the catchment itself, while for Waalre no local rain  
604 gauges were available. iii) The geometrical database underlying the FH model for Loenen is  
605 better known than for Waalre. The results for the RMSE of  $V_{SW}$  indicate that the more detailed  
606 model M3, i.e. RRO model for the runoff combined with the DR model for the sewer system, is

607 favoured when high quality information is available (in this case Loenen), while the less  
608 detailed model M2, RRO with SR, suffices when the information is of lower quality (Waalre).

609

610 One main source of uncertainty for Waalre likely stems from the calibrated rain radar input.

611 The rainfall in general seems reasonable with NS values for M2 or M3 > 0.6. In detail the

612 rainfall seems off in intensities and/or timing, an example of which can be found in figure 16.

613 Judging from the rainfall, the models responses in  $Q_{SW}$  are in accordance (main peak in the

614 outflow after main peak in the rainfall). However, in the measurements the main peak in the

615 outflow occurs right at the beginning of the rain event. The other events display a similar

616 mismatch between the rainfall and the outflow. This may also explain the very low values for

617 the parameters  $T_{lag}$  and  $K$ , see figure 13, as the calibration procedure tries to correct the

618 mismatch in the input data.

619

620 For  $V_{WWTP}$  the RMSE values in table 5 show that model M1 consistently performs worse than

621 M2 and M3 for all scenarios and both catchments. M2 and M3 generally perform on a similar

622 level, which is to be expected as the pumping regime in the SR and DR model structures is the

623 same.

624

625 The NS values reported in section 3.1 are based on the calibration parameters for each time

626 step, and the FP/FN in table 4 and RMSE in table 5 on  $V_{SW}$ . Each presents information on the

627 performance of the model structure. NS indicates the quality of the description of the sewer

628 systems behaviour in general, while the others are specific for CSO discharges. The difference

629 between the best performing model structure based on these criteria, especially for Loenen,

630 is striking. Model M2 and M3 have similar NS values > 0.9, but M3 is much more accurate

631 based on FP/FN and RMSE. Simplified sewer models are calibrated on measurements,

632 generally only water levels, but used to determine CSO discharges. These results show that  
633 care should be taken in choosing performance indicators suitable to the purpose of the model,  
634 likely leading to multiple indicators.

#### 635 **3.2.4. Uncalibrated FH models**

636 Finally the performance of the FH models is compared to the performance of the calibrated  
637 simplified models. The comparison is made for scenario 2, calibration for all events together,  
638 since there a single parameter set is derived for each model structure, similar to the single  
639 standard parameter set for the FH model.

640

641 Based on the determination of CSO event occurrences (table 4) the FH model performs at a  
642 similar level as M2 and M3. For Loenen one FP is noted for the FH model, while none for M2  
643 and M3. For Waalre it is reversed.

644

645 Taking the RMSE for  $V_{SW}$  (table 5) into account, the FH model is easily outperformed by both  
646 M2 and M3, while  $V_{WWTP}$  is worse for Loenen and better for Waalre. The results for the  
647 simplified models for  $V_{SW}$  (scenario 3) imply little loss of accuracy when the available data is  
648 split into a calibration and verification set. This suggests that, if a sufficiently large data set  
649 were available, the optimal parameter set should be applicable to other events without much  
650 loss of accuracy.

651

652 The simulation time for the FH models takes 1,000-5,000 times longer than for M2/M3 or  
653 250,000-475,000 times longer than for M1.

654

655 From the perspective of both the simulation time and accuracy of results it is concluded that it  
656 is better to apply simplified calibrated models in optimisation or RTC studies than uncalibrated  
657 FH models.  
658

659 **4. Conclusions and future research**

660 The research described dealt with the design and performance evaluation of a so called  
661 dynamic simplified sewer model for the accurate and rapid calculation of sewer system  
662 discharges for optimisation and RTC studies. The dynamic simplified sewer model (M3)  
663 consists of a calibrated rainfall runoff outflow (RRO) model and a dynamic reservoir (DR) model  
664 for the sewer behaviour. It contains characteristics derived from full hydrodynamic (FH) model  
665 simulations to account for the dynamic properties of the sewer system behaviour.

666

667 The performance of M3 was tested for two combined, pumped catchments and compared  
668 against two other simplified models, M2 (calibrated RRO model with a static reservoir (SR))  
669 and M1 (calibrated RRO model only), and uncalibrated FH models. The performance was not  
670 solely based on the goodness of fit of the calibration but primarily on the correct  
671 determination of CSO event occurrences, and secondly on the correct determination of the  
672 total discharged volumes to the surface water.

673

674 From this research the following conclusions can be drawn:

- 675 – Model M1 simulates > 100,000 times faster than the FH model; models M2/M3  
676 are > 1,000 times faster than the FH model.
- 677 – M1 is unsuitable to correctly predict CSO occurrences for pumped catchments.  
678 The model structure is unable to retain rain intensities higher than the pumping  
679 capacity reserved for WWF, resulting in too many CSO discharges.
- 680 – M2 and M3 are able to describe the behaviour of pumped sewer systems.
- 681 – Performance indicators for the selection of the most appropriate model structure  
682 should be chosen carefully in relation to the modelling objectives, likely leading to

683 multiple indicators, each one providing a specific approach of the models'  
684 performances.

685 – In case of detailed and trustworthy information available for the design and  
686 calibration of the model (Loenen), M3 outperforms M2 for all scenarios. If the  
687 available information is of lower quality (Waalre), M2 consistently performs  
688 slightly better indicating that the derivation of the more detailed DR model is not  
689 useful.

690 – For rainfall driven modelling trustworthy and local rain measurements remain  
691 necessary despite the availability of rain radar data, to either apply as direct input  
692 or the correction of radar data.

693 – M2 and M3 outperform the uncalibrated FH models based on the total discharge  
694 to the surface water. In optimisation or RTC studies the application of suitable  
695 calibrated simplified models is preferred over uncalibrated FH models.

696

697 Future research is recommended in the area of statistical substantiation of the results as the  
698 available data sets were too limited to allow a statistical analysis of the results themselves.  
699 Also the use of continuous data sets instead of the current intermittent ones would be  
700 interesting because more information on the initial conditions prior to events would be  
701 included.

702

703 Following the above, future research will focus on retrieving more reliable monitoring data  
704 (especially rainfall). For the catchment of Waalre, the impact of more reliable rainfall data on  
705 the performance of the detailed M3 model will be focussed on. Calibrated simplified sewer  
706 models will be derived for the catchments in the case study area of Eindhoven for application  
707 in an integrated model to research the possibilities for quality based RTC.



708 **Acknowledgements**

709 The authors would like to acknowledge Innovyze ([www.innovyze.com](http://www.innovyze.com)) for kindly supplying a  
710 research licence for the use of the software program InfoWorks ICM. Also the authors would  
711 like to thank the Van Gogh Programme for supplying a Travel Grant to cover the travel  
712 expenses for the cooperation between TU Delft and INSA Lyon.

713

714 The research is performed within the Dutch 'Kennisprogramma Urban Drainage' (Knowledge  
715 Programme Urban Drainage). The involved parties are: ARCADIS, Deltares, Evides, Gemeente  
716 Almere, Gemeente Arnhem, Gemeente Breda, Gemeente 's-Gravenhage, Gemeentewerken  
717 Rotterdam, Gemeente Utrecht, GMB Rioleringsstechniek, Grontmij, KWR Watercycle Research  
718 Institute, Royal HaskoningDHV, Stichting RIONED, STOWA, Tauw, vandervalk + degroot,  
719 Waterboard De Dommel, Waternet and Witteveen+Bos.

720

721 **References**

722 Bach, P.M., Rauch, W., Mikkelsen, P.S., McCarthy, D.T., Deletic, A., 2014. A critical review of  
723 integrated urban water modelling - Urban drainage and beyond. *Environ. Model. Softw.*  
724 54, 88–107.

725 Benedetti, L., Langeveld, J.G., Comeau, A., Corominas, L., Daigger, G., Martin, C., Mikkelsen,  
726 P.S., Vezzaro, L., Weijers, S.R., Vanrolleghem, P.A., 2013. Modelling and monitoring of  
727 integrated urban wastewater systems: review on status and perspectives. *Water Sci.*  
728 *Technol.* 68, 1203–1215.

729 Clemens, F.H.L.R., 2001. Hydrodynamic models in urban drainage: application and calibration.  
730 TU Delft.

731 Coutu, S., Del Giudice, D., Rossi, L., Barry, D.A., 2012. Parsimonious hydrological modeling of

732 urban sewer and river catchments. *J. Hydrol.* 464-465, 477–484.

733 De Niet, A.C., De Jonge, J., Korving, H., Langeveld, J.G., Van Nieuwenhuijzen, A., 2013. Het  
734 beste van twee werelden, correctie van neerslagradar op basis van grondstations voor  
735 toepassing in stedelijk gebied. *H2O online* 1–5.

736 Del Giudice, D., Reichert, P., Bareš, V., Albert, C., Rieckermann, J., 2015. Model bias and  
737 complexity – Understanding the effects of structural deficits and input errors on runoff  
738 predictions. *Environ. Model. Softw.* 64, 205–214.

739 Dotto, C.B.S., Kleidorfer, M., Deletic, A., Rauch, W., McCarthy, D.T., 2014. Impacts of measured  
740 data uncertainty on urban stormwater models. *J. Hydrol.* 508, 28–42.

741 Fach, S., Sitzenfrey, R., Rauch, W., 2009. Determining the spill flow discharge of combined  
742 sewer overflows using rating curves based on computational fluid dynamics instead of  
743 the standard weir equation. *Water Sci. Technol.* 60, 3035–43.

744 Ferreri, G.F., Freni, G., Tomaselli, P., 2010. Ability of Preissmann slot scheme to simulate  
745 smooth pressurisation transient in sewers. *Water Sci. Technol.* 62, 1848–1858.

746 Keating, E.H., Doherty, J., Vrugt, J.A., Kang, Q., 2010. Optimization and uncertainty assessment  
747 of strongly nonlinear groundwater models with high parameter dimensionality. *Water*  
748 *Resour. Res.* 46, 1–18.

749 Kleidorfer, M., Möderl, M., Fach, S., Rauch, W., 2009. Optimization of measurement campaigns  
750 for calibration of a conceptual sewer model. *Water Sci. Technol.* 59, 1523–30.

751 Korving, H., Clemens, F.H.L.R., 2005. Impact of dimension uncertainty and model calibration on  
752 sewer system assessment. *Water Sci. Technol.* 52, 35–42.

753 Krebs, G., Kokkonen, T., Valtanen, M., Setälä, H., Koivusalo, H., 2014. Spatial resolution  
754 considerations for urban hydrological modelling. *J. Hydrol.* 512, 482–497.

755 Langeveld, J.G., 2004. Interactions within wastewater systems. TU Delft.

756 Langeveld, J.G., Benedetti, L., De Klein, J., Nopens, I., Amerlinck, Y., Van Nieuwenhuijzen, A.,  
757 Flameling, T., Van Zanten, O., Weijers, S.R., 2013. Impact-based integrated real-time  
758 control for improvement of the Dommel River water quality. *Urban Water J.* 10, 312–329.

759 Lau, J., Butler, D., Schütze, M., 2002. Is combined sewer overflow spill frequency/volume a  
760 good indicator of receiving water quality impact? *Urban Water* 4, 181–189.

761 Leonhardt, G., Sun, S., Rauch, W., Bertrand-Krajewski, J.-L., 2014. Comparison of two model  
762 based approaches for areal rainfall estimation in urban hydrology. *J. Hydrol.* 511, 880–  
763 890.

764 Liefthing, H.J., 2012. Toetsing rioolmodel Waalre.

765 Mair, M., Kleidorfer, M., Rauch, W., 2012. Performance of auto-calibration algorithms in the  
766 field of urban drainage modelling, in: *Proceedings of UDM9*. Belgrade, pp. 1–10.

767 Mannina, G., Viviani, G., 2010. An urban drainage stormwater quality model: Model  
768 development and uncertainty quantification. *J. Hydrol.* 381, 248–265.

769 Meirlaen, J., Huyghebaert, B., Sforzi, F., Benedetti, L., Vanrolleghem, P.A., 2001. Fast,  
770 simultaneous simulation of the integrated urban wastewater system using mechanistic  
771 surrogate models. *Water Sci. Technol.* 43, 301–309.

772 Motiee, H., Chocat, B., Blanpain, O., 1997. A storage model for the simulation of the hydraulic  
773 behaviour of drainage networks. *Water Sci. Technol.* 36, 57–63.

774 Nash, J.E., Sutcliffe, J.V., 1970. River flow forecasting through conceptual models: Part I - A  
775 discussion of principles. *J. Hydrol.* 10, 282–290.

776 Rubinato, M., Shucksmith, J., Saul, A.J., Shepherd, W., 2013. Comparison between InfoWorks

777 hydraulic results and a physical model of an Urban drainage system. *Water Sci. Technol.*  
778 68, 372–379.

779 Sun, S., Bertrand-Krajewski, J.-L., 2013a. Input variable selection and calibration data selection  
780 for storm water quality regression models. *Water Sci. Technol.* 68, 50–58.

781 Sun, S., Bertrand-Krajewski, J.-L., 2013b. Separately accounting for uncertainties in rainfall and  
782 runoff: Calibration of event based conceptual hydrological models in small urban  
783 catchments using Bayesian method. *Water Resour. Res.* 49, 1–14.

784 Sun, S., Bertrand-Krajewski, J.-L., 2012. On calibration data selection: The case of stormwater  
785 quality regression models. *Environ. Model. Softw.* 35, 61–73.

786 Vaes, G., Berlamont, J., Bermont, J., 1999. Emission predictions with a multi-linear reservoir  
787 model. *Water Sci. Technol.* 39, 9–16.

788 Vaes, G., Willems, P., Berlamont, J., 2001. Rainfall input requirements for hydrological  
789 calculations. *Urban Water* 3, 107–112.

790 Van Bijnen, M., Korving, H., 2008. Application and results of automatic validation of sewer  
791 monitoring data, in: *Proceedings of ICUD11*. Edinburgh, pp. 1–10.

792 Van Daal-Rombouts, P.M.M., 2012. Personal communication.

793 Van Daal-Rombouts, P.M.M., Tralli, A., Verhaart, F., Langeveld, J.G., Clemens, F.H.L.R., 2014.  
794 Applicability of CFD modelling in determining accurate weir discharge - water level  
795 relationships, in: *Proceedings of ICUD13*. Sarawak, pp. 1–8.

796 Vrugt, J.A., Ter Braak, C.J.F., Clark, M.P., Hyman, J.M., Robinson, B.A., 2008. Treatment of input  
797 uncertainty in hydrologic modeling: Doing hydrology backward with Markov chain Monte  
798 Carlo simulation. *Water Resour. Res.* 44, 1–15.

- 799 Vrugt, J.A., Ter Braak, C.J.F., Gupta, H.V., Robinson, B.A., 2009. Equifinality of formal (DREAM)  
800 and informal (GLUE) Bayesian approaches in hydrologic modeling? *Stoch. Environ. Res.*  
801 *Risk Assess.* 23, 1011–1026.
- 802 Wolfs, V., Villazon, M.F., Willems, P., 2013. Development of a semi-automated model  
803 identification and calibration tool for conceptual modelling of sewer systems. *Water Sci.*  
804 *Technol.* 68, 167–175.
- 805 Wolfs, V., Willems, P., 2014. Development of discharge-stage curves affected by hysteresis  
806 using time varying models, model trees and neural networks. *Environ. Model. Softw.* 55,  
807 107–119.

1    **DESIGN AND PERFORMANCE EVALUATION OF A SIMPLIFIED DYNAMIC MODEL FOR**  
2    **COMBINED SEWER OVERFLOWS IN PUMPED SEWER SYSTEMS**

3

4    Petra VAN DAAL-ROMBOUITS<sup>1,2,\*</sup>, Siao SUN<sup>3</sup>, Jeroen LANGEVELD<sup>1,4</sup>, Jean-Luc BERTRAND-  
5    KRAJEWSKI<sup>5</sup>, François CLEMENS<sup>1,6</sup>

6

7    <sup>1</sup> Delft University of Technology, P.O. Box 5048, 2600 GA Delft, the Netherlands

8    <sup>2</sup> Witteveen+Bos, P.O. Box 233, 7400 AE Deventer, the Netherlands

9    <sup>3</sup> Key laboratory of Regional Sustainable Development Modeling, Institute of Geographical Sciences and  
10    Natural Resource Research, Chinese Academy of Sciences, Beijing, 100101, People's Republic of China

11    <sup>4</sup> Partners4UrbanWater, Javastraat 104A, 6524 MJ Nijmegen, the Netherlands

12    <sup>5</sup> University of Lyon, INSA Lyon, DEEP – EA 7429, F-69621 Villeurbanne Cedex, France

13    <sup>6</sup> Deltares, P.O. Box 177, 2600 MH Delft, the Netherlands

14

15    \*Corresponding author's e-mail: p.m.m.vandaal-rombouts@tudelft.nl

16

17

18    **Abstract**

19    Optimisation or real time control (RTC) studies in wastewater systems increasingly require  
20    rapid simulations of sewer systems in extensive catchments. To reduce the simulation time  
21    calibrated simplified models are applied, with the performance generally based on the  
22    goodness of fit of the calibration. In this research the performance of three simplified and a full  
23    hydrodynamic (FH) model for two catchments are compared based on the correct  
24    determination of CSO event occurrences and of the total discharged volumes to the surface  
25    water. Simplified model M1 consists of a rainfall runoff outflow (RRO) model only. M2  
26    combines the RRO model with a static reservoir model for the sewer behaviour. M3 comprises

27 the RRO model and a dynamic reservoir model. The dynamic reservoir characteristics were  
28 derived from FH model simulations. It was found that M2 and M3 are able to describe the  
29 sewer behaviour of the catchments, contrary to M1. The preferred model structure depends  
30 on the quality of the information (geometrical database and monitoring data) available for the  
31 design and calibration of the model. Finally, calibrated simplified models are shown to be  
32 preferable to uncalibrated FH models when performing optimisation or RTC studies.

33

34

35 **Keywords**

36 calibration, conceptual models, full hydrodynamic models, integrated modelling, monitoring,  
37 urban drainage systems

38

39 **1. Introduction**

40 Optimisation studies in wastewater management are increasingly common (Bach et al., 2014;  
41 Benedetti et al., 2013), requiring model simulations for the wastewater system as a whole, i.e.  
42 the contributing sewer systems, wastewater treatment plants (WWTP) and receiving surface  
43 waters. These model simulations are performed by coupling models for each sub system into  
44 an integrated model. In integrated modelling studies and real time control (RTC) applications  
45 two properties are of main importance: accuracy of the results and the required simulation  
46 time. Accurate results are essential for any modelling study. When working with integrated  
47 models this is especially true since faulty results from one sub model serve as input for the  
48 next sub model. As the simulation time increases with the model size, integrated model  
49 simulations take much time to perform. For example, simulating the full hydrodynamic sewer  
50 model for the Eindhoven case study (4,000 ha) as described in (Langeveld et al., 2013) for a  
51 period of 24 hours takes approximately 45 minutes on a regular laptop (4 cores of 2.8 GHz  
52 each). As optimisation studies generally consist of scenario analysis or the application of RTC,  
53 making evaluation of alternative scenarios beforehand or in real time necessary, the need for  
54 rapid simulation is evident.

55

56 To reduce the simulation time, simplified models, also commonly referred to as conceptual or  
57 surrogate models, are applied. Simplified models consist in many representations, see e.g.  
58 (Coutu et al., 2012; Mannina and Viviani, 2010; Motiee et al., 1997; Vaes et al., 1999; Wolfs  
59 and Willems, 2014), but all aim to compress the complexity of the real system in only a few  
60 characteristics and/or relationships. To ensure their representativeness, the simplified models  
61 are calibrated against field measurements. The model structure and parameter set that lead to  
62 the best overall fit with the measurements is accepted as the best simplified model. Attempts



63 to find appropriate calibration algorithms are described in e.g. (Krebs et al., 2014; Mair et al.,  
64 2012; Vrugt et al., 2009; Wolfs et al., 2013).

65

66 Previous research, see e.g. (Del Giudice et al., 2015; Dotto et al., 2014; Kleidorfer et al., 2009;  
67 Sun and Bertrand-Krajewski, 2013a, 2012; Vaes et al., 2001), made clear that the model input  
68 can have a major impact on the simplified models performance. When constructing simplified  
69 models for sewer systems in practice, however, usually only a few measurements are available  
70 for model calibration. Sewer systems that are not specifically monitored for research purposes  
71 will likely have water level measurements at the systems edges, at the discharges to the  
72 WWTP and surface water and flow measurements if sewerage is pumped to the WWTP. No  
73 flow measurements are generally available at free flow discharges to the WWTP and at  
74 combined sewer overflow (CSO) locations. Simplified models are therefore, in the majority of  
75 cases, calibrated based on the available water level measurements. The best performing  
76 model is obtained by adjusting model parameters to reproduce the measurements based on  
77 criteria such as Nash-Sutcliffe or root mean squared errors (RMSE).

78

79 The outputs of a (simplified) sewer model applied in integrated modelling are the discharges to  
80 the other sub systems: the WWTP and surface water. Although the quality of the calibration is  
81 a measure for the capability of the simplified sewer model to reproduce observations, it does  
82 not necessarily imply a sufficiently accurate determination of the discharges. Therefore, in the  
83 study presented here, simplified sewer models are calibrated with the established DREAM  
84 algorithm (Vrugt et al., 2008 and 2009), while the performance is evaluated on the correct  
85 determination of the occurrence of CSO events and the best estimation of the total volumes  
86 discharged to the surface water.

87

88 Three simplified models are used in this paper to represent the processes in sewer systems:  
89 i) rainfall runoff outflow (RRO) model, ii) static reservoir model (SR) and iii) dynamic reservoir  
90 model (DR). RRO models simulate the surface runoff generation process and the discharges at  
91 the outlet of small catchments equipped with sloped sewer systems. Among RRO models, (Sun  
92 and Bertrand-Krajewski, 2013b) have demonstrated the effectiveness of the standard linear  
93 reservoir model for such cases. However, the simple linear relation between the discharge and  
94 the storage in the fictitious reservoir of the model is likely not to be effective for looped sewer  
95 systems equipped with pumping stations and CSO structures. Other process descriptions are  
96 needed in order to characterize the flow behaviour in these more complicated systems. In this  
97 study, a standard RRO model is thus complemented with either the SR model or the more  
98 elaborate DR model to represent looped, pumped, systems. For the derivation of the SR  
99 models geometrical information and pumping station settings are taken from a full  
100 hydrodynamic (FH) model, i.e. a 1D model taking into account hydrodynamic processes in the  
101 sewer system. For the DR models additional key relationships between variables are obtained  
102 through FH model simulations. In the development of SR and DR models, simplicity was  
103 constantly balanced against physical representativeness. Simplicity, and by that reproducibility  
104 and applicability in practical RTC situations, was pursued.

105

106 This paper thus presents a comparison of three simplified models: i) a single RRO model, ii) a  
107 combination RRO + SR models and iii) a combination RRO + DR models for the simulation of  
108 CSO events and volumes. Finally, the performances of the simplified and FH models are  
109 compared. This study has been conducted for two catchment areas in the Netherlands: Loenen  
110 and Waalre. Both catchments consist of pumped, combined sewer systems, but differ in size,  
111 structure and average ground level slope.

112

113 **2. Materials and method**

114 **2.1. Catchment areas**

115 Two combined sewer systems have been selected to test the simplified models: Loenen and  
116 Waalre. Loenen is located in the central east of the Netherlands in a mildly sloping area. This  
117 system has a partly looped and partly branched character. It is equipped with one pumping  
118 station and two CSOs. One CSO, referred to as primary, is located downstream in the sewer  
119 system and discharges much more and more often than the upstream, secondary, CSO. At the  
120 location of the pumping station an additional inflow from a small neighbouring sewer system is  
121 incorporated. Sewer system characteristics and layout can be found in table 1 and figure 1  
122 (left).

123

124 Waalre is located in the south of the Netherlands. The sewer system is looped with one  
125 pumping station, a primary CSO equipped with a settling tank and a secondary CSO that rarely  
126 discharges. Additionally Waalre is connected to a neighbouring catchment in the east.

127 Although water can flow both ways, it serves as a discharge for Waalre. Characteristics of the  
128 sewer systems are listed in table 1, while figure 1 (right) displays the sewer system layout.

129 **2.2. Monitoring data**

130 For Loenen monitoring data is available at a one minute interval from June 2001 to January  
131 2002, collected as part of a dedicated research project. Flow measurements are available at  
132 the pumping station and an inflow into the pumping station from a neighbouring catchment.  
133 Level measurements are available in the pumping chamber and at the CSO locations, as  
134 displayed in figure 1 (left). Additionally, two rain gauges were installed in the catchment. Due  
135 to various reasons no continuous data set is available for the measuring period.

136

137 For Waalre monitoring data at the sewer system edges is available at a one minute interval.  
138 Flow is measured at the pumping station. Level measurements are available in the pumping  
139 chamber, inside the settling tank and at the secondary CSO location. The measuring locations  
140 are indicated in figure 1 (right). Additional one minute interval rain gauge measurements are  
141 performed at several locations approximately 10 km around Waalre. All measurements are  
142 recorded permanently. Data validation was performed applying the algorithms described in  
143 (Van Bijnen and Korving, 2008). Rain radar data with a five minute interval and pixel size of one  
144 square kilometre are available from the Royal Netherlands Meteorological Institute (KNMI).  
145 The radar data is calibrated against the rain gauge measurements using a procedure based on  
146 conditional merging as described in (De Niet et al., 2013). The rain radar calibration was  
147 performed only during wet weather days and when the rain gauges functioned in the period of  
148 April 2011 to January 2012.

149

### 150 **Dry Weather Flow (DWF)**

151 Daily dry weather flow (DWF) profiles have been derived from the monitoring data for both  
152 catchments. For Waalre it was based on the pump flow measurements in 2011. The mean  
153 hourly pumped discharge at DWF days was used to represent a typical daily DWF profile. DWF  
154 days are defined as having received less than 0.05 mm of precipitation after exponential  
155 smoothing (80% accounted to the current day and 20% to the following day) to prevent false  
156 detection of DWF days due to the absence of rain gauges inside the catchment. Unrealistic  
157 measurements and periods with snowfall have been manually discarded. The DWF profile for  
158 Loenen was previously derived by (Langeveld, 2004) based on the pump flow measurements  
159 using a similar strategy. The resulting profiles can be found in figure 2.

### 160 **2.3. Full hydrodynamic (FH) models**

161 FH models for both catchments are available in InfoWorks ICM ([www.innovyze.com](http://www.innovyze.com)). The FH  
162 model for Loenen was calibrated by (Langeveld, 2004), following the procedure described by  
163 (Clemens, 2001). The calibration involved a detailed check of the geometrical database and  
164 tuning of several parameters to match measured and modelled water levels at up to ten  
165 locations. As the calibration resulted in very close resemblance between the modelled and  
166 measured water levels (deviations < 5 cm), it was concluded that the geometrical database  
167 was virtually without errors. The FH model for Waalre was validated following the procedure  
168 described in (Langeveld et al., 2013). It involved the comparison of measured and modelled  
169 water levels as a function of time at the three monitoring locations. No parameter  
170 optimisation was performed. As mentioned in the report (Liefing, 2012) the measured and  
171 modelled water levels resembled one another in general and it was concluded that no large  
172 errors in the geometrical database existed. Nevertheless, occasional deviations in measured  
173 and modelled water levels of up to 50 cm occurred.

174

175 The FH models are applied in this study for three purposes: i) properties of the geometrical  
176 database and pumping station settings are utilized in the design of the SR and DR models,  
177 ii) key relationships between variables are obtained by means of FH model simulations and  
178 applied in the DR model, and iii) the performance of the simplified models is compared to the  
179 performance of the FH models. For all simulations with the FH models for any of the above  
180 purposes, a standard (uncalibrated) parameter set is employed as (Korving and Clemens, 2005)  
181 showed that the portability of event specific parameter sets for FH models is low. The main  
182 distinction between the calibrated FH model for Loenen and validated FH model for Waalre  
183 lies therefore in the trustworthiness of the underlying geometrical database.

184

185 The simulations performed with the FH model for the second purpose, application in the  
186 design of the DR model, are based on ten years (1955-1964) of 15 minute interval rainfall  
187 measurements in De Bilt in the Netherlands. The simulations were executed with a one minute  
188 time step, recording for every time step the volume, water level and flows in all manholes,  
189 conduits, pumps, CSOs etc. The derivation of the required relationships is described in detail in  
190 section 2.4.3.

## 191 **2.4. Model structures**

192 The general structure of the three simplified models tested in this paper is shown in figure 3.  
193 Model M1 includes only a RRO model. Model M2 combines a RRO model and a SR model,  
194 while model M3 combines a RRO model and a DR model. Rainfall, DWF and optional additional  
195 flows are model inputs, while flows to the surface water ( $Q_{SW}$ ) and to the WWTP ( $Q_{WWTP}$ ) are  
196 model outputs. In the following sections, all models are explained in more detail.

### 197 **2.4.1. Rainfall runoff outflow (RRO) model**

198 The standard linear reservoir model is a typical RRO model, see e.g. (Sun and Bertrand-  
199 Krajewski, 2013b). It comprises of a rainfall loss model followed by a linear reservoir. The  
200 rainfall loss model consists of initial ( $I_{ini}$  [mm]) and proportional ( $P_{cons}$  [-]) rainfall losses, i.e.  
201 depression losses and ratio of contributing and total area. The resulting net rainfall ( $I_{net}$  [mm])  
202 occurs with a time lag ( $T_{lag}$  [min]) and feeds the linear reservoir with a reservoir constant ( $K$   
203 [min]). The outflow of the standard linear reservoir ( $Q_{out}$ ) is derived from the inputs using:

204

$$205 \quad Q_{out}(t) = \exp\left(-\frac{\Delta t}{K}\right) Q_{out}(t - \Delta t) + \left[1 - \exp\left(-\frac{\Delta t}{K}\right)\right] I_{net}(t - T_{lag})A, \quad (1)$$

206

207 with A the catchment area [ha]. For more details on the standard linear reservoir model the  
208 reader is referred to (Sun and Bertrand-Krajewski, 2013b).  
209  
210 To determine the total inflow into the sewer models ( $Q_{in}$  in figure 3) for models M2 and M3,  
211  $Q_{DWF}$  and  $Q_{optional}$  are simply added to  $Q_{out}$ . For model M1,  $Q_{out}$  together with  $Q_{DWF}$  and  $Q_{optional}$   
212 represent both the surface runoff and the subsequent flow routing within the sewer system. It  
213 is split in the two sewer discharges  $Q_{SW}$  and  $Q_{WWTP}$  on the assumption that as much water is  
214 pumped to the WWTP as possible, i.e. all discharges up to the maximum pumping capacity is  
215 accounted to  $Q_{WWTP}$  as illustrated in figure 4 for Loenen. For Waalre,  $Q_{WWTP}$  is determined using  
216 the same method. From the remainder the discharge through the connection to the  
217 neighbouring catchment (determined from FH model simulations as it is not monitored) is  
218 subtracted before accounting it to  $Q_{SW}$ .

#### 219 **2.4.2. Static reservoir (SR) model**

220 The SR model aims to represent processes within the sewer system that the basic RRO model  
221 cannot explicitly simulate. FH model properties of the geometrical database and pumping  
222 station settings are applied in its design. A schematic representation of the SR model for  
223 Loenen is shown in figure 5. It consists of a single basin for the sewer system which is filled by  
224  $Q_{in}$  as described in the previous section. It empties through a pump resulting in  $Q_{WWTP}$ , and a  
225 single CSO resulting in  $Q_{SW}$ .

226

227 Several characteristics or relationships are applied in the SR model, numbered S SR1-SR3 in  
228 figure 5. Their representation and derivation were performed as follows:

229 SR1. Static storage-level curve

230 The static storage-level curve is used to convert the sewer volume ( $V_s$ ) into the water  
231 level in the sewer ( $H_s$ ). It is derived from the geometrical database of the FH model as  
232 the cumulative volume of all manholes, conduits, etc. of the sewer system under each  
233 possible water level.

234 SR2. Discharge through pump

235 The discharge through the pump ( $Q_{s,p}$ ) is calculated through  $H_s$  and the pump  
236 characteristic. The pump characteristic is taken from the FH model. The DWF and  
237 maximum capacity are 115 and 209  $m^3/h$  respectively. The switch on level is 15.00 m,  
238 and the switch off level 14.05 m above Normal Amsterdam Water Level (m AD).

239 SR3. Discharge through CSO

240 The discharge through the CSO ( $Q_{CSO}$ ) is taken to be only caused by the primary CSO.

241 The discharge is calculated through  $H_s$  and the standard weir equations for frontal  
242 weirs:

243

$$244 \quad Q_{free} = c_1 h^{c_2} \quad (2)$$

245

246 for free outflow, with flow  $Q_{free}$  [ $m^3/s$ ],  $h$  [m] water level above the weir crest,  $c_1$   
247 [ $m^{3-c_2}/s$ ] taken to be 1.36 times the weir width [m] and  $c_2$  [-] taken to be 1.5. Or

248

$$249 \quad Q_{sub} = c_3 h_{DS} \sqrt{2g(h_{US} - h_{DS})} \quad (3)$$

250

251 for submerged outflow, with flow  $Q_{sub}$  [ $m^3/s$ ],  $h_{US}$  and  $h_{DS}$  [m] the upstream and  
252 downstream water level above the weir crest,  $c_3$  [m] taken to be 0.8 times the weir  
253 width [m] and  $g$  the standard acceleration due to gravity [ $9.81 m/s^2$ ]. Submerged



254 outflow is assumed to occur when  $2/3 \cdot h_{US} < h_{DS}$ . For Loenen only free outflow is  
255 assumed.

256

257 A schematic representation of the SR model for Waalre is depicted in figure 6. It consists of a  
258 basin for the sewer system and a basin for the settling tank. The sewer basin is filled by  $Q_{in}$  and  
259 has three discharges: one through the pump resulting in  $Q_{WWTP}$ , one through the connection  
260 with the neighbouring catchment and one through a single CSO to the settling tank. The  
261 discharge through the CSO fills the settling tank that is emptied either through a pump back  
262 into the sewer basin, or through a CSO to the surface water resulting in  $Q_{SW}$ .

263

264 Again several characteristics or relationships have been applied in the model, numbered SR4-  
265 SR10 in figure 6. Their representation and derivation were performed as follows:

266 SR4. Static storage-level curve sewer

267 See SR1, and excluding the settling tank.

268 SR5. Discharge sewer through pump

269 The discharge through the pump ( $Q_{S,p}$ ) is calculated through the water level in the  
270 sewer ( $H_s$ ) and the pump characteristic. The pump characteristic is derived from  
271 analysis of the water level and flow measurements at the pumping station, and (Van  
272 Daal-Rombouts, 2012). The DWF and maximum capacity are 85 and 400 m<sup>3</sup>/h  
273 respectively. The switch on level is 17.15 m AD, the switch off level 16.30 m AD.

274 SR6. Discharge sewer through connection

275 From simulations with the FH model it was found that water only flows from Waalre to  
276 the neighbouring catchment. The discharge through the connection ( $Q_{CONN}$ ) is  
277 calculated through  $H_s$  and the standard equation for a free outflow over a V-notch  
278 weir,

279

280 
$$Q = c_1 \tan (\theta/2) h^{5/2}, \quad (4)$$

281

282 as the connecting sewer is egg shaped. Here Q is the flow [ $m^3/s$ ],  $c_1$  a constant [ $m^{1/2}/s$ ]  
283 taken to be 1.4,  $\theta$  the notch angle taken to be  $67^\circ$ , and h [m] the water level over the  
284 weir crest. Free outflow is assumed at all times and the bottom of the notch is taken to  
285 be the highest invert of the connecting conduit.

286 SR7. Discharge sewer through CSO

287 The discharge through the CSO ( $Q_{CSO}$ ) is taken to be caused only by the primary CSO  
288 and is calculated through  $H_S$  and equations 2 and 3. Both free and submerged outflow  
289 are allowed (only free outflow is displayed).

290 SR8. Static storage-level curve settling tank

291 The static storage-level curve is used to convert the settling tank volume ( $V_T$ ) into the  
292 water level in the tank ( $H_T$ ). It is derived from the FH model, similar to SR1.

293 SR9. Discharge settling tank through pump

294 The discharge of the settling tank through the pump ( $Q_{T,p}$ ) is based on  $H_T$  and the pump  
295 characteristic. The pump characteristic was taken from the FH model, where the  
296 pumping capacity was adjusted to match the monitoring data.

297 SR10. Discharge settling tank

298 The discharge of the settling tank ( $Q_T$ ) is calculated through  $H_T$  and equation 2.

### 299 **2.4.3. Dynamic reservoir (DR) model**

300 The DR models for the sewer systems are similar to the SR models, but contain additional  
301 relationships derived from FH model simulations to better account for the dynamic behaviour  
302 of a sewer system. A schematic representation of the DR model for Loenen is shown in figure 7

303 and can be compared to the SR model in figure 5. Differences are expressed in the storage-  
304 level curve applied (SR1 - DR1) and the water level applied in the CSO discharge (DR2 - no  
305 equivalent in the SR model).

306

307 The characteristics or relationships applied in the DR model are numbered DR1-DR4 in figure 7.

308 Their representation and derivation are explained below:

309 DR1. Hybrid storage-level curve

310 A so called hybrid storage-level curve is used to convert the sewer volume ( $V_s$ ) into the  
311 water level in the sewer ( $H_s$ ). The hybrid curve follows the static storage-level curve  
312 (see SR1) for low water levels to correctly model DWF circumstances and pumping  
313 behaviour, and gradually turns to the dynamic storage-level curve for high water levels  
314 (with possibly pressurised flow conditions) to take the dynamic properties of the sewer  
315 system under wet weather flow (WWF) conditions and CSO discharges into account.

316 Figure 8 (left) displays the static, dynamic, and hybrid storage curves for Loenen.

317 The dynamic storage-level curve was derived from simulations performed with the FH  
318 model as described in section 2.3. The resulting water volumes in the entire sewer  
319 system (every minute for 10 years) were grouped in one cm intervals of the  
320 corresponding water level at the pumping station. The grouped volumes were  
321 averaged and smoothed to obtain the dynamic storage-level curve, as displayed in  
322 figure 8 (right). Note that the dynamic storage-level curve converges towards the static  
323 storage-level curve for DWF conditions or low rain intensities as the water level in the  
324 sewer system levels off.

325 DR2. Level at CSO

326  $H_s$  is converted into the water level at the primary CSO location ( $H_{CSO}$ ). The relationship  
327 is based on FH model simulations, where a linear relation is fitted through the

328 simulated water levels at the pumping station and the CSO location. Only elevated  
329 water levels (WWF conditions) are taken into account.

330 DR3. Discharge through pump

331 See SR2.

332 DR4. Discharge through CSO

333 See SR3, only now  $H_{CSO}$  is applied.

334

335 A schematic representation of the DR model for Waalre is shown in figure 9 and can be  
336 compared to the SR model in figure 6. Differences are expressed in the storage-level curve  
337 applied (DR5-SR4), the water level applied in the CSO discharge (DR6-no equivalent in the SR  
338 model) and the water level applied in and the calculation of the flow through the connection  
339 (DR7-no equivalent in SR model, DR9-SR6).

340

341 The characteristics or relationships applied in the DR for Waalre are numbered DR5-DR13 in  
342 figure 9. Their representation and derivation are explained as follows:

343 DR5. Hybrid storage-level curve sewer

344 A hybrid storage-level curve is used to convert  $V_S$  into  $H_S$ . The derivation follows DR1.

345 The resulting curves for Waalre are displayed in Figure 10: (left) the static, dynamic,  
346 and hybrid storage curves, (right) the derivation of the dynamic storage-level curve  
347 from the FH model simulation results.

348 DR6. Level sewer at CSO

349 Similar to DR2, a relationship has been derived between  $H_{CSO}$  and  $H_S$ . As Waalre is  
350 equipped with the settling tank two linear segments that connect at the highest weir  
351 crest level of the settling tank have been applied. Only elevated water levels (WWF  
352 conditions) are taken into account.

353 DR7. Level sewer at connection  
354 Similar to  $H_{CSO}$  in DR6, a relationship between the water level at the connection to the  
355 neighbouring catchment ( $H_{CONN}$ ) and  $H_s$  is derived from the FH model simulations. A  
356 linear relation was fitted, taking only elevated water levels (WWF conditions) into  
357 account.

358 DR8. Discharge sewer through pump  
359 See SR5.

360 DR9. Discharge sewer through connection  
361 The discharge of the sewer through the connection to the neighbouring catchment  
362 ( $Q_{CONN}$ ) is based on  $H_{CONN}$  and a relationship derived from the FH model simulations.  
363 The simulated water levels at the connection and the corresponding flow through the  
364 connection were fitted with a third order polynomial equation. To prevent unrealistic  
365 (negative) output a maximum value is set for  $H_{CONN}$ .

366 DR10. Discharge sewer through CSO  
367 See SR7, where  $H_{CSO}$  is applied in the calculation of the discharge from the sewer.

368 DR11. Static storage-level curve settling tank  
369 See SR8.

370 DR12. Discharge settling tank through pump  
371 See SR9.

372 DR13. Discharge settling tank  
373 See SR10.

## 374 **2.5. Calibration procedure**

### 375 **2.5.1. DREAM algorithm**

376 Calibration, which adjusts model parameters by minimizing the difference between model  
377 outputs and measurements, is an important step before applying simplified models. The  
378 research on calibration methods in the area of rainfall-runoff modelling is comprehensive,  
379 leading to the application of automatic calibration methods instead of traditional manual  
380 calibration mainly based on trial and error approaches. In this study an automatic calibration  
381 method (the differential evolution adaptive metropolis (DREAM) method (Vrugt et al., 2008,  
382 2009)) was applied for the calibration of the RRO models. The DREAM method is based on the  
383 Bayesian theorem, which considers model parameters as probabilistic variables revealing the  
384 probabilistic belief on the parameters according to observed model outputs. In DREAM the  
385 probability distribution function of parameters is derived using an iterative approximation  
386 method (the Markov chain Monte Carlo (MCMC) method) coupled with multiple chains in  
387 parallel in order to provide a robust exploration of the search space. In addition to an optimal  
388 model parameter set, DREAM also results in an evaluation of model parameter uncertainty,  
389 which provides important information on model reliability. The effectiveness of DREAM in  
390 water related model calibration has been demonstrated in many previous studies, e.g. (Keating  
391 et al., 2010; Leonhardt et al., 2014).

### 392 **2.5.2. Parameter optimisation**

393 The DREAM algorithm is applied to calibrate the parameters of the RRO model to find the  
394 minimal difference between the simplified model output and the measurements. Table 2  
395 shows the parameters, units and the searching range for the calibration procedure.

396

397 The algorithm minimises the sum of squared errors (SSE) between the model output and  
398 measurements. Water level measurements are applied in the calibration as they are the actual  
399 monitoring data available, containing all information on the sewer systems behaviour. For

400 Loenen the water level measurement at the primary CSO location is used to calibrate M2 and  
401 M3. For Waalre the water level measurements at the pumping station and inside the settling  
402 tank are applied, by minimising the sum of the SSEs for each model output-measurement  
403 combination. Only periods with elevated water levels are considered in the calibration, as the  
404 RRO model parameters are connected to rainfall only. Since water levels do not have  
405 significance in M1, it's calibration is based on the total outflow from the sewer system, i.e. the  
406 sum of the measured pump flow and the calculated outflow at the CSO locations (determined  
407 with the measured water levels and equation 2) for Loenen and Waalre. For Waalre the  
408 outflow through the connection with the neighbouring catchment is added. As this flow is not  
409 monitored, it is based on FH model simulations for the respective rain events.

410

411 The information content on which the models are calibrated is similar, especially for the  
412 elevated water levels relevant for CSO discharges. M2 and M3 are calibrated on measured  
413 water levels at the CSO locations. The discharge to the surface water in M2 and M3 is  
414 calculated using the modelled water level and equation 2. The same equation with the  
415 measured water levels is applied to determine the outflow for the calibration of M1.  
416 Additionally, the pumped outflow supplies information during low intensity rainfall, as  
417 contained in the level measurements at the pumping station (in case of Waalre) or the primary  
418 CSO location (for Loenen) when it is not yet discharging.

419

420 The calibration is performed using 10,000 iterations in DREAM, as it was found from test runs  
421 that the cumulative density functions of the parameters do not change (within the parameter  
422 stability) after several thousand iterations. The last 5,000 iterations are used for further  
423 analysis: the optimal parameter set and model output are derived, and the model is run with

424 all 5,000 parameter sets to determine the 95% confidence intervals for the water levels and  
425 discharges.

### 426 **2.5.3. Events**

427 For each catchment six rain events are available for the parameter optimisation, e.g. they led  
428 to a significant rise in water level in the sewer system, with or without discharge to the surface  
429 water, no external influences were known and monitoring data was available and judged  
430 reliable after data validation. The selected events and their characteristics are summarised in  
431 table 3.

432

433 (Korving and Clemens, 2005) showed that the portability of event specific parameter sets for  
434 FH models is low. (Sun and Bertrand-Krajewski, 2012) investigated the impact of calibration  
435 data selection on the model performance of regression models. Given the limited dataset, full  
436 consideration of this aspect is considered beyond the scope of this paper. It is clear, however,  
437 that comparison of the model structures on single event calibration is insufficient. Therefore  
438 three scenarios have been explored:

- 439 1. Calibration of single rain events,
- 440 2. Calibration on all events together,
- 441 3. Calibration on any set of 3 events and verification with the remaining 3 events.

### 442 **2.6. Performance evaluation**

443 The performance of the calibrated simplified model structures should be evaluated on the  
444 capability to correctly represent the sewer systems functioning at the edges of the system. As  
445 argued in the introduction this is not obtained by comparing the best fits between the  
446 measured and modelled water levels but by comparing the discharges from the system, i.e. to



447 the WWTP and the surface water. As the RRO models are calibrated, i.e. all calibration  
448 parameters are related to rainfall, the focus of the performance evaluation will be on the CSO  
449 discharges to the surface water. As the discharge to the WWTP is also relevant for integrated  
450 studies it will be reported for completeness.

451

452 Common sense dictates that the impact of CSO events depends foremost on the occurrence of  
453 such events, with the absolute discharged flows of secondary consequence. This is supported  
454 by literature stating that impact based RTC can influence the systems performance for small  
455 and moderate events, contrary to large events on which it has no influence (Langeveld et al.,  
456 2013), and that up to a certain point overflow frequency is a good indicator of receiving water  
457 impact (Lau et al., 2002). Therefore the first evaluation criterion for the simplified sewer  
458 models is the correct determination of CSO event occurrences. The second evaluation criterion  
459 is the correct determination of the total discharged volume.

460

461 Based on the monitored water levels at the CSO locations in the sewer systems and settling  
462 tank, for each event and catchment the discharge to the surface water ( $Q_{SW}$ ) is calculated  
463 through application of equation 2. Additionally the total discharge to the WWTP ( $Q_{WWTP}$ ) is  
464 calculated from the pump flow measurements. For each model structure and scenario the  
465 modelled the total discharged volumes ( $V_{SW}$  and  $V_{WWTP}$ ) are determined as the integral of the  
466 model outputs  $Q_{SW}$  and  $Q_{WWTP}$ .

467

468 CSO event occurrences are analysed through false positives (FP) and false negatives (FN). A FP  
469 is defined as a CSO event occurrence ( $V_{SW} > 0$ ) in the model output but not in the  
470 measurements, a FN as a CSO event occurrence in the measurements but not in the model  
471 output. For the comparison of discharged volumes, differences in  $V_{SW}$  (and  $V_{WWTP}$ ) between the

472 model output and the measurements are calculated and listed for each event and scenario.

473 Cumulative results for each scenario are determined by taking the root mean squared errors

474 (RMSE) over all events.

475

476 For comparison purposes the selected rain events have also been simulated using the FH

477 models. The comparison between simplified models with calibrated inflow parameters and FH

478 models with uncalibrated inflow parameters is relevant since the FH models simulate the

479 sewer systems behaviour in greatest detail and hence are deemed to be most accurate (Ferreri

480 et al., 2010; Meirlaen et al., 2001; Rubinato et al., 2013). This might hold true for calibrated FH

481 models but not for the much more commonly applied uncalibrated models, as proper

482 calibration of FH models is very time consuming and requires a very large monitoring data set.

483

484 Finally, the simulation time needed by different simplified model structures and the FH model

485 will be compared.

486

487 **3. Results and discussion**

488 **3.1. Calibration**

489 As described in the previous section the performance of the simplified model structures will be  
490 evaluated based upon the correct determination of CSO occurrences and the total discharge to  
491 the surface water. The calibration results, however, provide useful insight into the models  
492 functioning. Therefore, a typical calibration result for each catchment will be presented. Nash-  
493 Sutcliffe efficiency indexes (NS) (Nash and Sutcliffe, 1970) are supplied for easy comparison of  
494 the calibration results. Optimal parameter sets will be given for all events and scenarios.

495

496 The results for the individual calibration of rain events 2001-08-27 (Loenen) and 2011-08-14  
497 (Waalre) for all model structures are displayed in figures 11 and 12 respectively. From top to  
498 bottom the applied rainfall is shown, followed by the model results for M1 (based on the total  
499 sewer outflow), and M2 and M3 (based on the water level in the sewer system). For Waalre  
500 additional water level measurements in the settling tank were applied, the results of which  
501 have been added to the bottom of figure 12. For each model structure the optimal results are  
502 displayed together with their 95% confidence bands.

503

504 Figures 11 and 12 show that M2 and M3 are in general well able to describe the sewer systems  
505 behaviour: the measurements applied in the calibration are closely followed during the filling  
506 of the basins, once they are full and during emptying, resulting in NS values  $> 0.95$  for Loenen  
507 and  $> 0.75$  for Waalre. Small differences occur between these models especially during filling  
508 and in the response to temporal changes in the rainfall. M1 cannot describe the sewer systems  
509 behaviour in detail as it has only the reservoir constant K to account for surface storage and in-

510 sewer storage. The response to rainfall is therefore more smoothed, which is best  
511 demonstrated in figure 11. NS values  $< 0.4$  are found.  
512  
513 For both catchments and all model structures the 95% confidence bands are mostly  $< 1\%$ .  
514 Logically, the influence of the (inflow) calibration parameters on water levels in sewer systems  
515 is most apparent at the onset of a rain event or during temporal changes, resulting in  
516 confidence bands up to 10% for M2 and M3, while they stay  $< 1\%$  for M1.  
517  
518 For all scenarios for Loenen NS values for M2 and M3  $> 0.90$ . For M1, values differ strongly  
519 from -8.52 to 0.44. For Waalre for M2 and M3 in scenario 1, NS values range between 0.61 and  
520 0.96, with one event around zero. In scenario 2 the values drop to 0.5 to 0.6. The NS values for  
521 M1 again differ strongly between events and scenarios from -9.42 to 0.82.  
522  
523 Figure 13 shows the optimal parameter values for Loenen (left) and Waalre (right) for all  
524 model structures. In asterisks the results for scenario 1 (calibration on single rain events) are  
525 given, the line indicates the parameter values for scenario 2 (all events together). Results for  
526 all twenty possible combinations of three calibration events in scenario 3 can be found in  
527 figure 14. The optimal parameter values reflect the results for the water levels and NS values:  
528 the parameters for M2 and M3 show much resemblance within a catchment, while M1  
529 deviates. Especially the difference in K stands out, as the RRO model in M1 has to account for  
530 the surface and in-sewer storage, while in M2 and M3 only for the surface storage. The  
531 optimal parameter values between scenarios 2 (line in figure 13) and 3 (figure 14) are  
532 consistent, indicating that the exact split in a calibration and verification set does not have a  
533 major impact on the outcome.

### 534 **3.2. Performance evaluation**

535 **3.2.1. Model discharge**

536 As the calibration of the simplified models is performed on rainfall related parameters, the  
537 focus of the performance evaluation will be on the discharge to the surface water ( $Q_{SW}$ ) while  
538 the discharge to the WWTP ( $Q_{WWTP}$ ) is included for completeness.

539

540 Optimal  $Q_{SW}$  and  $Q_{WWTP}$  for all model structures for the calibration of the single events of 2001-  
541 08-27 (Loenen) and 2011-08-14 (Waalre) are displayed in figures 15 and 16 as well as the  
542 discharges determined from the measurements. The difference between M1 and M2/M3  
543 observed in the calibration results are also clear from these figures, as  $Q_{SW}$  for M1 tends to be  
544 more smoothed because of the higher value for K.

545 **3.2.2. Determination of CSO events**

546 FPs and FNs for all events for each model structure and scenario, based on the optimal  
547 parameter sets, are given in table 4. For scenarios 1 and 2 the total number is reported, for  
548 scenario 3 the results have been averaged over all combinations and multiplied by two for easy  
549 comparison. Additionally, results for the FH model have been added.

550

551 Based on the FPs and FNs in table 4, M1 can be immediately discarded for these catchments.  
552 For each scenario and catchment two FPs were recorded, the exact number of rain events that  
553 did not lead to a CSO event. This is easily explained since a rain event leading to a significant  
554 rise in water level in a pumped sewer system will likely contain rain intensities higher than the  
555 pumping capacity of the sewer system reserved for WWF (design guideline in the Netherlands:  
556 0.7 mm/h). In M1 all rainfall in excess of this capacity has to be discharged to the surface  
557 water, leading to a CSO event. The calibration algorithm unsuccessfully tries to overcome this

558 inadequacy in the model structure by delaying the rainfall (high  $T_{lag}$ ) and smoothing the  
559 response (high  $K$ ), as can be found from the optimal parameter values in figure 13.  
560  
561 For M2 and M3 the results are less conclusive. Single FPs or FNs occur depending on the  
562 catchment and scenario applied. The floating point values for scenario 3 for Waalre (due to  
563 averaging over all possible combinations) and the optimal parameter values in figure 13  
564 further indicate that the inflow parameters are calibrated differently depending on the  
565 selection of calibration/verification events. Only for M3 for Loenen no FPs or FNs occur in any  
566 scenario signalling that the M3, combining the RRO and DR models, is likely the best  
567 performing model for Loenen.

### 568 **3.2.3. Determination of discharged volumes**

569 The total volumes discharged to the surface water ( $V_{sw}$ ) for each model structure and  
570 scenarios 1 and 2 are displayed in figure 17 for Loenen and 18 for Waalre.  $V_{sw}$  is the integrated  
571 model output  $Q_{sw}$ , for which the optimal values and 95% confidence bands are determined as  
572 described in section 2.5.2. The calculation of the 95% confidence intervals for the  
573 measurements is based on an uncertainty in the standard weir equation of 25%. This  
574 percentage is estimated on previous work by (Van Daal-Rombouts et al., 2014) on scale models  
575 and (Fach et al., 2009) on computational fluid dynamics. Both studies indicate deviations  
576 between the actual (measured or calculated) CSO discharge and the discharge determined  
577 with the standard weir equation of up to 50%. They also indicate that this strongly depends on  
578 the water level over the weir crest leading to under and over estimations of the flow.  
579 Therefore an intermediate value was chosen. For the FH model an uncertainty of 50% was  
580 applied based on the possibility to calibrate FH models up to 5 cm difference in water levels  
581 and equation 2.

582

583 The cumulative results for  $V_{SW}$  and  $V_{WWTP}$ , given in table 5, were determined by taking the  
584 RMSE of the results from the optimal parameter sets over all events. The RMSE for scenario 3  
585 have been averaged over all possible combinations and values for the FH model have been  
586 added.

587

588 The results for  $V_{SW}$  in figures 17 and 18 and table 5 support the preliminary conclusion that M3  
589 outperforms M2 for Loenen. For all scenarios the RMSE and the uncertainty bands for M3 are  
590 smaller than for M2. Despite the inability of M1 to correctly determine CSO event occurrences,  
591 it outperforms M2 based on  $V_{WS}$ . For Waalre the performance of M2 and M3 are similar,  
592 corresponding to the determination of the CSO events. Nevertheless, M2 consistently  
593 performs better than M3. Similar to Loenen, M1 generally performs well based on  $V_{SW}$ . The  
594 difference in the performance of M2 and M3 between the catchments is also reflected in the  
595 optimal parameter values (figure 13). The parameter values for Waalre are close resulting in  
596 similar RMSE values in table 5, while for Loenen there is more variety between the model  
597 structures especially for  $I_{ini}$  and  $K$ .

598

599 These results can be explained by the information available for the simplified model design  
600 and calibration as described in sections 2.2 and 2.3. All information is better known or of  
601 higher quality for Loenen: i) The monitoring data for Loenen was gathered for research  
602 purposes, while the monitoring campaign for Waalre received less dedicated attention. ii) For  
603 Loenen two rain gauges were installed in the catchment itself, while for Waalre no local rain  
604 gauges were available. iii) The geometrical database underlying the FH model for Loenen is  
605 better known than for Waalre. The results for the RMSE of  $V_{SW}$  indicate that the more detailed  
606 model M3, i.e. RRO model for the runoff combined with the DR model for the sewer system, is

607 favoured when high quality information is available (in this case Loenen), while the less  
608 detailed model M2, RRO with SR, suffices when the information is of lower quality (Waalre).

609

610 One main source of uncertainty for Waalre likely stems from the calibrated rain radar input.

611 The rainfall in general seems reasonable with NS values for M2 or M3 > 0.6. In detail the

612 rainfall seems off in intensities and/or timing, an example of which can be found in figure 16.

613 Judging from the rainfall, the models responses in  $Q_{SW}$  are in accordance (main peak in the

614 outflow after main peak in the rainfall). However, in the measurements the main peak in the

615 outflow occurs right at the beginning of the rain event. The other events display a similar

616 mismatch between the rainfall and the outflow. This may also explain the very low values for

617 the parameters  $T_{lag}$  and  $K$ , see figure 13, as the calibration procedure tries to correct the

618 mismatch in the input data.

619

620 For  $V_{WWTP}$  the RMSE values in table 5 show that model M1 consistently performs worse than

621 M2 and M3 for all scenarios and both catchments. M2 and M3 generally perform on a similar

622 level, which is to be expected as the pumping regime in the SR and DR model structures is the

623 same.

624

625 The NS values reported in section 3.1 are based on the calibration parameters for each time

626 step, and the FP/FN in table 4 and RMSE in table 5 on  $V_{SW}$ . Each presents information on the

627 performance of the model structure. NS indicates the quality of the description of the sewer

628 systems behaviour in general, while the others are specific for CSO discharges. The difference

629 between the best performing model structure based on these criteria, especially for Loenen,

630 is striking. Model M2 and M3 have similar NS values > 0.9, but M3 is much more accurate

631 based on FP/FN and RMSE. Simplified sewer models are calibrated on measurements,



632 generally only water levels, but used to determine CSO discharges. These results show that  
633 care should be taken in choosing performance indicators suitable to the purpose of the model,  
634 likely leading to multiple indicators.

#### 635 **3.2.4. Uncalibrated FH models**

636 Finally the performance of the FH models is compared to the performance of the calibrated  
637 simplified models. The comparison is made for scenario 2, calibration for all events together,  
638 since there a single parameter set is derived for each model structure, similar to the single  
639 standard parameter set for the FH model.

640

641 Based on the determination of CSO event occurrences (table 4) the FH model performs at a  
642 similar level as M2 and M3. For Loenen one FP is noted for the FH model, while none for M2  
643 and M3. For Waalre it is reversed.

644

645 Taking the RMSE for  $V_{SW}$  (table 5) into account, the FH model is easily outperformed by both  
646 M2 and M3, while  $V_{WWTP}$  is worse for Loenen and better for Waalre. The results for the  
647 simplified models for  $V_{SW}$  (scenario 3) imply little loss of accuracy when the available data is  
648 split into a calibration and verification set. This suggests that, if a sufficiently large data set  
649 were available, the optimal parameter set should be applicable to other events without much  
650 loss of accuracy.

651

652 The simulation time for the FH models takes 1,000-5,000 times longer than for M2/M3 or  
653 250,000-475,000 times longer than for M1.

654

655 From the perspective of both the simulation time and accuracy of results it is concluded that it  
656 is better to apply simplified calibrated models in optimisation or RTC studies than uncalibrated  
657 FH models.  
658

659 **4. Conclusions and future research**

660 The research described dealt with the design and performance evaluation of a so called  
661 dynamic simplified sewer model for the accurate and rapid calculation of sewer system  
662 discharges for optimisation and RTC studies. The dynamic simplified sewer model (M3)  
663 consists of a calibrated rainfall runoff outflow (RRO) model and a dynamic reservoir (DR) model  
664 for the sewer behaviour. It contains characteristics derived from full hydrodynamic (FH) model  
665 simulations to account for the dynamic properties of the sewer system behaviour.

666

667 The performance of M3 was tested for two combined, pumped catchments and compared  
668 against two other simplified models, M2 (calibrated RRO model with a static reservoir (SR))  
669 and M1 (calibrated RRO model only), and uncalibrated FH models. The performance was not  
670 solely based on the goodness of fit of the calibration but primarily on the correct  
671 determination of CSO event occurrences, and secondly on the correct determination of the  
672 total discharged volumes to the surface water.

673

674 From this research the following conclusions can be drawn:

- 675 – Model M1 simulates > 100,000 times faster than the FH model; models M2/M3  
676 are > 1,000 times faster than the FH model.
- 677 – M1 is unsuitable to correctly predict CSO occurrences for pumped catchments.  
678 The model structure is unable to retain rain intensities higher than the pumping  
679 capacity reserved for WWF, resulting in too many CSO discharges.
- 680 – M2 and M3 are able to describe the behaviour of pumped sewer systems.
- 681 – Performance indicators for the selection of the most appropriate model structure  
682 should be chosen carefully in relation to the modelling objectives, likely leading to

683 multiple indicators, each one providing a specific approach of the models'  
684 performances.

685 – In case of detailed and trustworthy information available for the design and  
686 calibration of the model (Loenen), M3 outperforms M2 for all scenarios. If the  
687 available information is of lower quality (Waalre), M2 consistently performs  
688 slightly better indicating that the derivation of the more detailed DR model is not  
689 useful.

690 – For rainfall driven modelling trustworthy and local rain measurements remain  
691 necessary despite the availability of rain radar data, to either apply as direct input  
692 or the correction of radar data.

693 – M2 and M3 outperform the uncalibrated FH models based on the total discharge  
694 to the surface water. In optimisation or RTC studies the application of suitable  
695 calibrated simplified models is preferred over uncalibrated FH models.

696

697 Future research is recommended in the area of statistical substantiation of the results as the  
698 available data sets were too limited to allow a statistical analysis of the results themselves.  
699 Also the use of continuous data sets instead of the current intermittent ones would be  
700 interesting because more information on the initial conditions prior to events would be  
701 included.

702

703 Following the above, future research will focus on retrieving more reliable monitoring data  
704 (especially rainfall). For the catchment of Waalre, the impact of more reliable rainfall data on  
705 the performance of the detailed M3 model will be focussed on. Calibrated simplified sewer  
706 models will be derived for the catchments in the case study area of Eindhoven for application  
707 in an integrated model to research the possibilities for quality based RTC.

708 **Acknowledgements**

709 The authors would like to acknowledge Innovyze ([www.innovyze.com](http://www.innovyze.com)) for kindly supplying a  
710 research licence for the use of the software program InfoWorks ICM. Also the authors would  
711 like to thank the Van Gogh Programme for supplying a Travel Grant to cover the travel  
712 expenses for the cooperation between TU Delft and INSA Lyon.

713

714 The research is performed within the Dutch 'Kennisprogramma Urban Drainage' (Knowledge  
715 Programme Urban Drainage). The involved parties are: ARCADIS, Deltares, Evides, Gemeente  
716 Almere, Gemeente Arnhem, Gemeente Breda, Gemeente 's-Gravenhage, Gemeentewerken  
717 Rotterdam, Gemeente Utrecht, GMB Rioleringsstechniek, Grontmij, KWR Watercycle Research  
718 Institute, Royal HaskoningDHV, Stichting RIONED, STOWA, Tauw, vandervalk + degroot,  
719 Waterboard De Dommel, Waternet and Witteveen+Bos.

720

721 **References**

722 Bach, P.M., Rauch, W., Mikkelsen, P.S., McCarthy, D.T., Deletic, A., 2014. A critical review of  
723 integrated urban water modelling - Urban drainage and beyond. *Environ. Model. Softw.*  
724 54, 88–107.

725 Benedetti, L., Langeveld, J.G., Comeau, A., Corominas, L., Daigger, G., Martin, C., Mikkelsen,  
726 P.S., Vezzaro, L., Weijers, S.R., Vanrolleghem, P.A., 2013. Modelling and monitoring of  
727 integrated urban wastewater systems: review on status and perspectives. *Water Sci.*  
728 *Technol.* 68, 1203–1215.

729 Clemens, F.H.L.R., 2001. Hydrodynamic models in urban drainage: application and calibration.  
730 TU Delft.

731 Coutu, S., Del Giudice, D., Rossi, L., Barry, D.A., 2012. Parsimonious hydrological modeling of

732 urban sewer and river catchments. *J. Hydrol.* 464-465, 477–484.

733 De Niet, A.C., De Jonge, J., Korving, H., Langeveld, J.G., Van Nieuwenhuijzen, A., 2013. Het  
734 beste van twee werelden, correctie van neerslagradar op basis van grondstations voor  
735 toepassing in stedelijk gebied. *H2O online* 1–5.

736 Del Giudice, D., Reichert, P., Bareš, V., Albert, C., Rieckermann, J., 2015. Model bias and  
737 complexity – Understanding the effects of structural deficits and input errors on runoff  
738 predictions. *Environ. Model. Softw.* 64, 205–214.

739 Dotto, C.B.S., Kleidorfer, M., Deletic, A., Rauch, W., McCarthy, D.T., 2014. Impacts of measured  
740 data uncertainty on urban stormwater models. *J. Hydrol.* 508, 28–42.

741 Fach, S., Sitzenfrey, R., Rauch, W., 2009. Determining the spill flow discharge of combined  
742 sewer overflows using rating curves based on computational fluid dynamics instead of  
743 the standard weir equation. *Water Sci. Technol.* 60, 3035–43.

744 Ferreri, G.F., Freni, G., Tomaselli, P., 2010. Ability of Preissmann slot scheme to simulate  
745 smooth pressurisation transient in sewers. *Water Sci. Technol.* 62, 1848–1858.

746 Keating, E.H., Doherty, J., Vrugt, J.A., Kang, Q., 2010. Optimization and uncertainty assessment  
747 of strongly nonlinear groundwater models with high parameter dimensionality. *Water*  
748 *Resour. Res.* 46, 1–18.

749 Kleidorfer, M., Möderl, M., Fach, S., Rauch, W., 2009. Optimization of measurement campaigns  
750 for calibration of a conceptual sewer model. *Water Sci. Technol.* 59, 1523–30.

751 Korving, H., Clemens, F.H.L.R., 2005. Impact of dimension uncertainty and model calibration on  
752 sewer system assessment. *Water Sci. Technol.* 52, 35–42.

753 Krebs, G., Kokkonen, T., Valtanen, M., Setälä, H., Koivusalo, H., 2014. Spatial resolution  
754 considerations for urban hydrological modelling. *J. Hydrol.* 512, 482–497.

755 Langeveld, J.G., 2004. Interactions within wastewater systems. TU Delft.

756 Langeveld, J.G., Benedetti, L., De Klein, J., Nopens, I., Amerlinck, Y., Van Nieuwenhuijzen, A.,  
757 Flameling, T., Van Zanten, O., Weijers, S.R., 2013. Impact-based integrated real-time  
758 control for improvement of the Dommel River water quality. *Urban Water J.* 10, 312–329.

759 Lau, J., Butler, D., Schütze, M., 2002. Is combined sewer overflow spill frequency/volume a  
760 good indicator of receiving water quality impact? *Urban Water* 4, 181–189.

761 Leonhardt, G., Sun, S., Rauch, W., Bertrand-Krajewski, J.-L., 2014. Comparison of two model  
762 based approaches for areal rainfall estimation in urban hydrology. *J. Hydrol.* 511, 880–  
763 890.

764 Liefthing, H.J., 2012. Toetsing rioolmodel Waalre.

765 Mair, M., Kleidorfer, M., Rauch, W., 2012. Performance of auto-calibration algorithms in the  
766 field of urban drainage modelling, in: *Proceedings of UDM9*. Belgrade, pp. 1–10.

767 Mannina, G., Viviani, G., 2010. An urban drainage stormwater quality model: Model  
768 development and uncertainty quantification. *J. Hydrol.* 381, 248–265.

769 Meirlaen, J., Huyghebaert, B., Sforzi, F., Benedetti, L., Vanrolleghem, P.A., 2001. Fast,  
770 simultaneous simulation of the integrated urban wastewater system using mechanistic  
771 surrogate models. *Water Sci. Technol.* 43, 301–309.

772 Motiee, H., Chocat, B., Blanpain, O., 1997. A storage model for the simulation of the hydraulic  
773 behaviour of drainage networks. *Water Sci. Technol.* 36, 57–63.

774 Nash, J.E., Sutcliffe, J.V., 1970. River flow forecasting through conceptual models: Part I - A  
775 discussion of principles. *J. Hydrol.* 10, 282–290.

776 Rubinato, M., Shucksmith, J., Saul, A.J., Shepherd, W., 2013. Comparison between InfoWorks

777 hydraulic results and a physical model of an Urban drainage system. *Water Sci. Technol.*  
778 68, 372–379.

779 Sun, S., Bertrand-Krajewski, J.-L., 2013a. Input variable selection and calibration data selection  
780 for storm water quality regression models. *Water Sci. Technol.* 68, 50–58.

781 Sun, S., Bertrand-Krajewski, J.-L., 2013b. Separately accounting for uncertainties in rainfall and  
782 runoff: Calibration of event based conceptual hydrological models in small urban  
783 catchments using Bayesian method. *Water Resour. Res.* 49, 1–14.

784 Sun, S., Bertrand-Krajewski, J.-L., 2012. On calibration data selection: The case of stormwater  
785 quality regression models. *Environ. Model. Softw.* 35, 61–73.

786 Vaes, G., Berlamont, J., Bermont, J., 1999. Emission predictions with a multi-linear reservoir  
787 model. *Water Sci. Technol.* 39, 9–16.

788 Vaes, G., Willems, P., Berlamont, J., 2001. Rainfall input requirements for hydrological  
789 calculations. *Urban Water* 3, 107–112.

790 Van Bijnen, M., Korving, H., 2008. Application and results of automatic validation of sewer  
791 monitoring data, in: *Proceedings of ICUD11*. Edinburgh, pp. 1–10.

792 Van Daal-Rombouts, P.M.M., 2012. Personal communication.

793 Van Daal-Rombouts, P.M.M., Tralli, A., Verhaart, F., Langeveld, J.G., Clemens, F.H.L.R., 2014.  
794 Applicability of CFD modelling in determining accurate weir discharge - water level  
795 relationships, in: *Proceedings of ICUD13*. Sarawak, pp. 1–8.

796 Vrugt, J.A., Ter Braak, C.J.F., Clark, M.P., Hyman, J.M., Robinson, B.A., 2008. Treatment of input  
797 uncertainty in hydrologic modeling: Doing hydrology backward with Markov chain Monte  
798 Carlo simulation. *Water Resour. Res.* 44, 1–15.



799 Vrugt, J.A., Ter Braak, C.J.F., Gupta, H.V., Robinson, B.A., 2009. Equifinality of formal (DREAM)  
800 and informal (GLUE) Bayesian approaches in hydrologic modeling? *Stoch. Environ. Res.*  
801 *Risk Assess.* 23, 1011–1026.

802 Wolfs, V., Villazon, M.F., Willems, P., 2013. Development of a semi-automated model  
803 identification and calibration tool for conceptual modelling of sewer systems. *Water Sci.*  
804 *Technol.* 68, 167–175.

805 Wolfs, V., Willems, P., 2014. Development of discharge-stage curves affected by hysteresis  
806 using time varying models, model trees and neural networks. *Environ. Model. Softw.* 55,  
807 107–119.

**Table 1.** Sewer system characteristics for Loenen and Waalre.

property	unit	Loenen	Waalre
number of inhabitants	-	2,100	6,200
contributing area	ha	23.4	52.3
average slope ground level	%	0.91	0.14
static storage volume	m <sup>3</sup> - mm	947 - 4.0	2,704 - 5.2
WWF pumping capacity	m <sup>3</sup> /h	209	400
number of CSO structures	-	2	2 (incl. 1 SST)
length of conduits	km	12.3	27.6

**Table 2.** Calibration parameters with searching range.

parameter	abbreviation	unit	searching range
initial rainfall loss	$I_{ini}$	mm	0 - 4
proportional rainfall loss	$P_{cons}$	-	0 - 1
lag time	$T_{lag}$	min	0 - 120
reservoir constant	K	min	0 - 240

**Table 3.** Selected rain events with key characteristics.

catchment area	event [dd-mm-yyyyy]	rainfall depth [mm]	max rain intensity [mm/h]	duration [hh:mm]	discharge to surface water [y/n]
Loenen	30-06-2001	9.9	24.8	6:12	y
	18-07-2001	13.9	25.4	14:36	y
	19-07-2001	12.2	34.0	12:15	n
	23-07-2001	12.3	19.4	7:48	y
	27-08-2001	17.0	24.0	7:45	y
	23-10-2001	7.4	6.0	7:39	n
Waalre	29-04-2011	6.5	5.2	6:20	n
	14-08-2011	27.0	23.4	10:35	y
	18-08-2011	12.0	14.9	7:20	n
	22-08-2011	39.2	68.8	23:04	y
	14-12-2011	15.4	11.9	23:31	y
	16-12-2011	33.4	8.5	22:15	y

**Table 4.** FPs and FNs for all 6 events for each model structure and scenario based on the optimal parameter sets. The results for scenario 3 have been averaged over all combinations and multiplied by two for easy comparison.

scenario	1: individual events		2: all events together		3: 3 events calibration, 3 verification			
	total	total	total	total	mean	mean	mean	mean
catchment / model structure	FP	FN	FP	FN	FP	FN	FP	FN
<b>Loenen</b>								
M1	2	0	2	0	2.0	0.0	2.0	0.0
M2	1	0	0	0	1.0	0.0	1.0	0.0
M3	0	0	0	0	0.0	0.0	0.0	0.0
FH			1	0				
<b>Waalre</b>								
M1	2	0	2	0	2.0	0.0	1.9	0.0
M2	0	1	1	0	0.4	0.2	0.6	0.1
M3	0	1	1	0	0.4	0.2	0.6	0.1
FH			0	0				

**Table 5.** RMSE for  $V_{SW}$  and  $V_{WWTP}$  for all 6 events for each model structure and scenario (1: individual events, 2: all events together, 3: calibrate and verify on 3 events each) based on the optimal parameters sets.

catchment / model structure	RMSE [ $m^3$ ]							
	$V_{SW}$				$V_{WWTP}$			
	1	2	3 calibra- tion	3 verifica- tion	1	2	3 calibra- tion	3 verifica- tion
<b>Loenen</b>								
M1	112	150	147	178	445	242	248	255
M2	416	197	346	364	67	150	135	158
M3	57	145	94	125	124	143	133	132
FH		661				399		
<b>Waalre</b>								
M1	3,470	2,469	2,448	2,157	3,072	2,075	2,307	2,240
M2	5,202	967	2,593	2,212	422	1,331	995	1,330
M3	5,398	1,480	2,788	2,487	556	1,346	1,027	1,354
FH		2,658				619		

1 **Figure 1.** Sewer system layout for Loenen (left) and Waalre (right). Monitoring locations and  
2 locations of pumping stations and CSOs are indicated. Line colour and width indicate pipe  
3 diameter ranges:  $\geq 1500$  mm (thick black),  $\geq 1000$  (black),  $\geq 600$  (thick grey),  $\geq 400$  (grey)  
4 and  $< 400$  mm (light grey).

5

6 **Figure 2.** Daily DWF profiles per person for Loenen and Waalre.

7

8 **Figure 3.** The three simplified models M1-M3 convert the three inputs to two discharges to the  
9 surface water ( $Q_{SW}$ ) and the WWTP ( $Q_{WWTP}$ ). RRO: rainfall runoff outflow, SR: static reservoir,  
10 DR: dynamic reservoir.

11

12 **Figure 4.** The output of the RRO model is split into  $Q_{SW}$  and  $Q_{WWTP}$  based on the maximum  
13 pumping capacity of the catchment ( $209 \text{ m}^3/\text{h}$  for Loenen).

14

15 **Figure 5.** Schematic representation of the SR model for Loenen. Applied characteristics or  
16 relationships as displayed in graphs SR1-SR3 are elaborated upon in the main text.

17

18 **Figure 6.** Schematic representation of the SR model for Waalre. Applied characteristics or  
19 relationships as displayed in graphs SR4-SR10 are elaborated upon in the main text.

20

21 **Figure 7.** Schematic representation of the DR model for Loenen. Applied characteristics or  
22 relationships as displayed in graphs DR1-DR4 are elaborated upon in the main text.

23

24 **Figure 8.** Hybrid storage-level curve (left) and derivation of the dynamic storage-level curve  
25 from the FH model simulation results (right) for Loenen.

26

27 **Figure 9.** Schematic representation of the DR model for Waalre. Applied characteristics or  
28 relationships as displayed in graphs DR5-DR13 are elaborated upon in the main text.

29

30 **Figure 10.** Hybrid storage-level curve (left) and derivation of the dynamic storage-level curve  
31 from the FH model simulation results (right) for Waalre.

32

33 **Figure 11.** Results for the individual calibration of rain event 2001-08-27 for all model  
34 structures for Loenen.

35

36 **Figure 12.** Results for the individual calibration of rain event 2011-08-14 for all model  
37 structures for Waalre.

38

39 **Figure 13.** Optimal parameter values for scenarios 1 (individual calibrated events (asterisks))  
40 and scenario 2 (all events together (line)) for Loenen (left) and Waalre (right). The horizontal  
41 axis presents event numbers. Please note the changing scale for  $T_{lag}$  and  $K$ .

42

43 **Figure 14.** Optimal parameter values for scenario 3 for Loenen (left) and Waalre (right). The  
44 horizontal axis presents the 20 possible combinations to take 3 events from 6. Please note the  
45 changing scale for  $T_{lag}$  and  $K$ .

46

47 **Figure 15.**  $Q_{SW}$  and  $Q_{WWTP}$  for the individually calibrated event of 2001-08-27 for Loenen.

48

49 **Figure 16.**  $Q_{SW}$  and  $Q_{WWTP}$  for the individually calibrated event of 2011-08-14 for Waalre.

50



51 **Figure 17.**  $V_{sw}$  with 95% confidence bands for all events and each model structure for Loenen.  
52 For scenarios 1 (individual events, top) and 2 (all events together, bottom). The horizontal axis  
53 presents event numbers.

54

55 **Figure 18.**  $V_{sw}$  with 95% confidence bands for all events and each model structure for Waalre.  
56 For scenarios 1 (individual events, top) and 2 (all events together, bottom). The horizontal axis  
57 presents event numbers.

**Figure 1 - left**

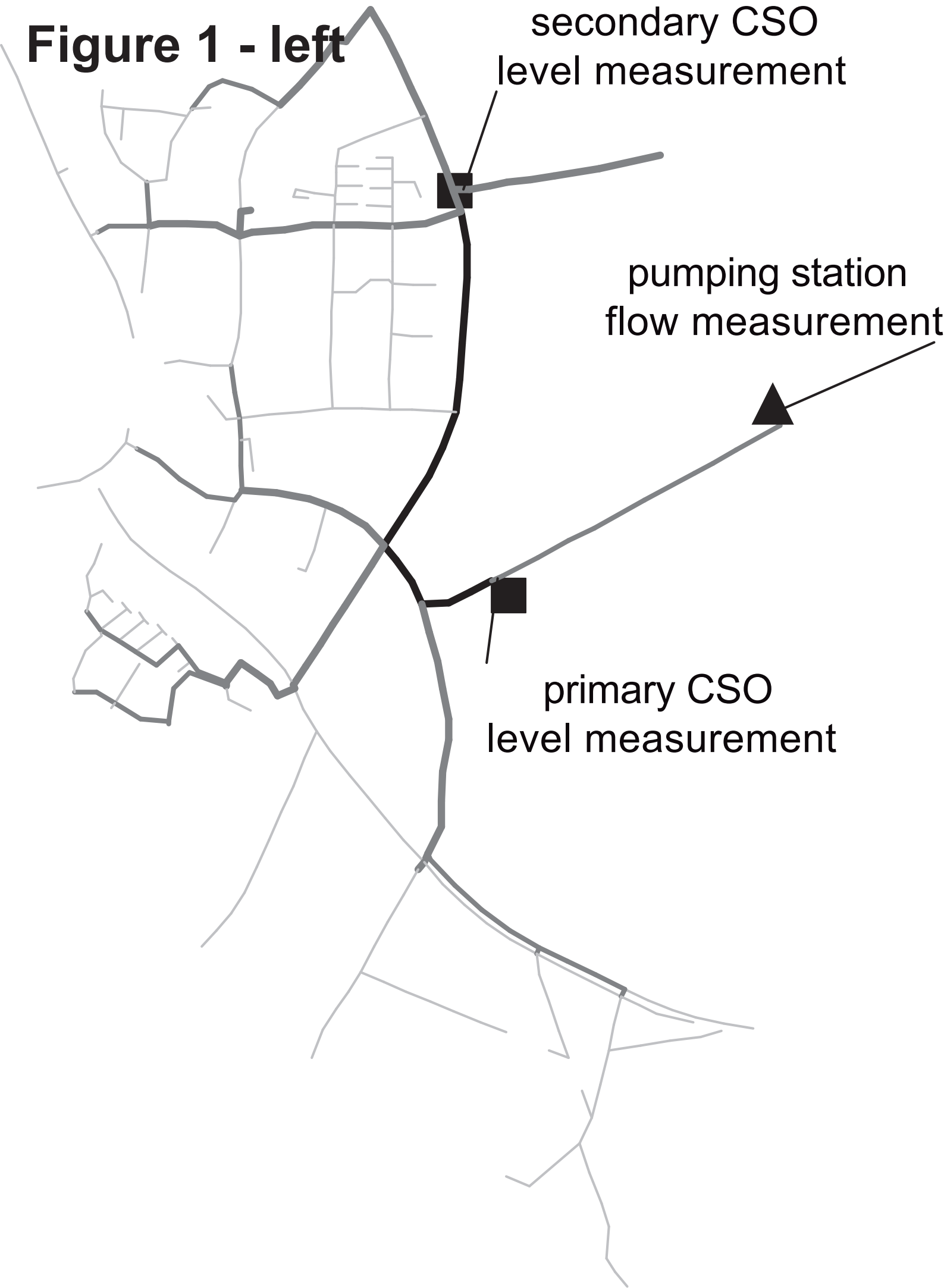


**Figure 1 - right**

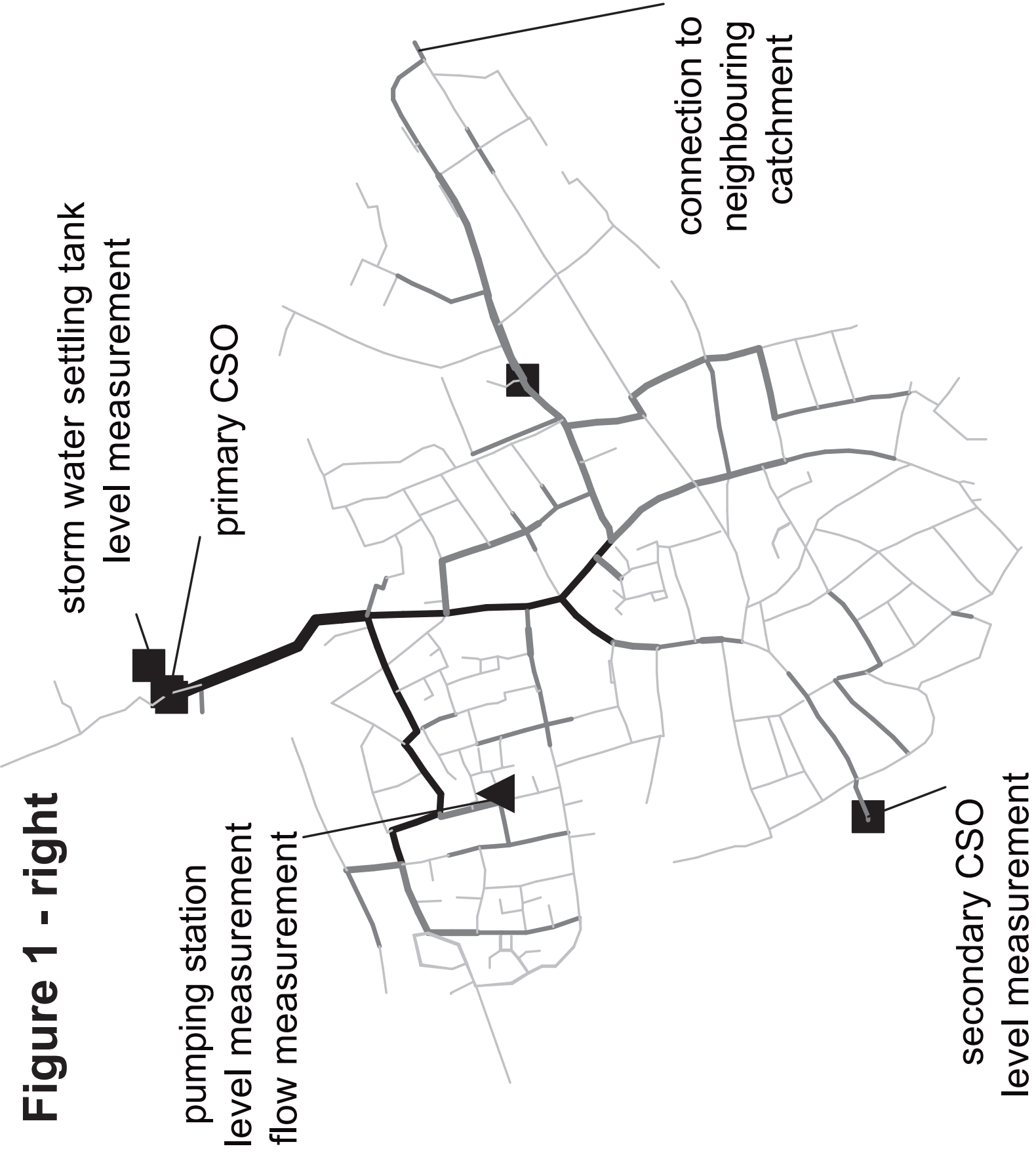


Figure 2

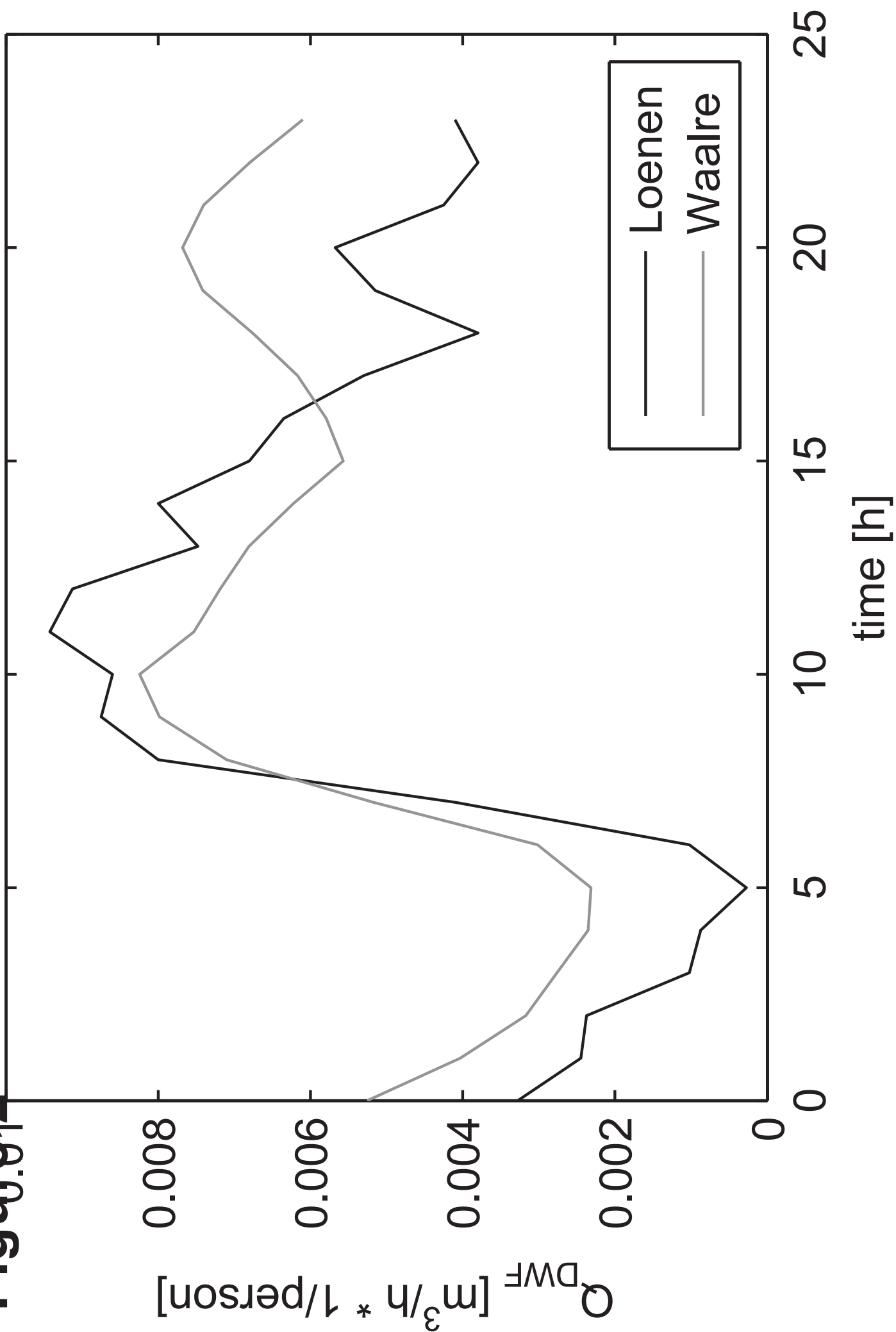
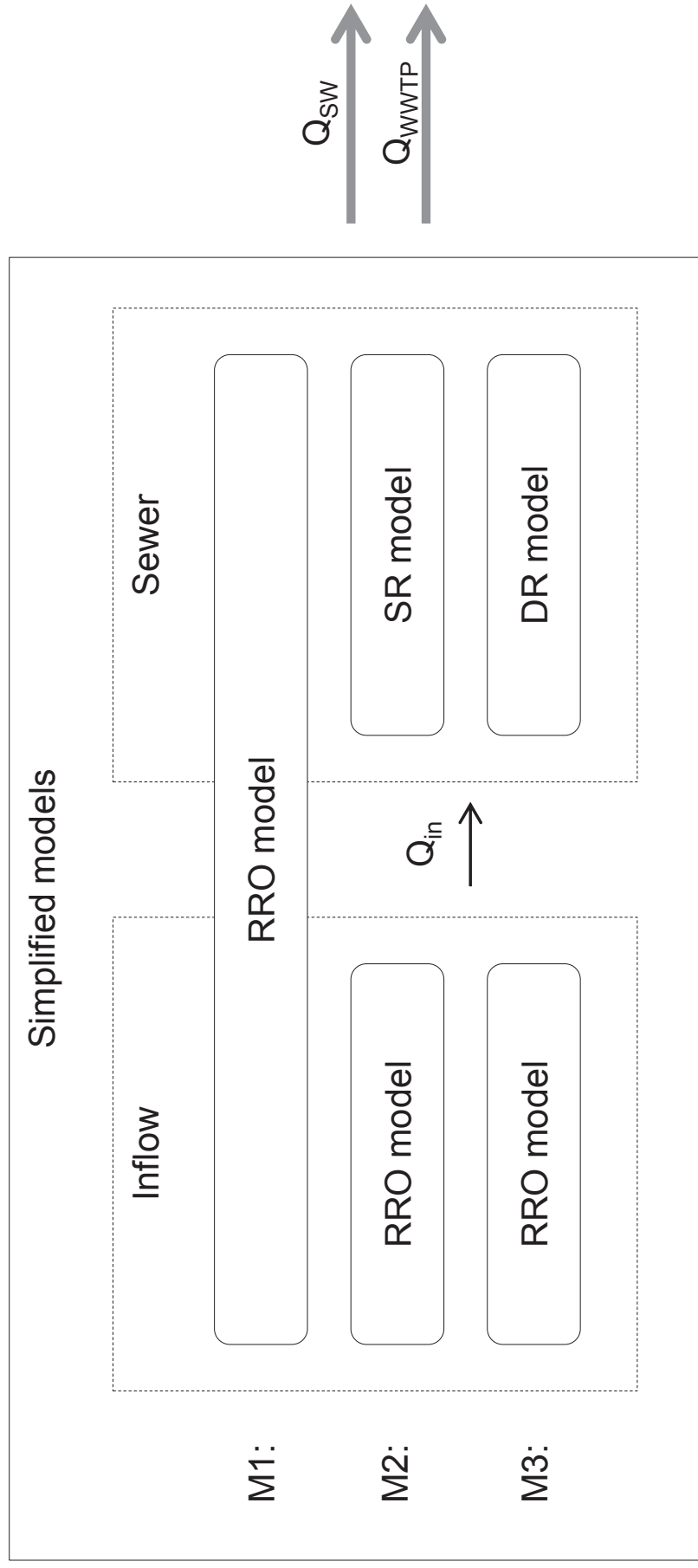


Figure 3



**Figure 4**

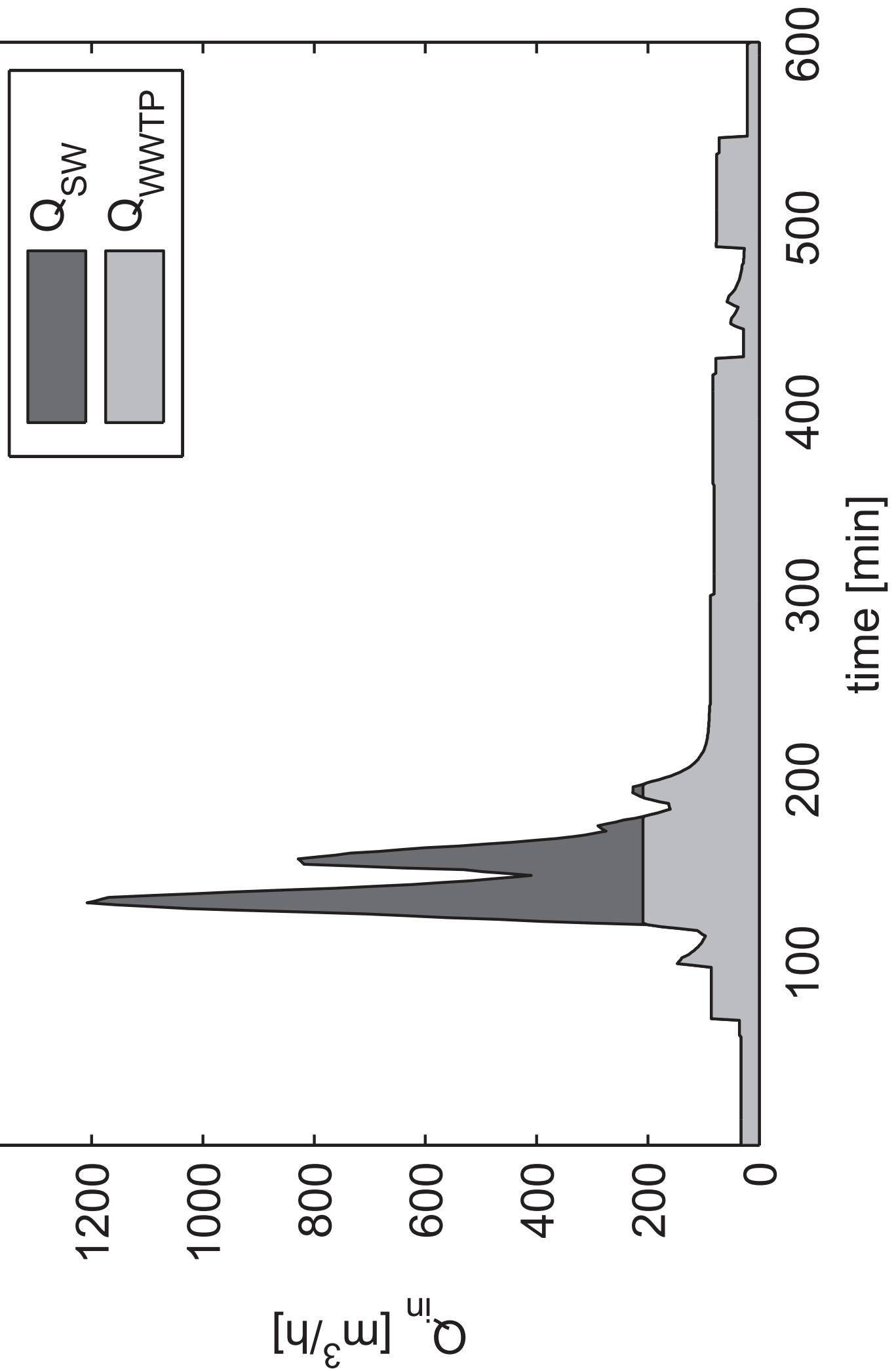
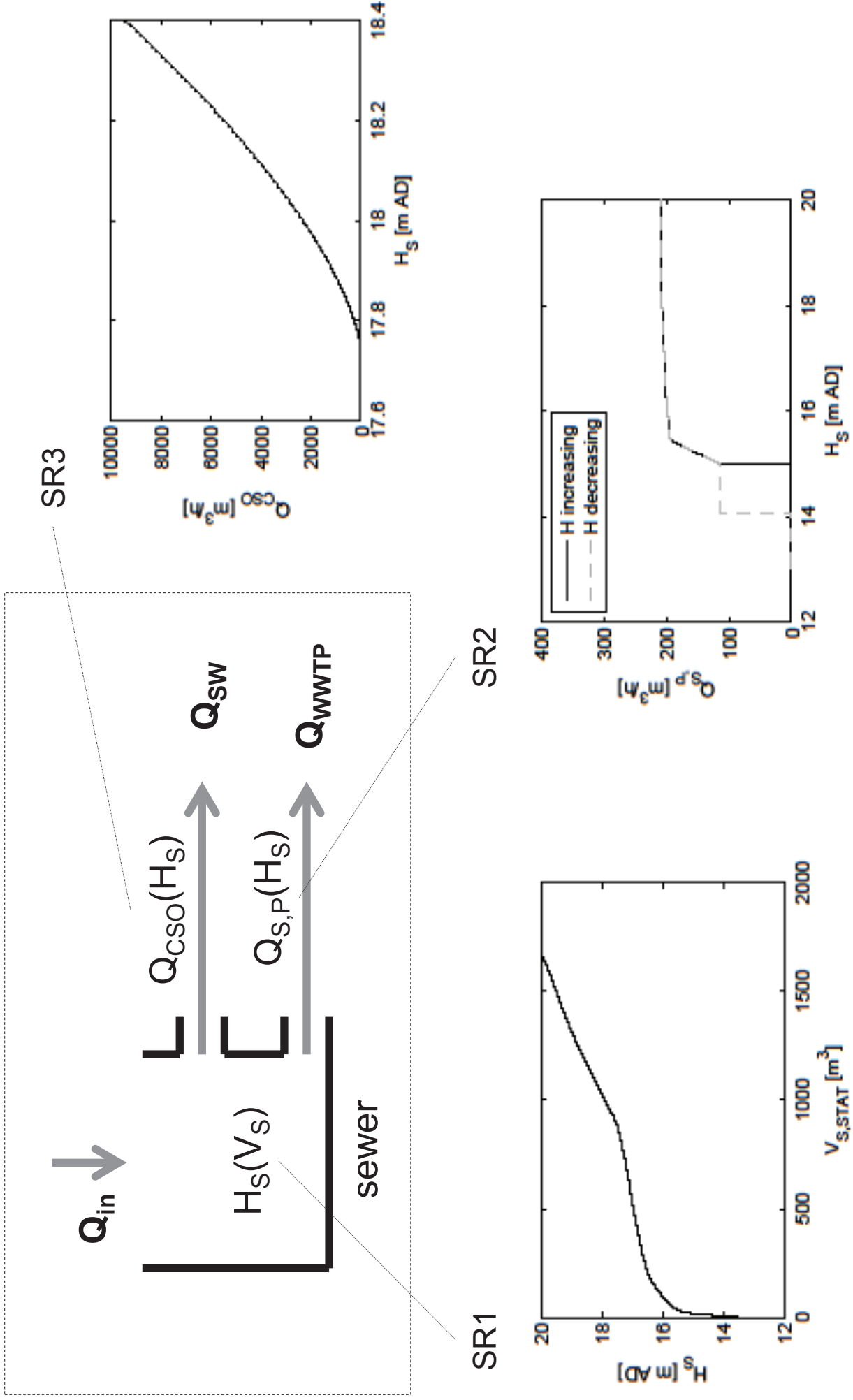


Figure 5 - total SR model Loenen with graphs SR1-SR3



**Figure 5 - high res SR1**

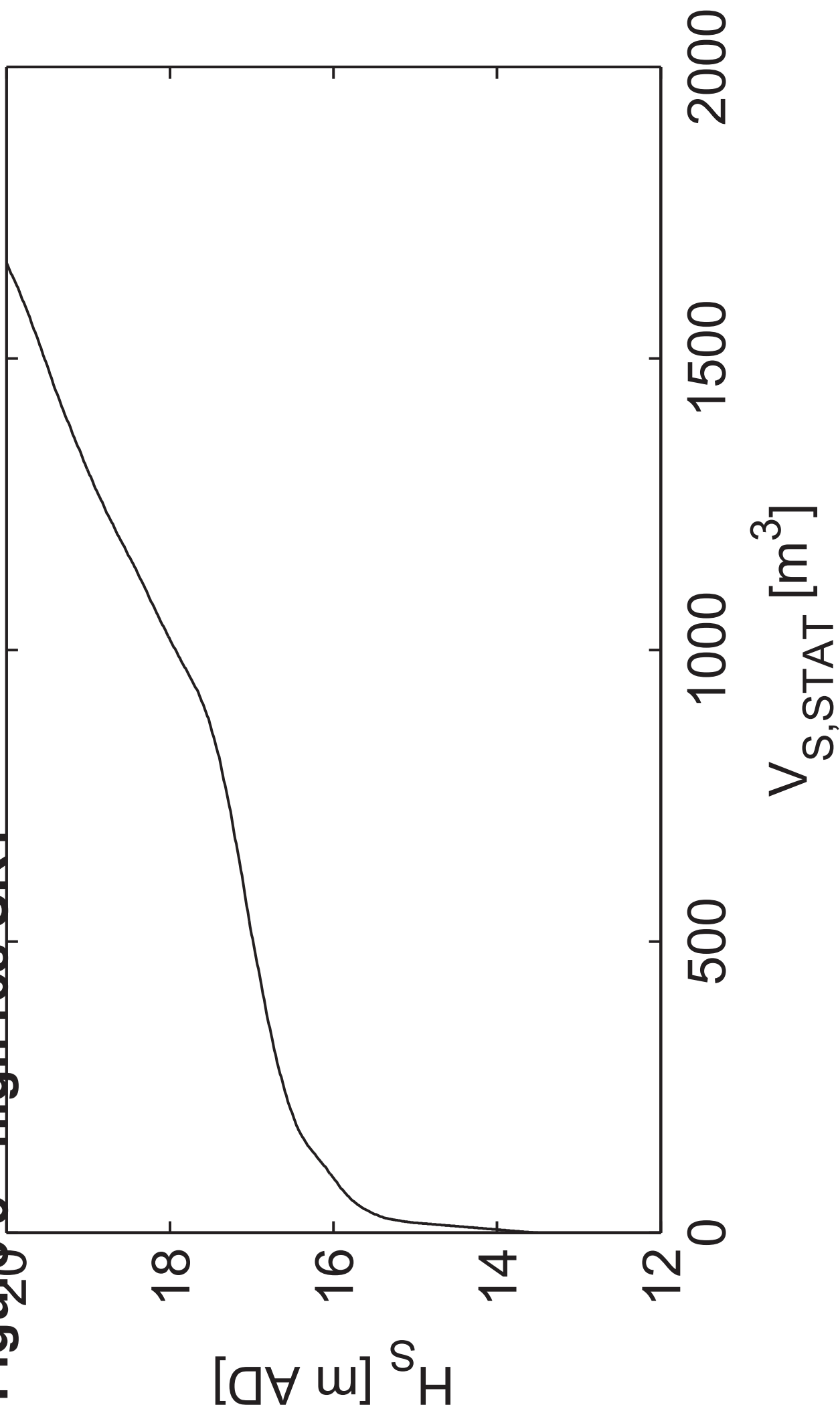
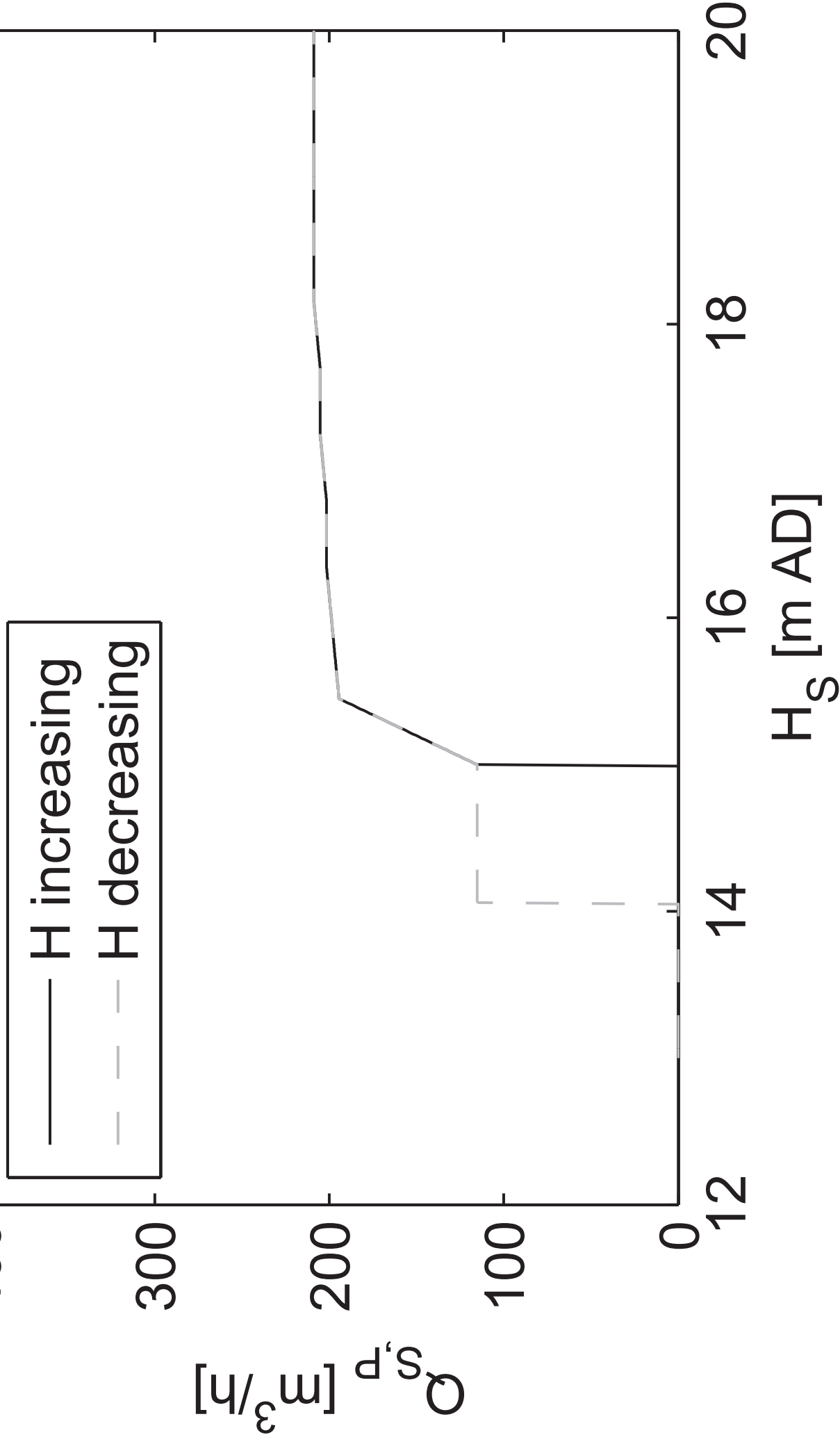




Figure 5 - high res SR2



**Figure 500 high res SR3**

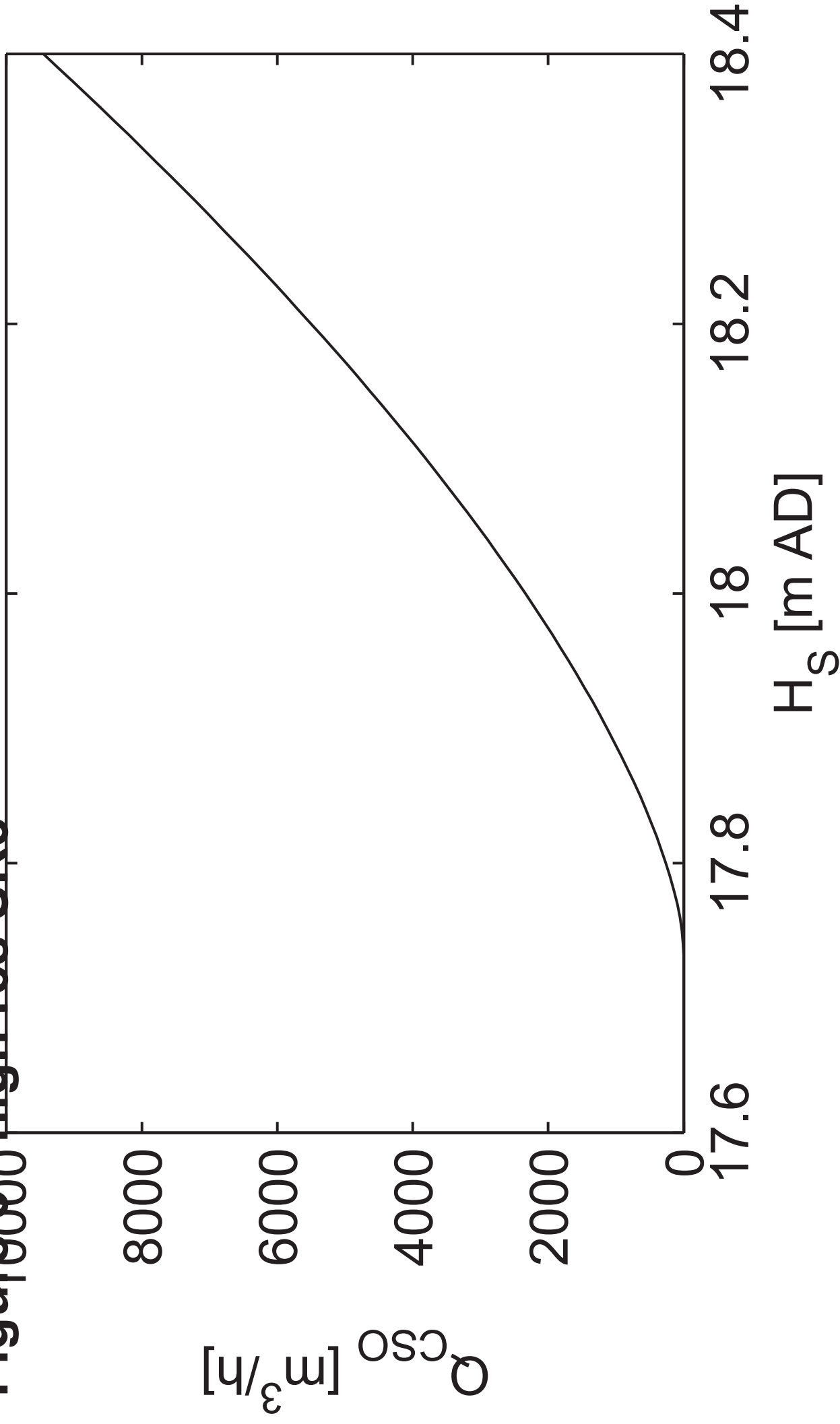
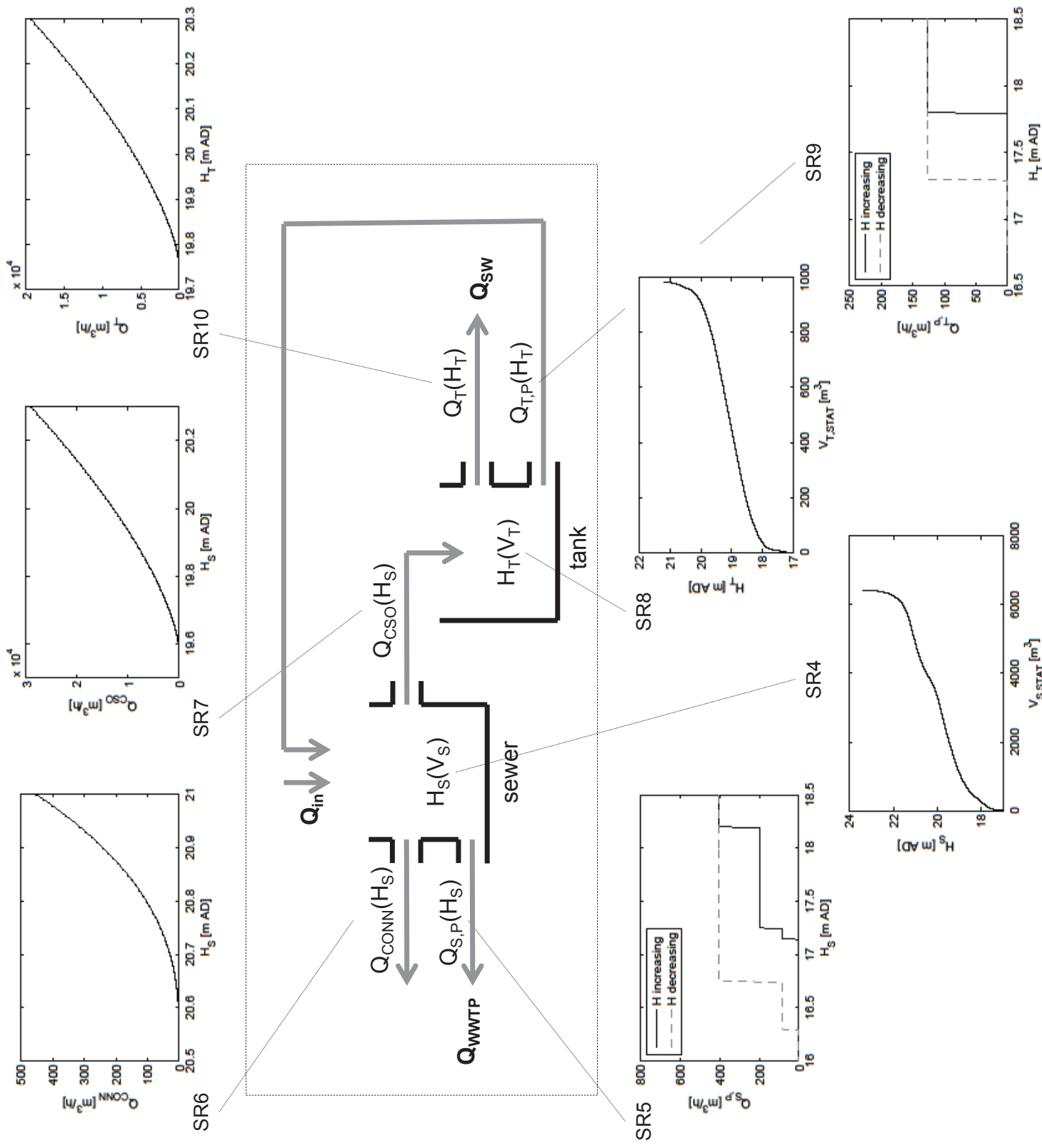
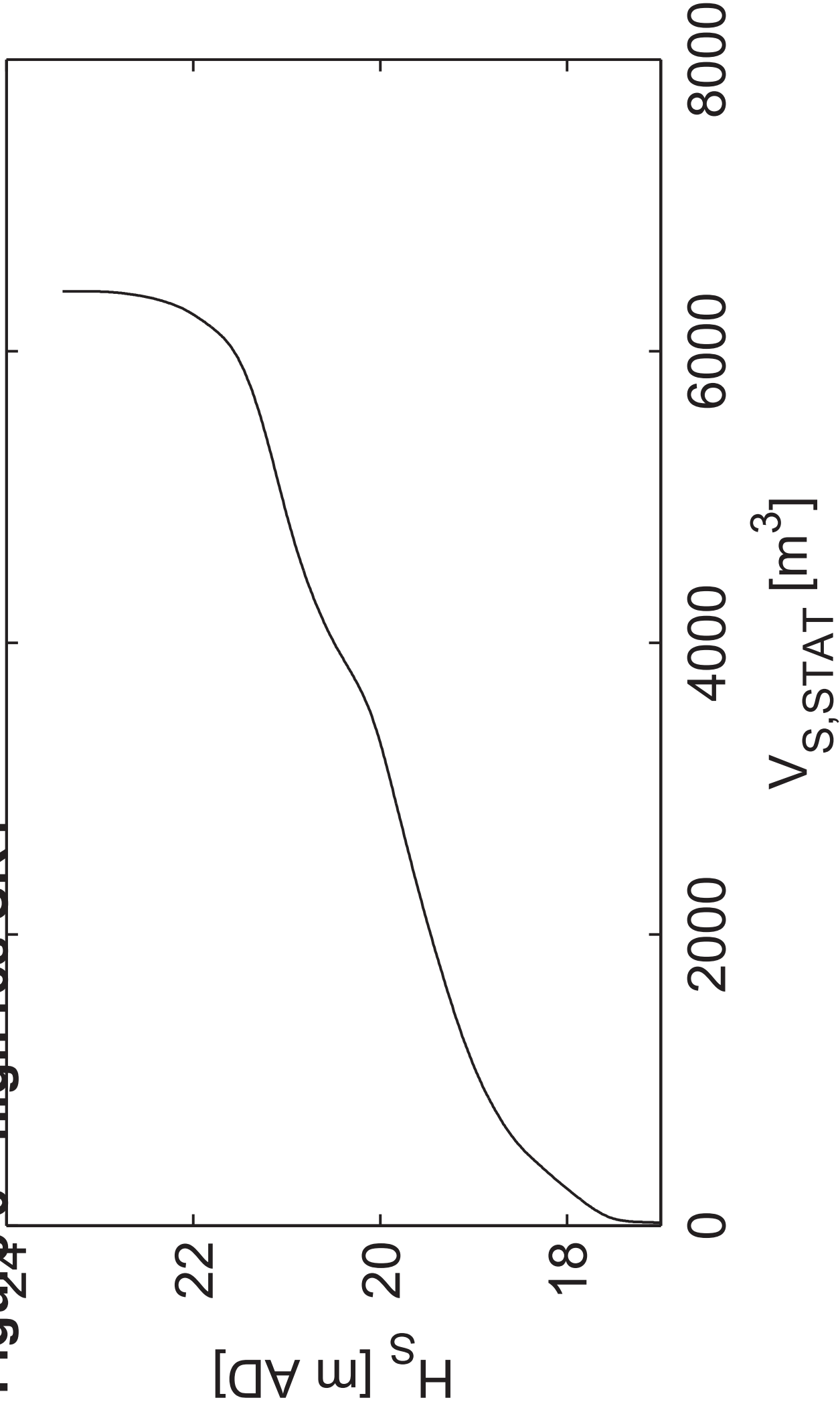


Figure 6 - total SR model Waalre with graphs SR4-SR10



**Figure 6 - high res SR4**



**Figure 6 - high res SR5**

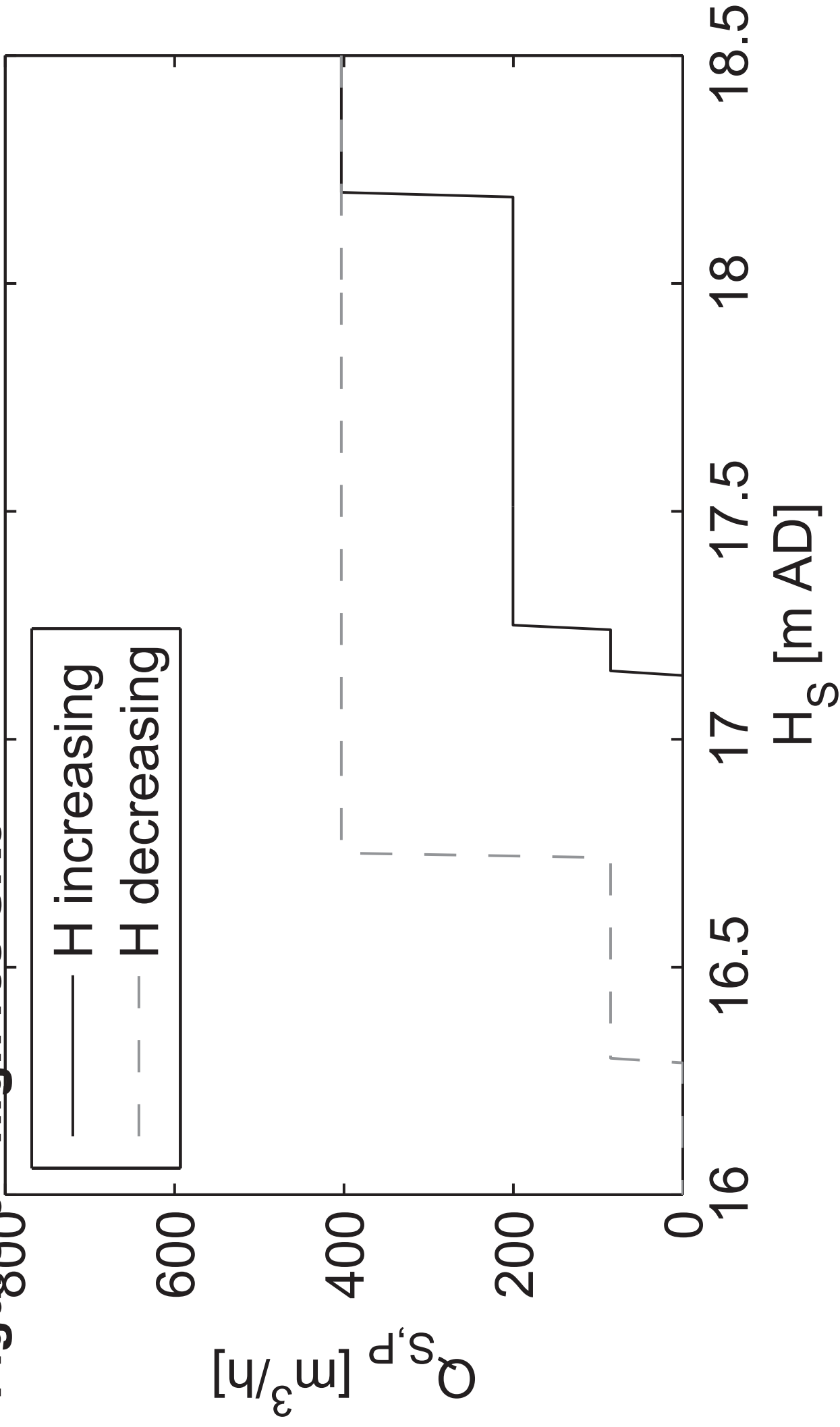


Figure 6 - high res SR6

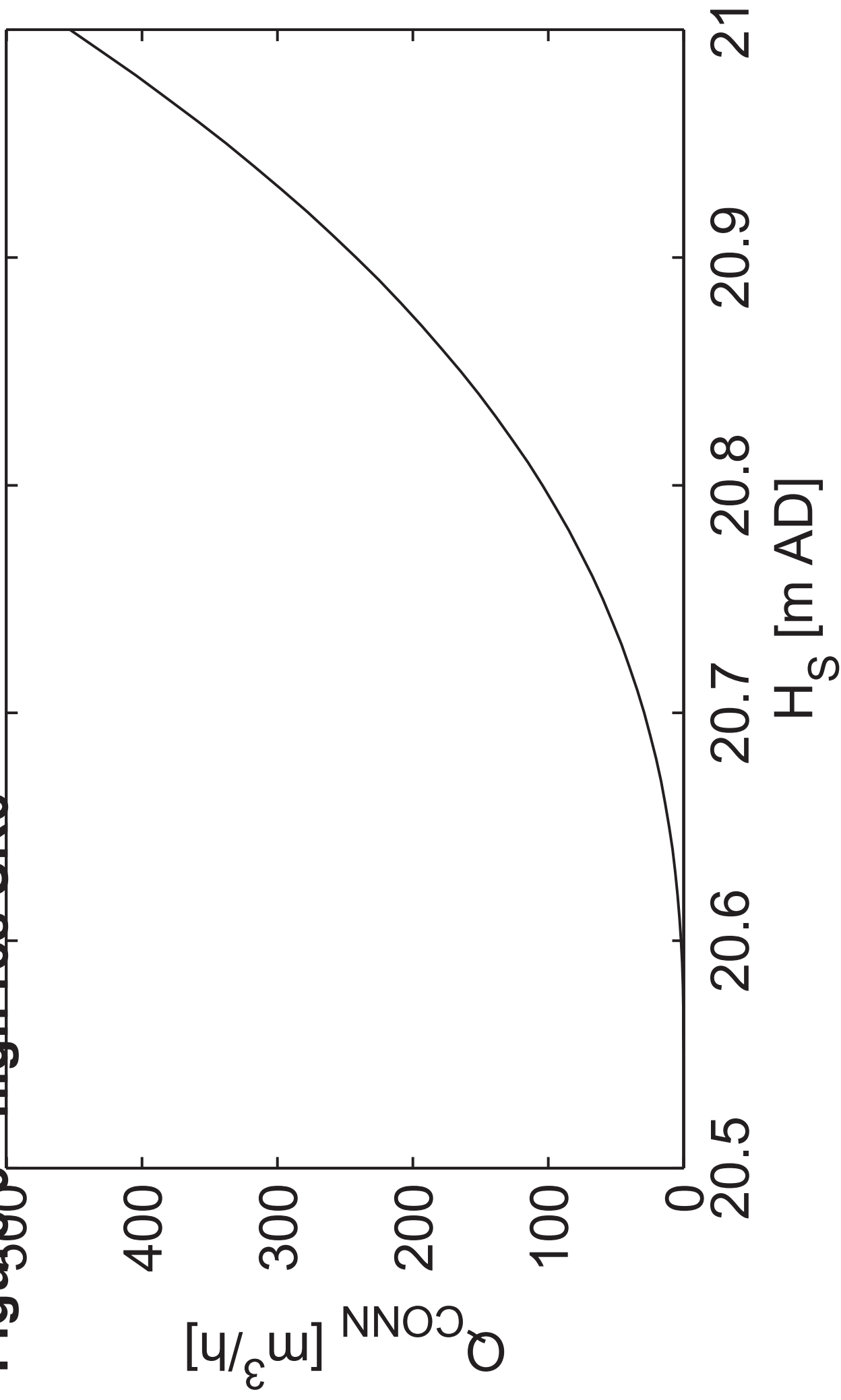
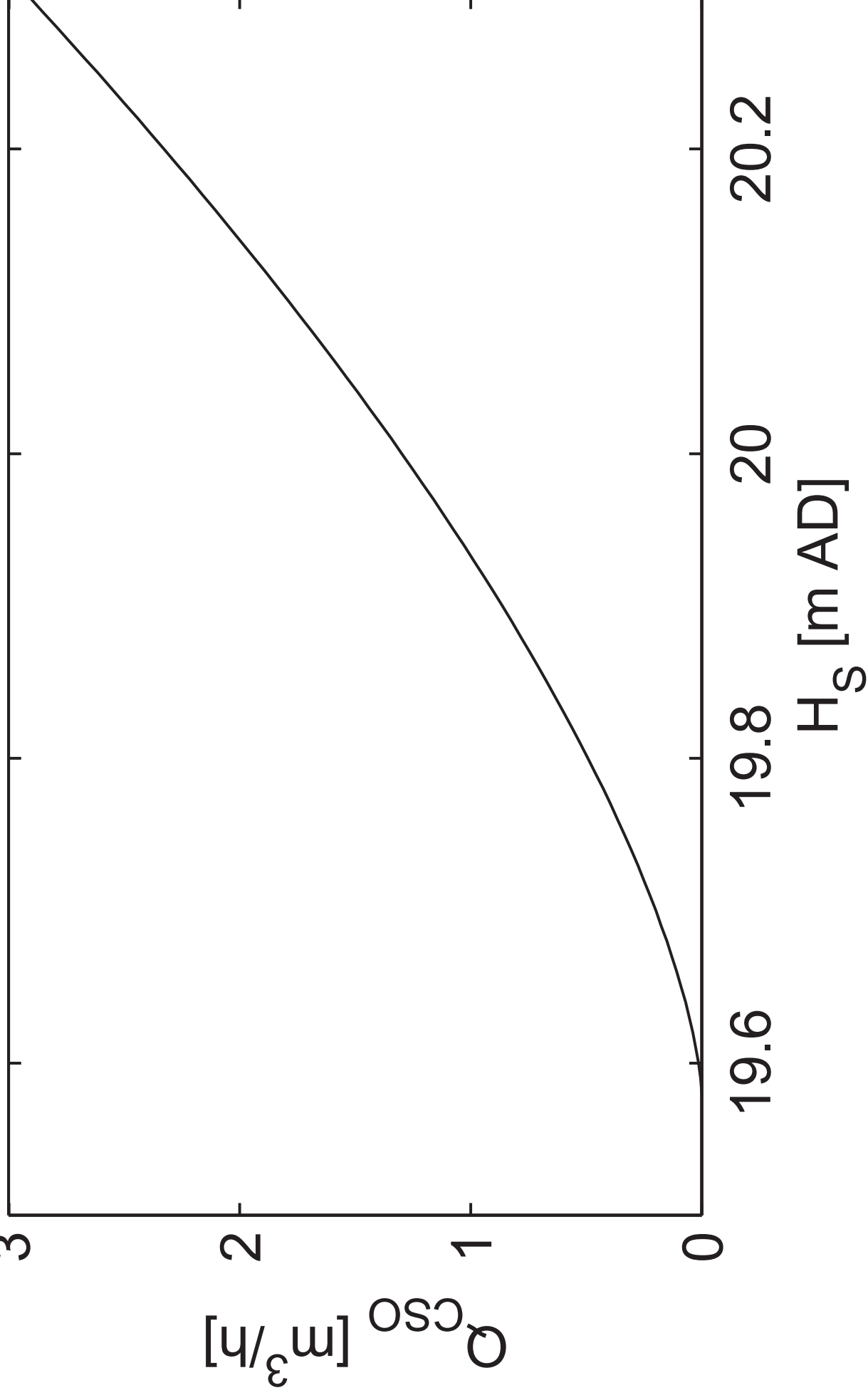
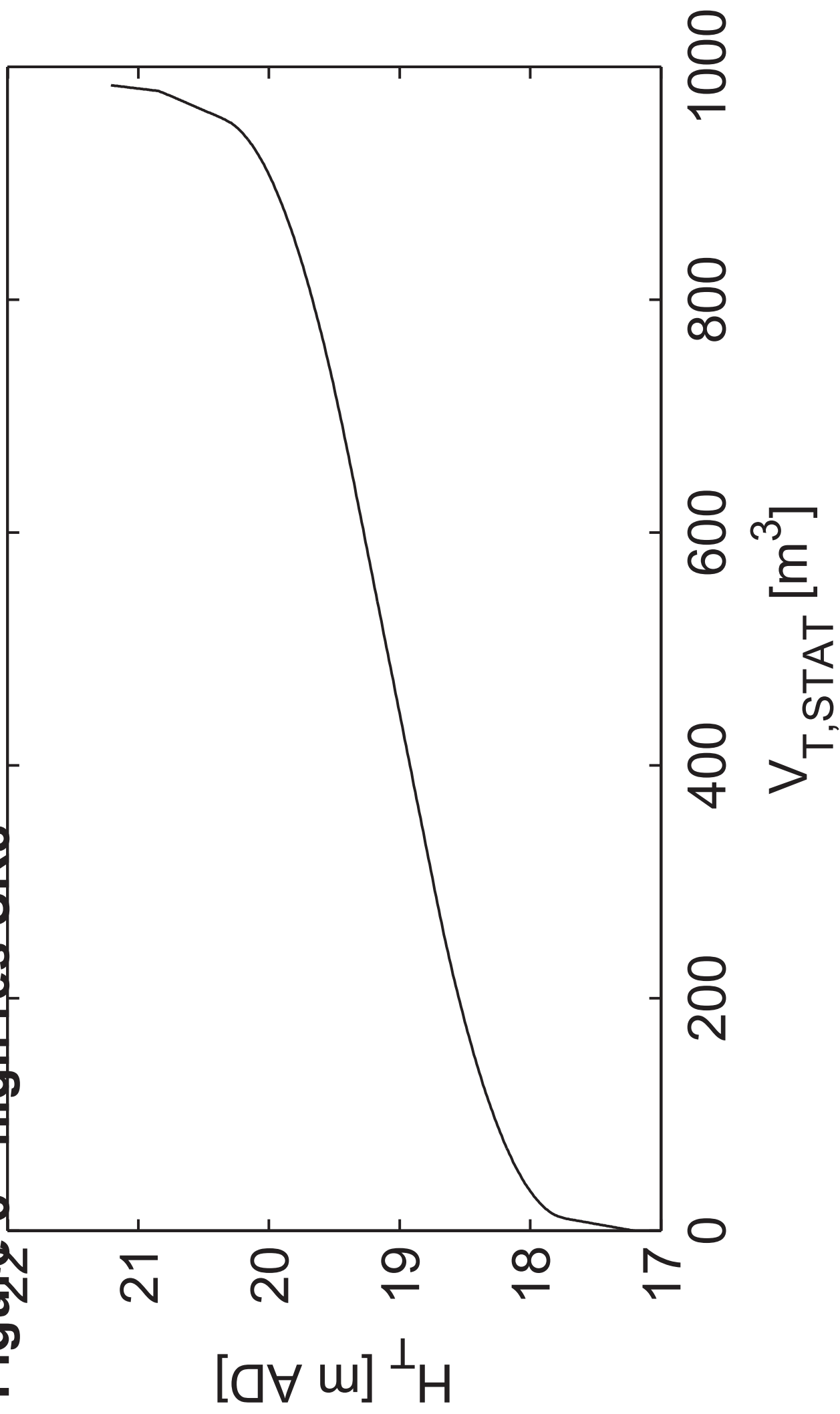


Figure 6-10<sup>4</sup> high res SR7



**Figure 6 - high res SR8**





**Figure 506 - high res SR9**

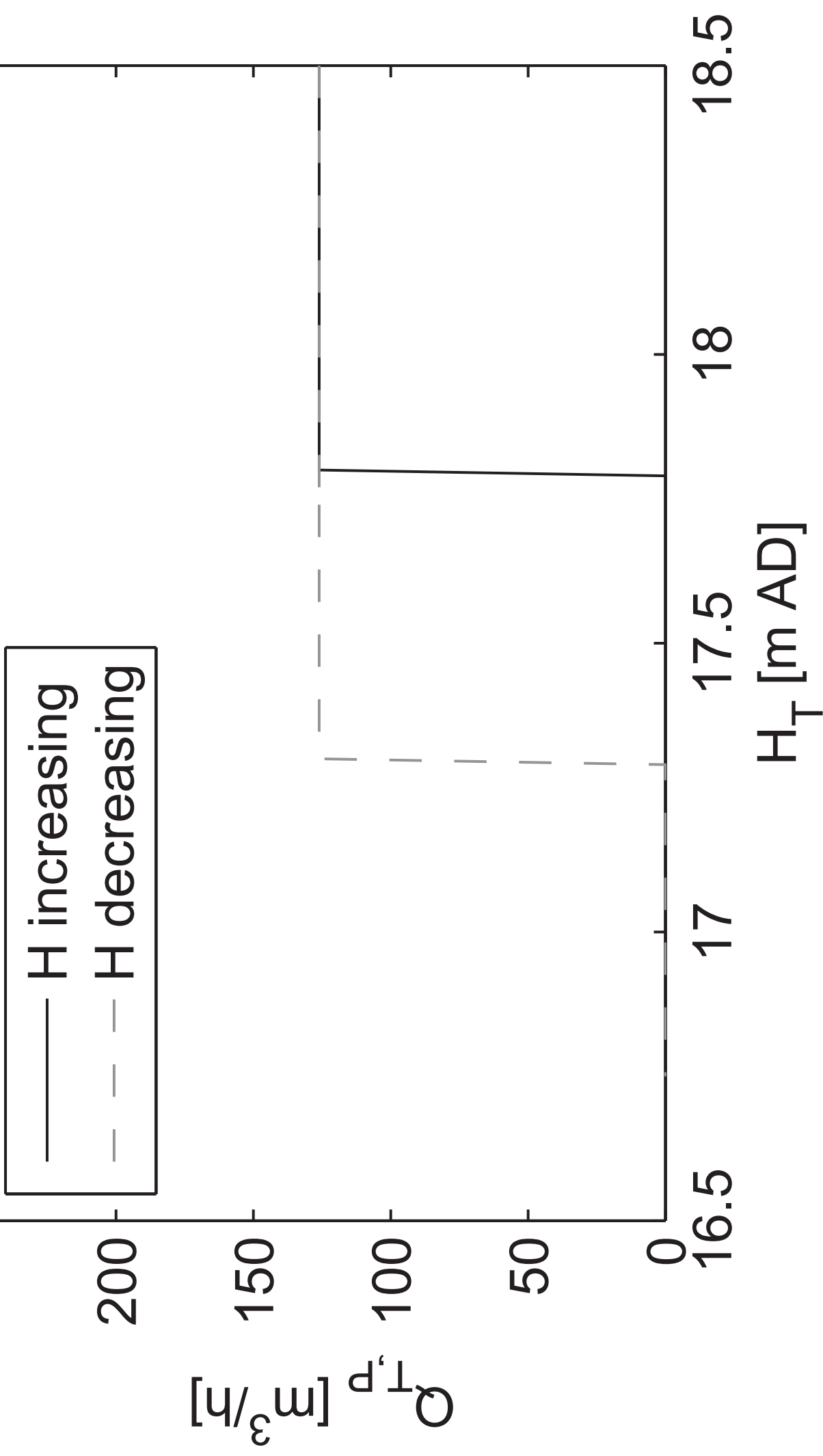


Figure 6-10<sup>4</sup> High res SR10

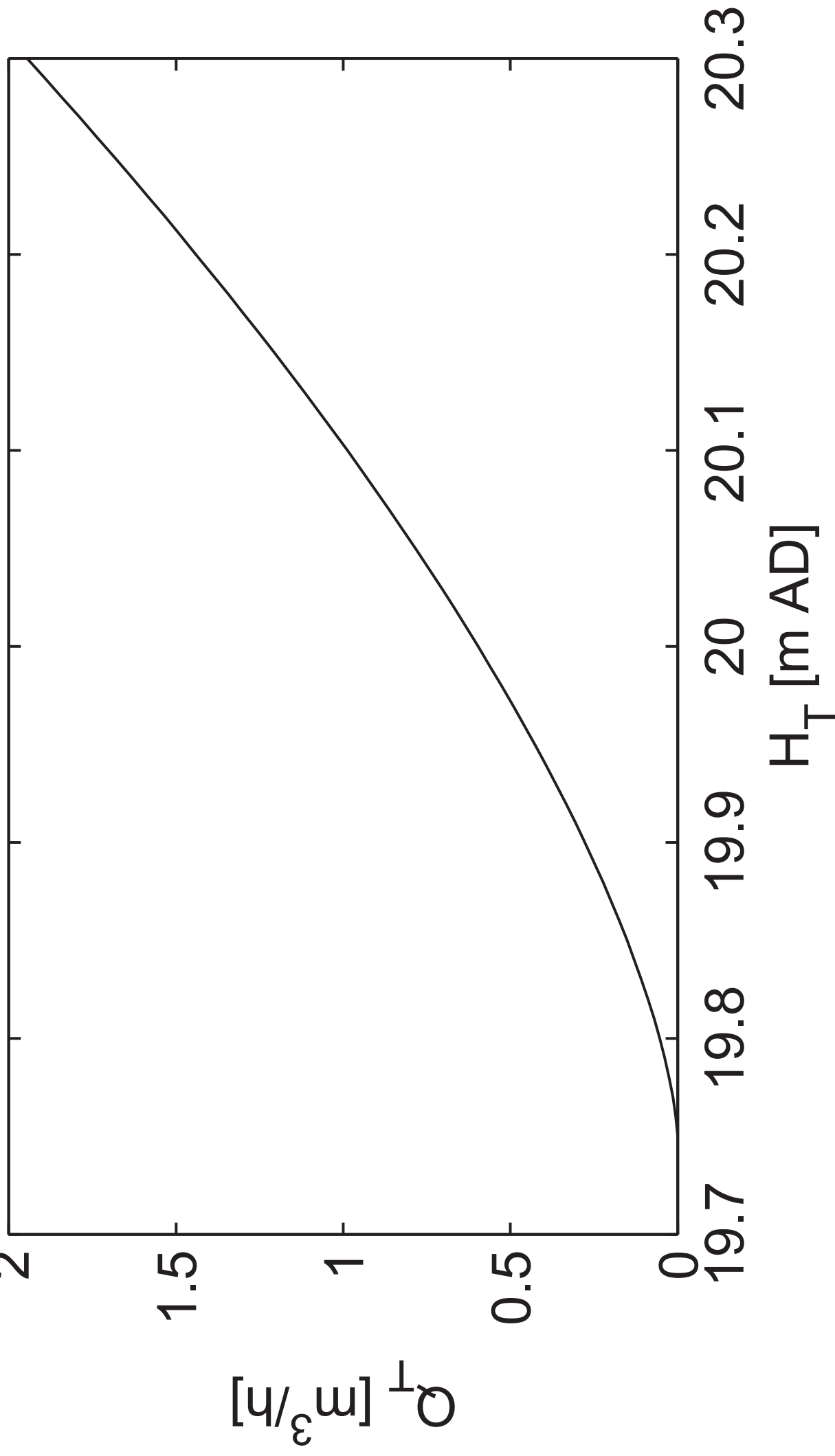


Figure 7 - total DR model Loenen with graphs DR1-DR4

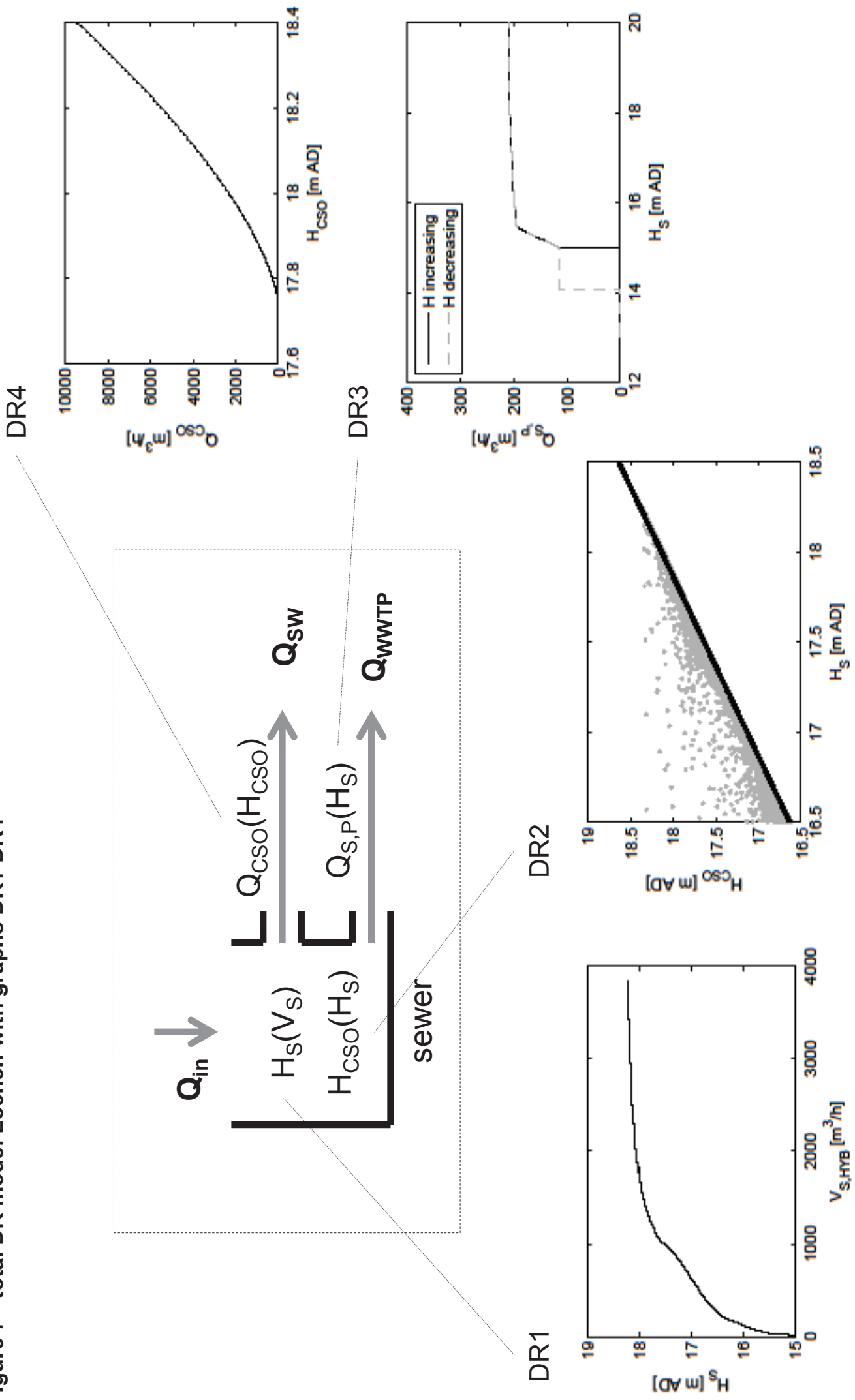


Figure 7 - high res DR1

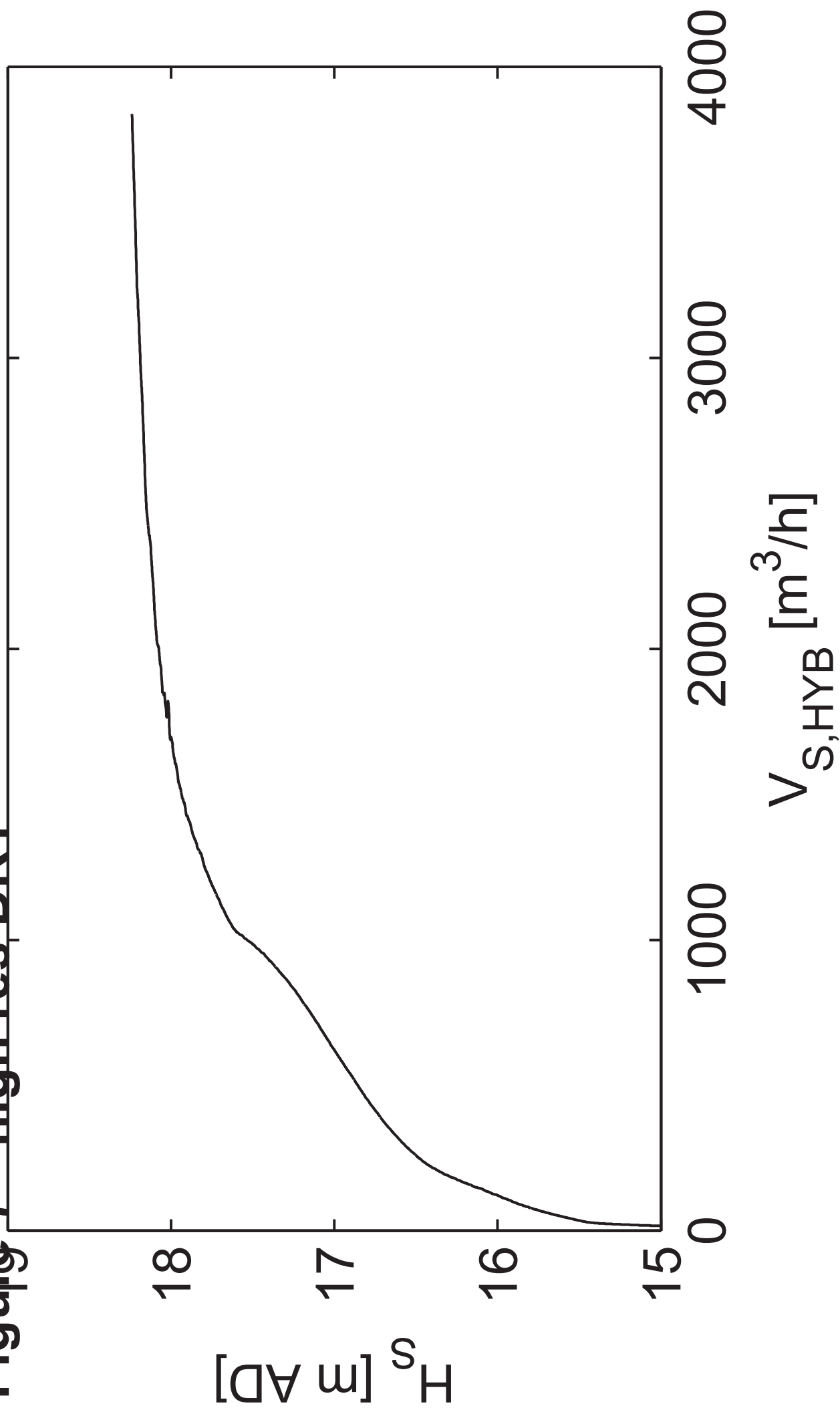


Figure 7 - high res DR2

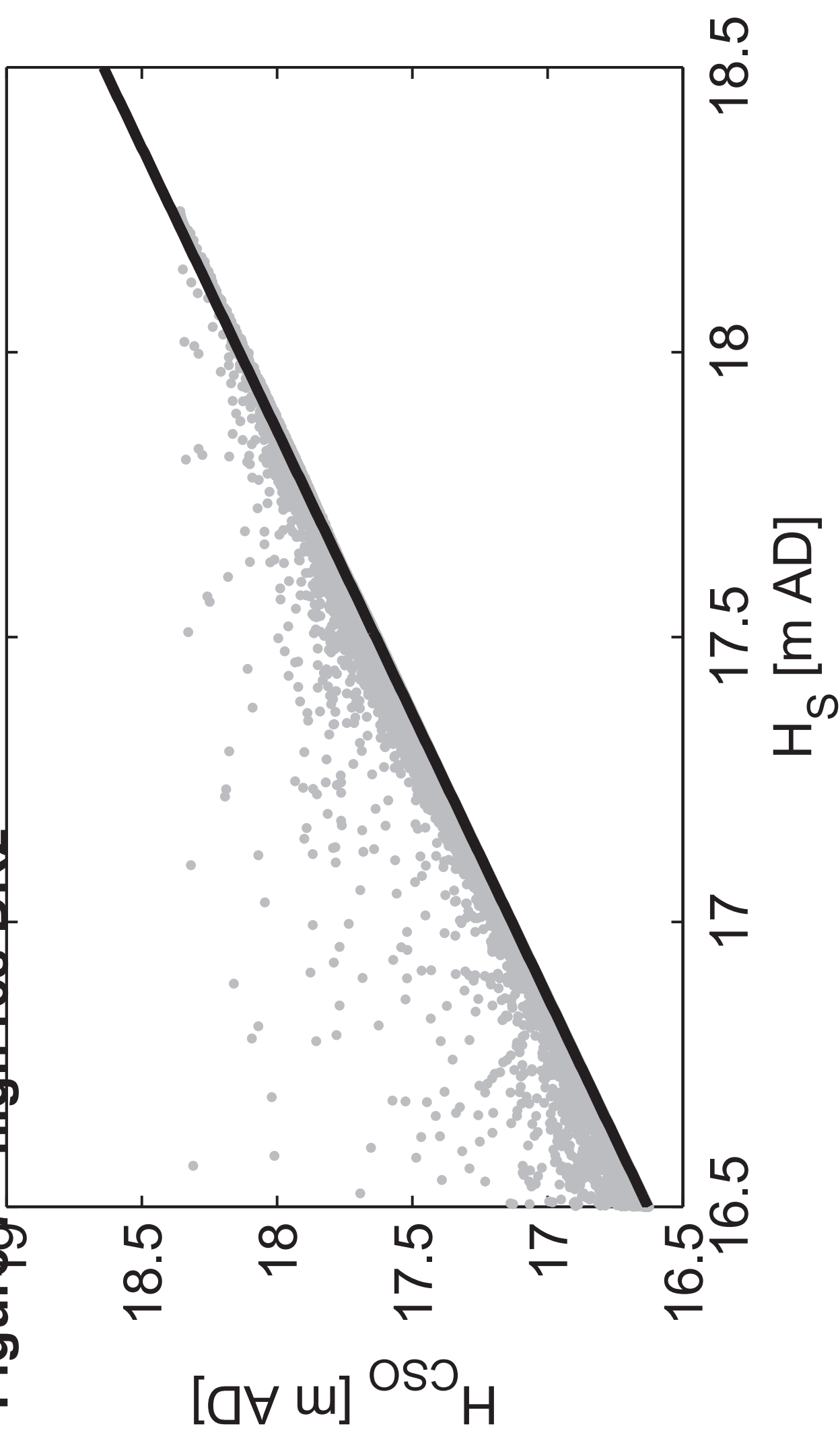
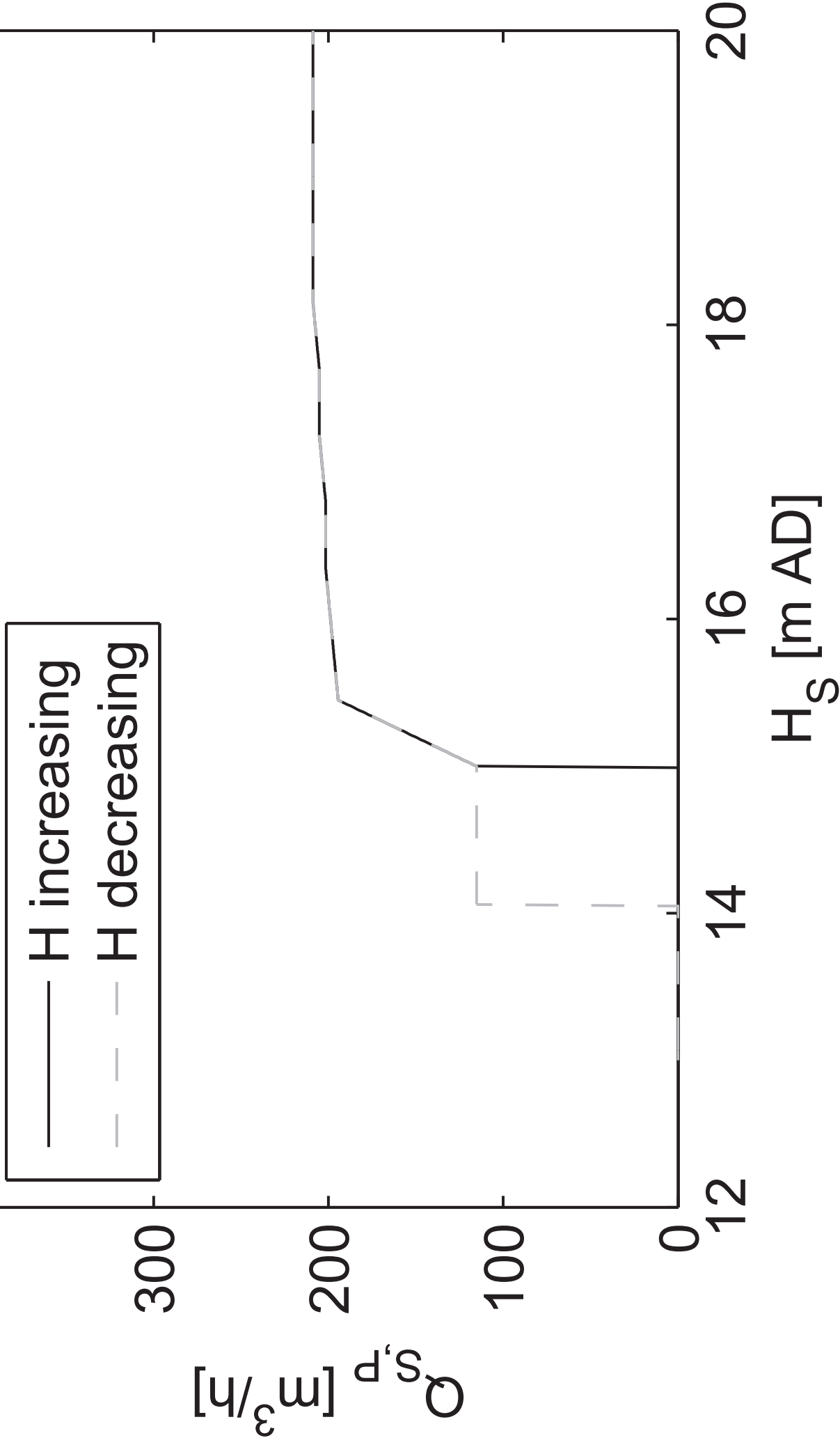


Figure 7 - high res DR3



**Figure 700 high res DR4**

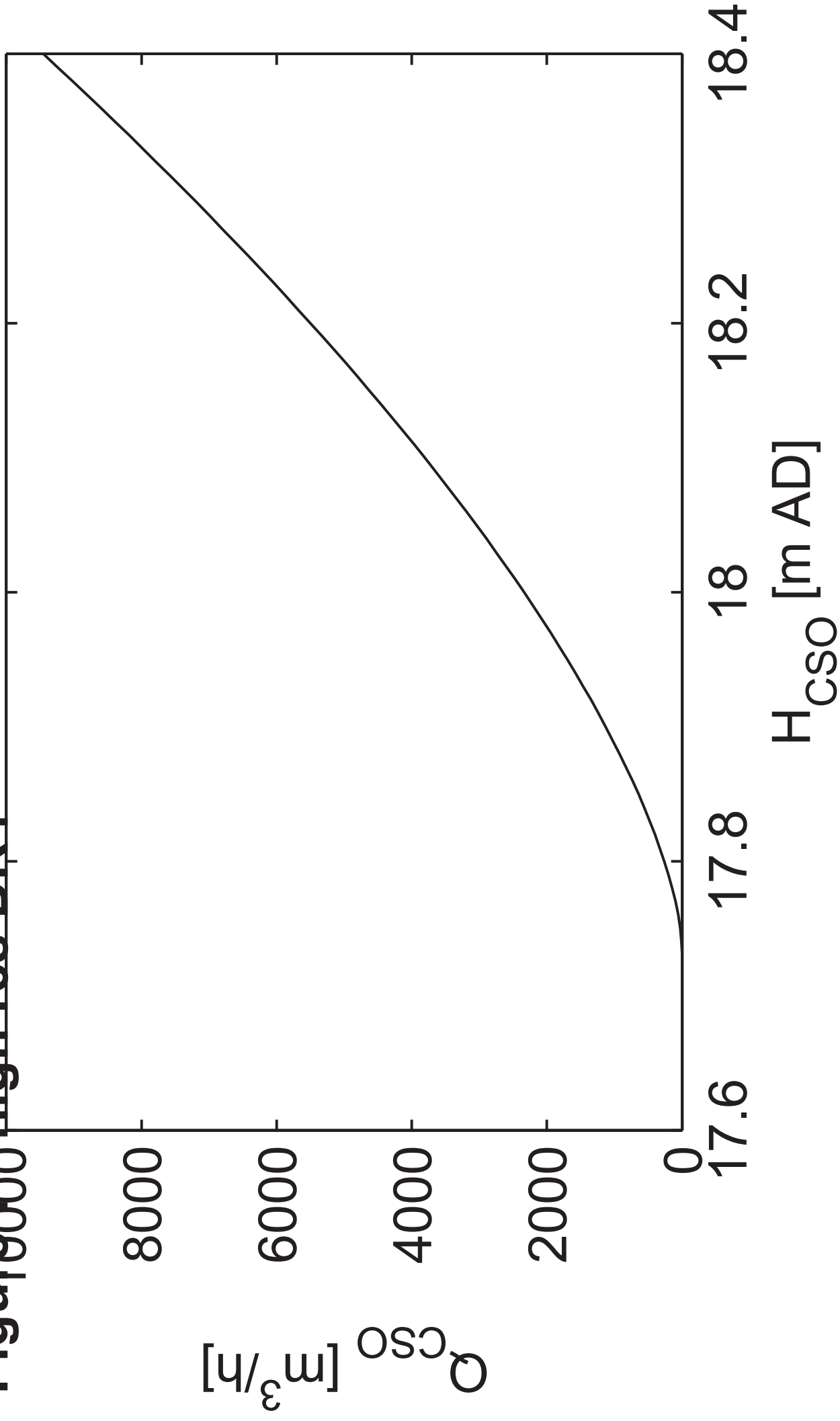
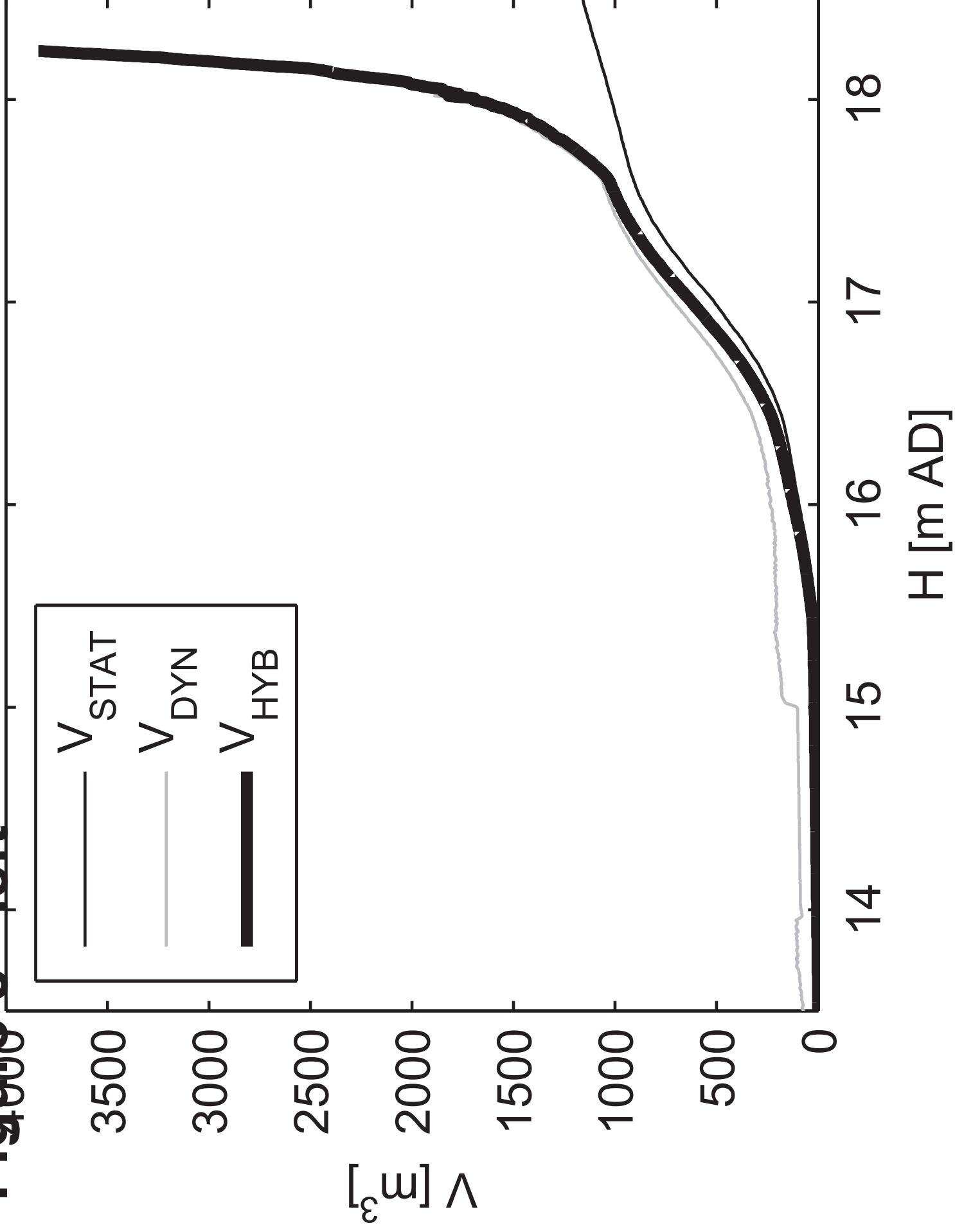


Figure 8 - left





**Figure 8 - right**

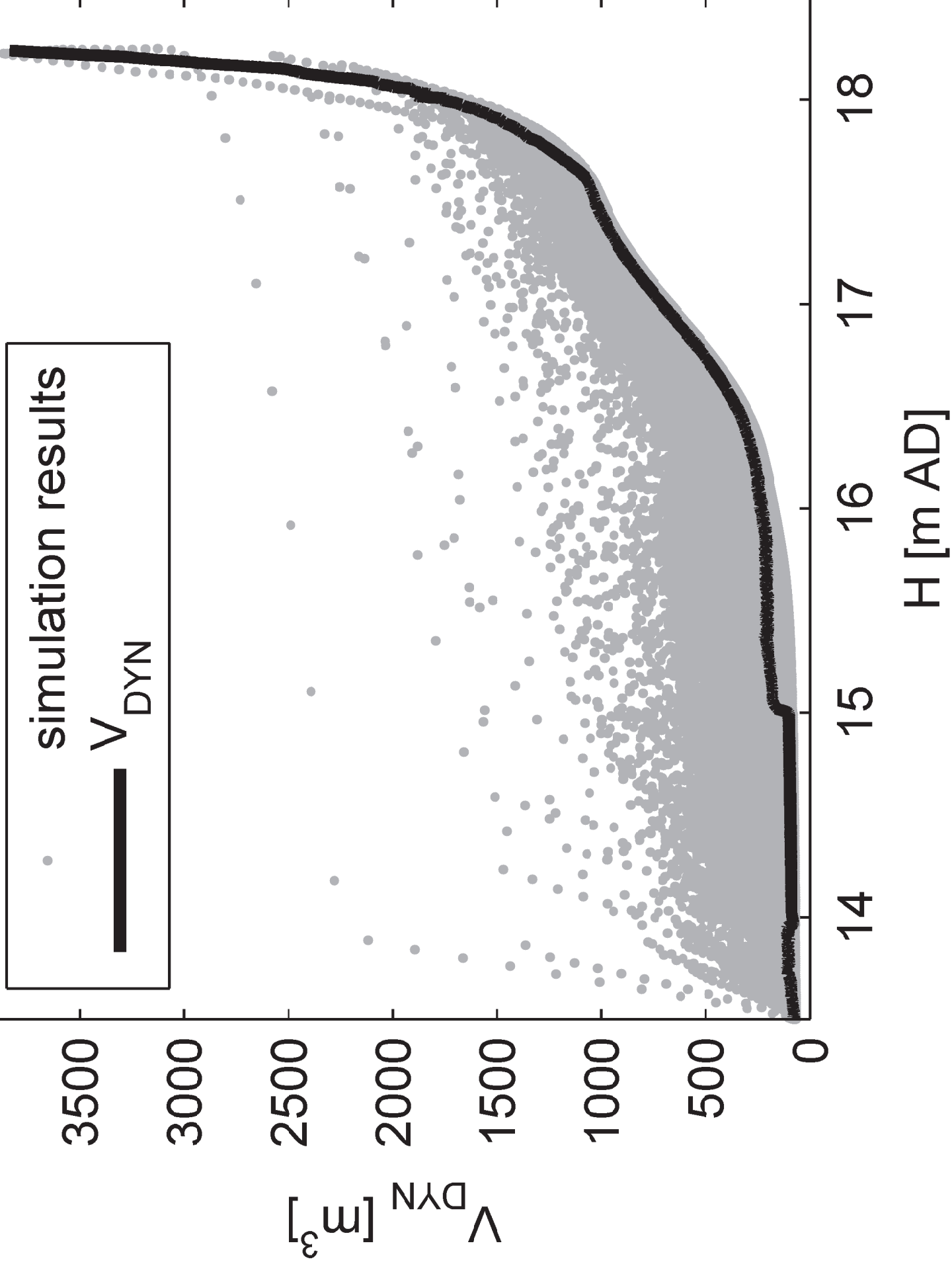


Figure 9 - total DR model Waalre with graphs DR5-DR13

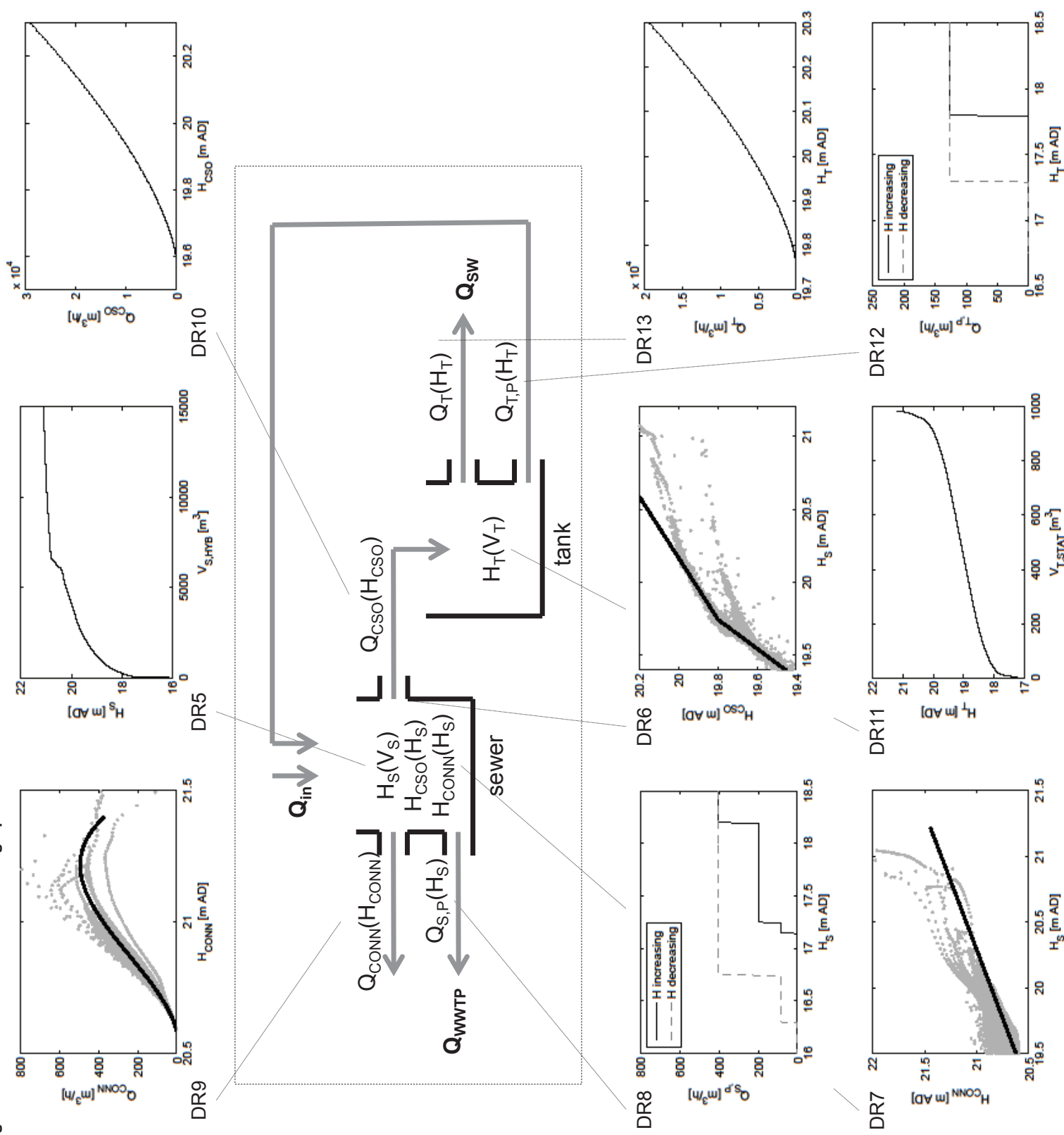


Figure 9 - high res DR5

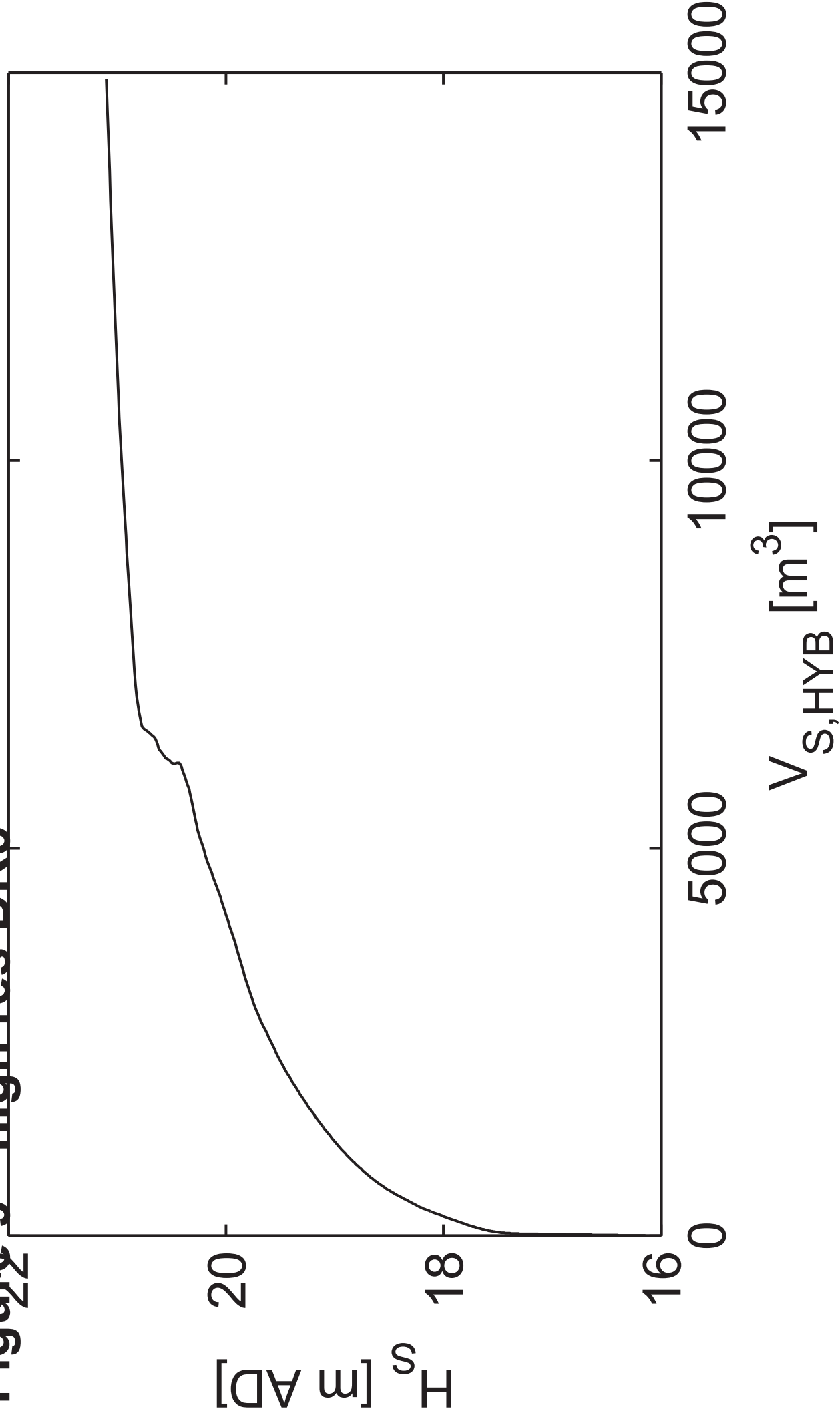


Figure 9 - high res DR6

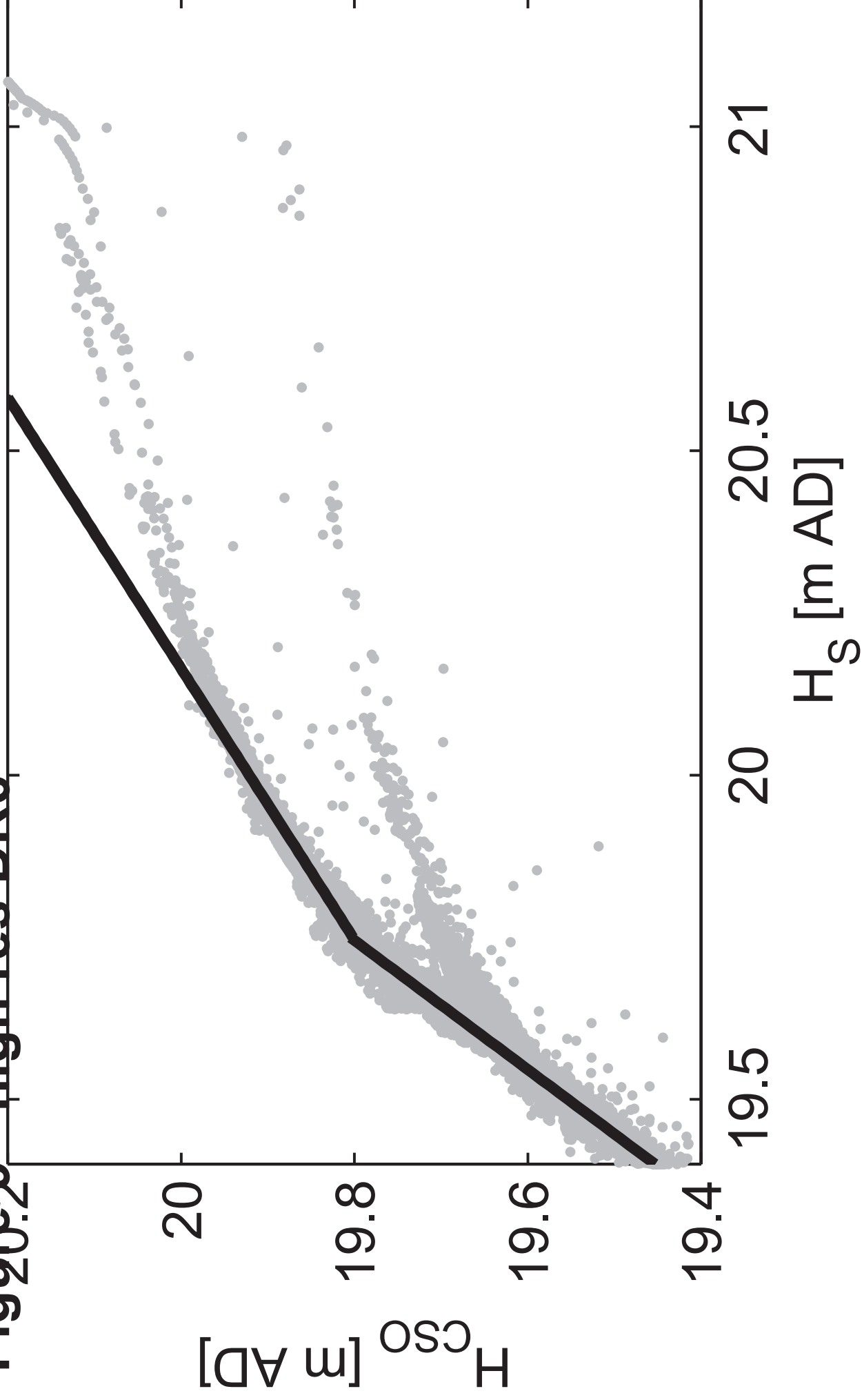


Figure 9 - high res DR7

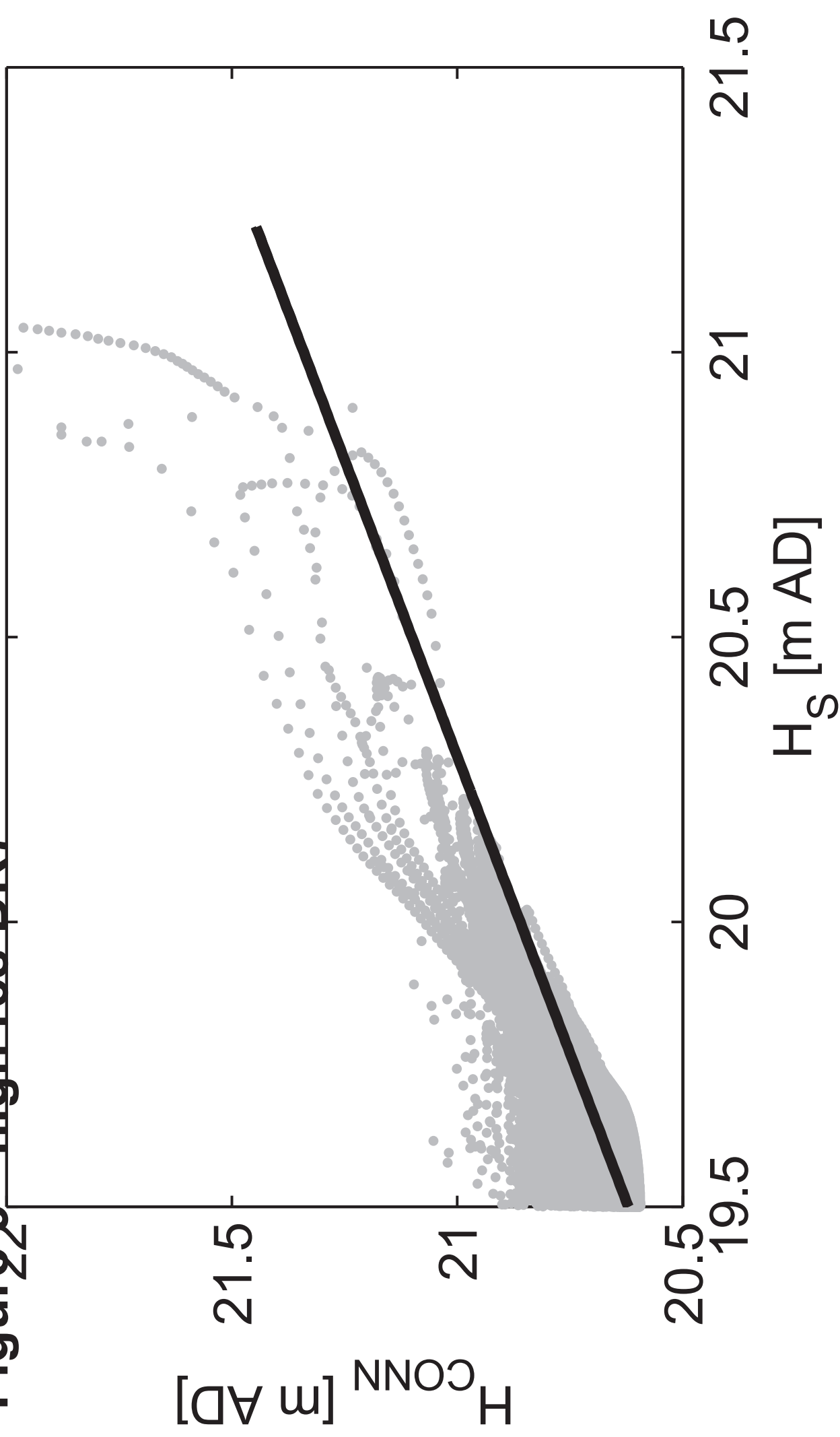


Figure 9 - high res DR8

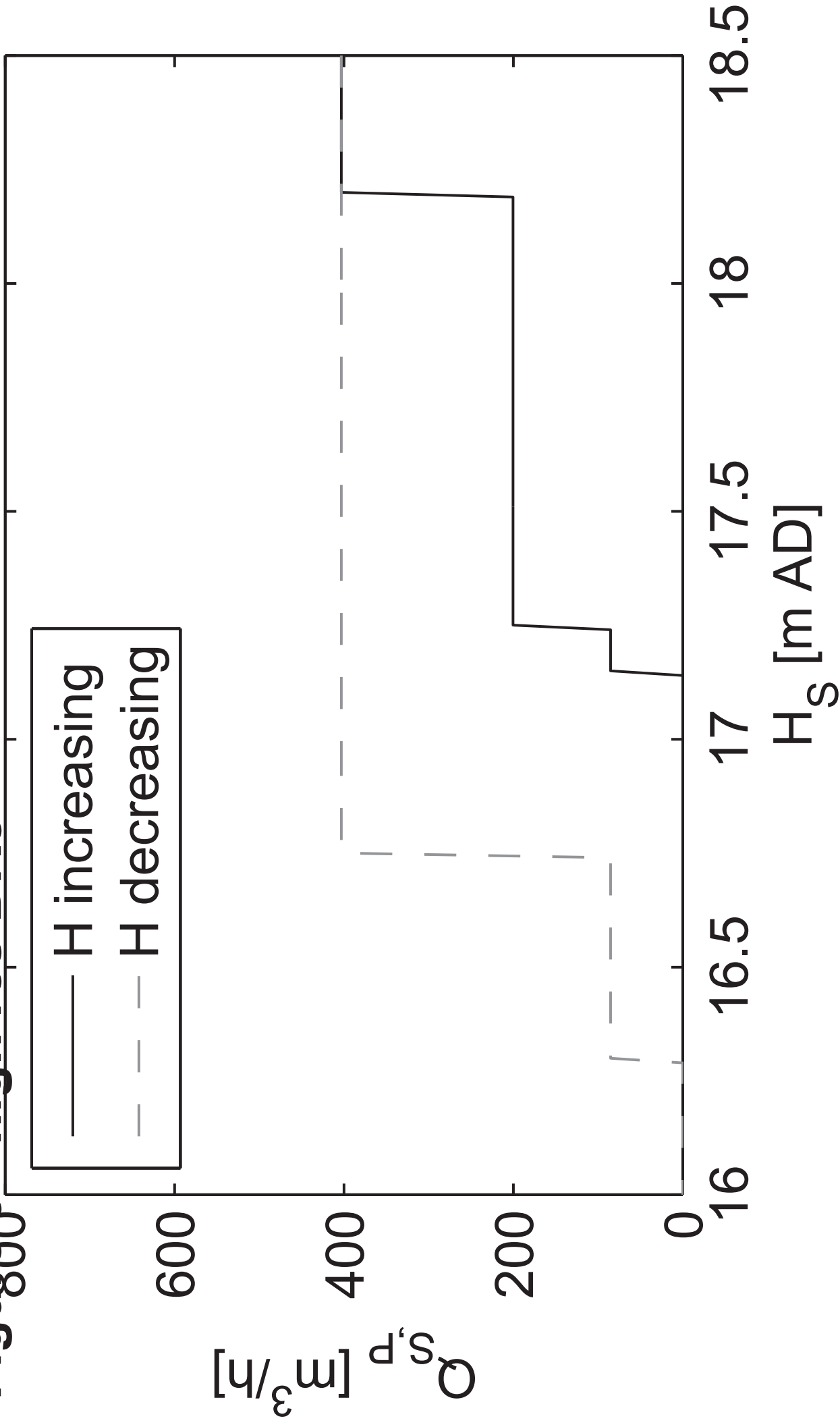


Figure 9-10<sup>4</sup> high res DR10

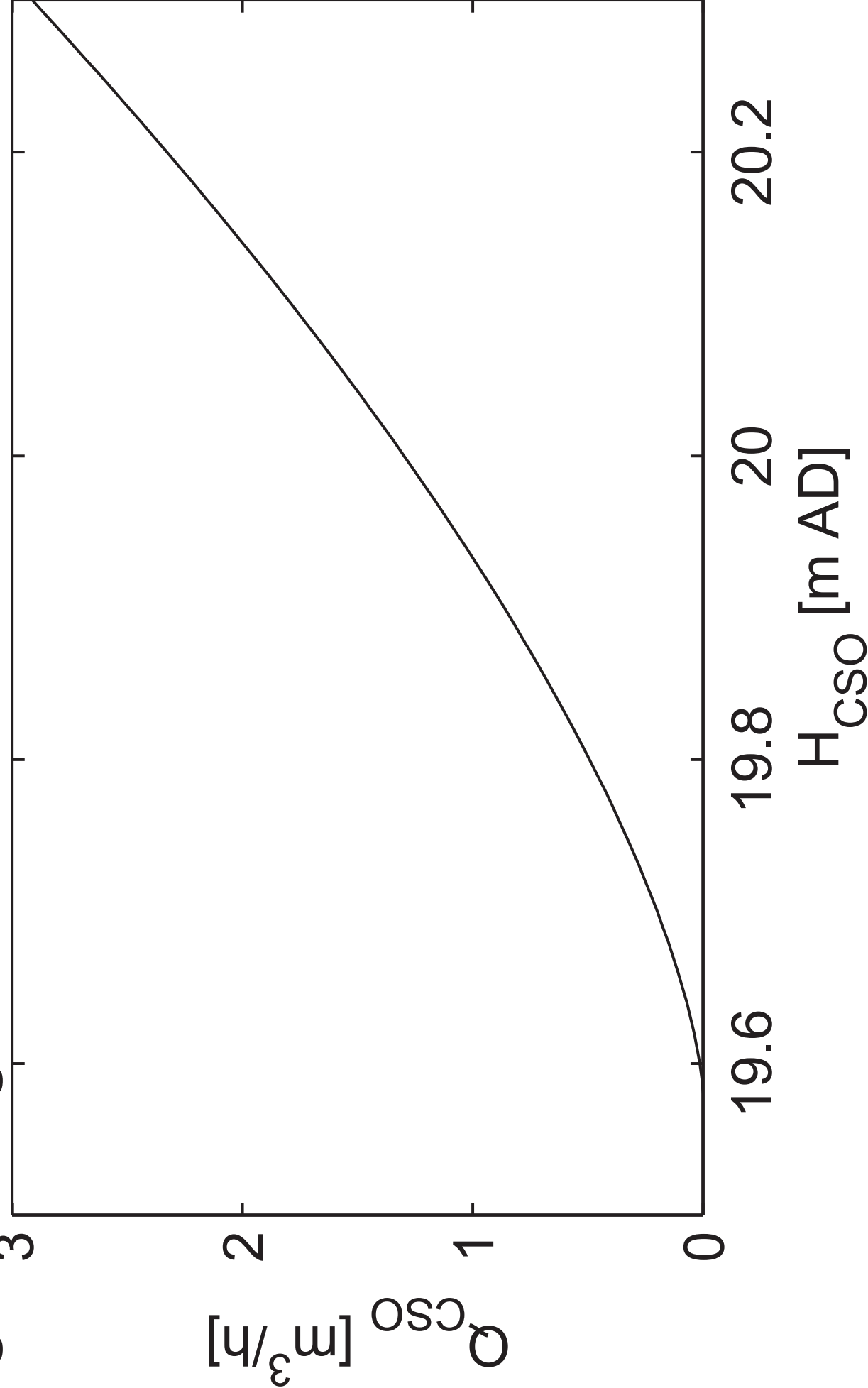


Figure 9 - high res DR9

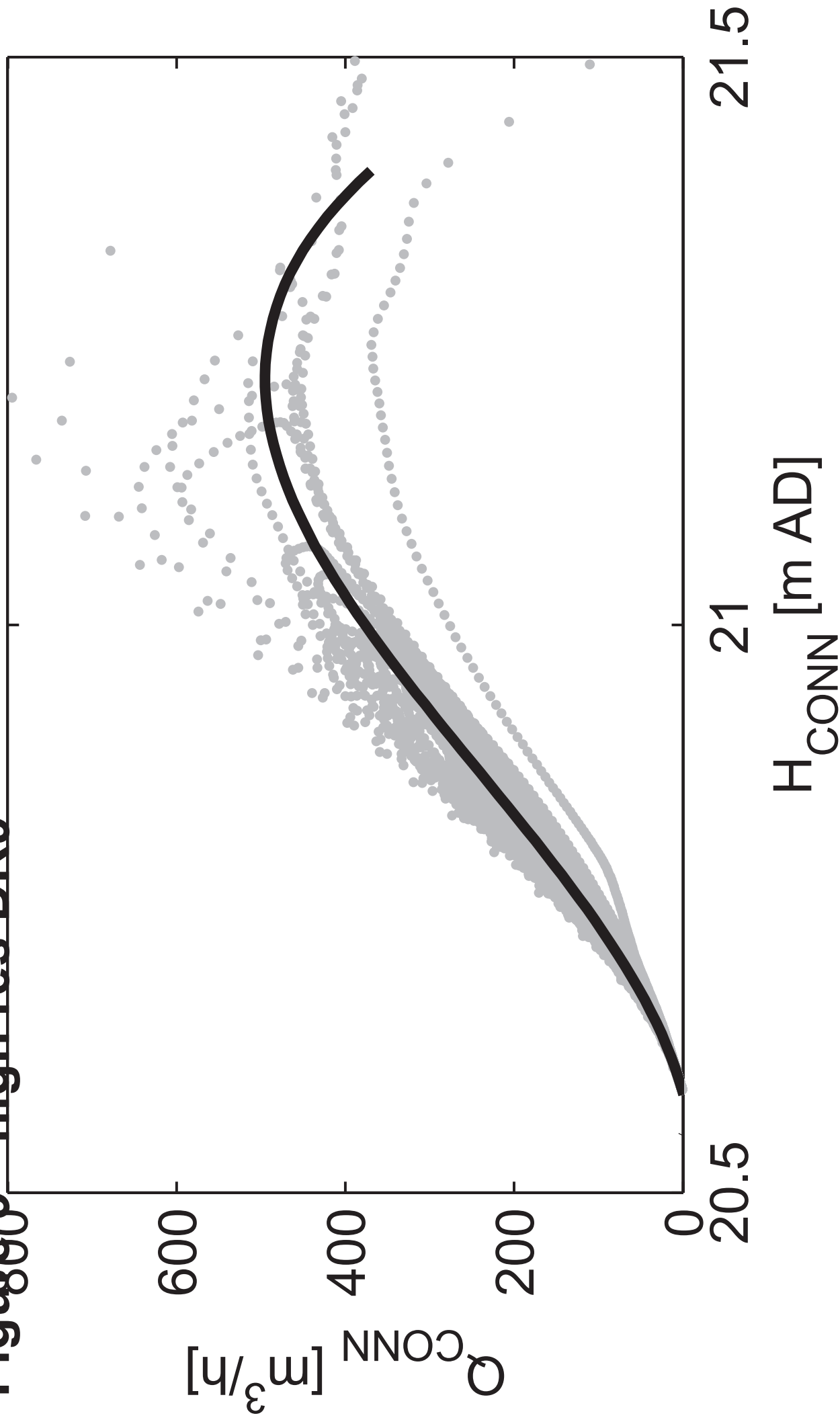




Figure 9 - high res DR11

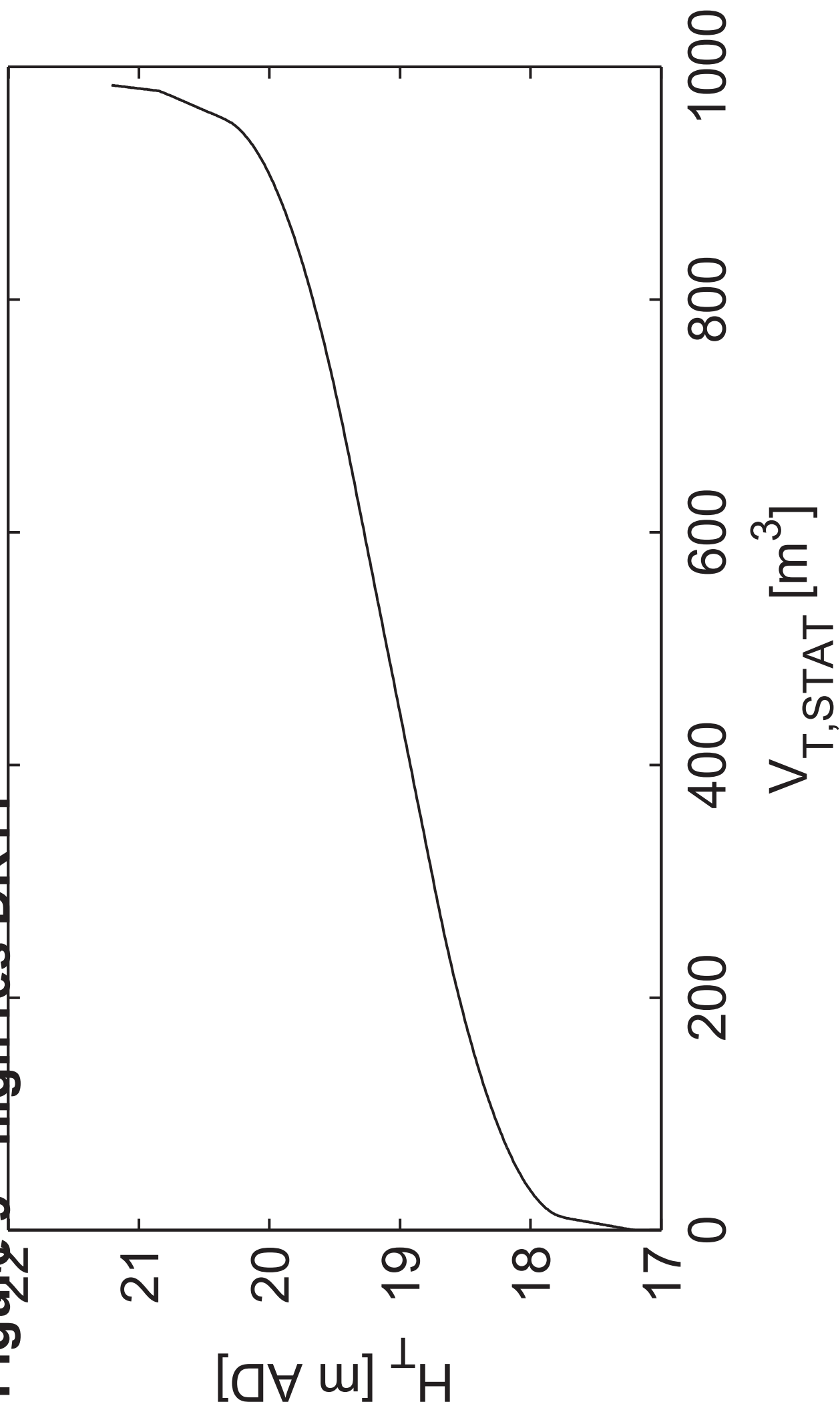


Figure 9 - high res DR12

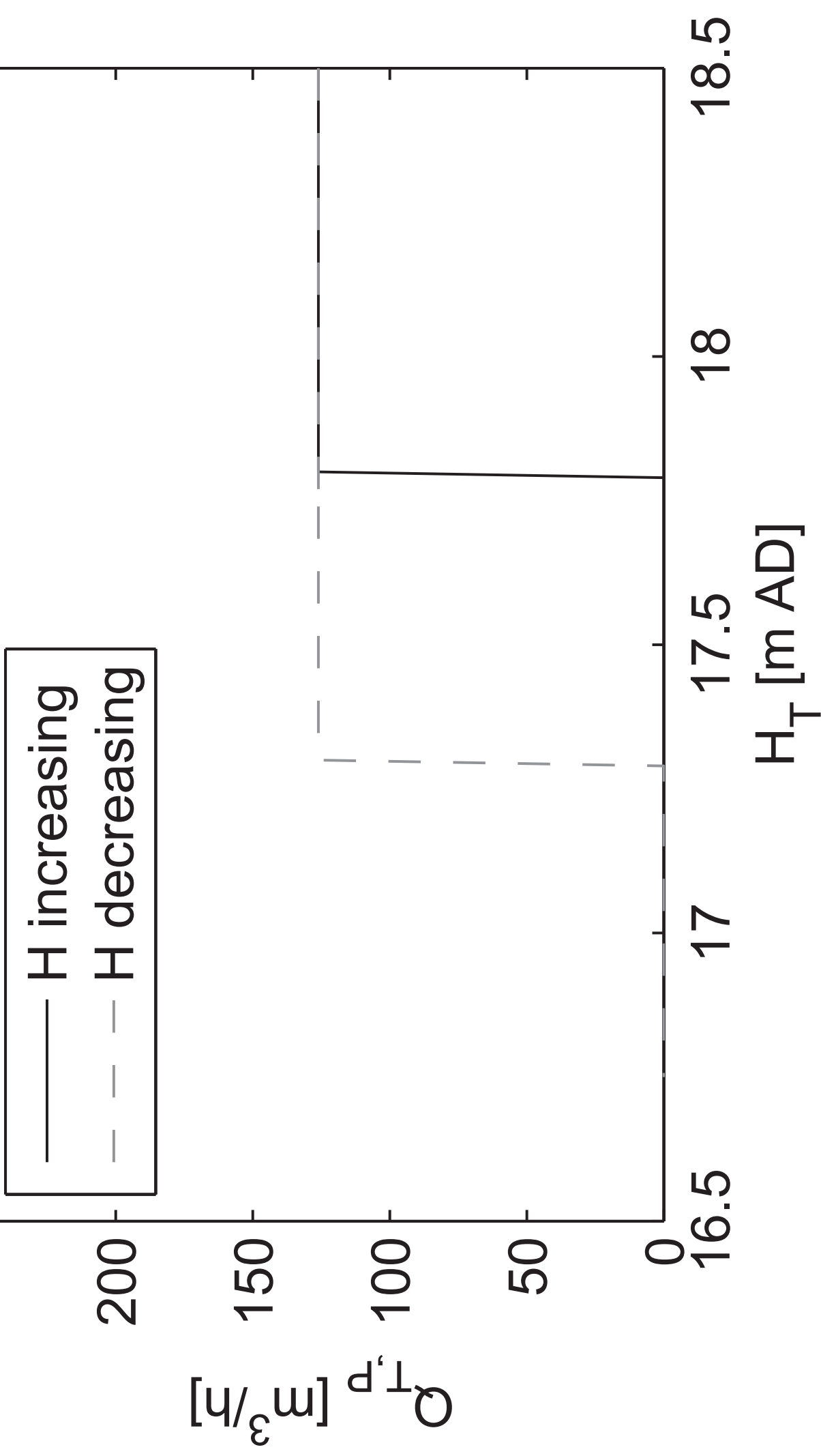


Figure 9-16<sup>4</sup> High res DR13

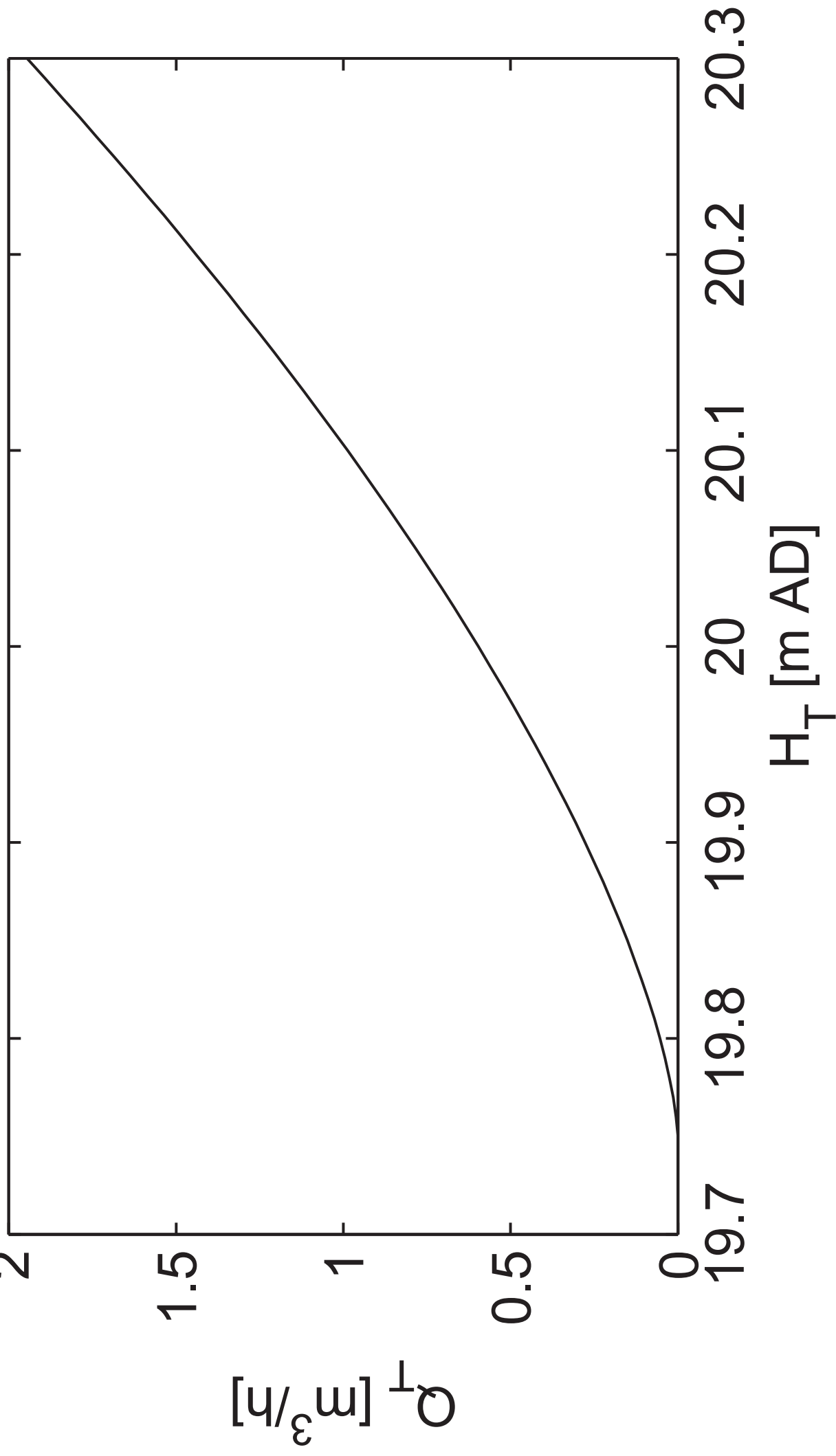


Figure 10 - left

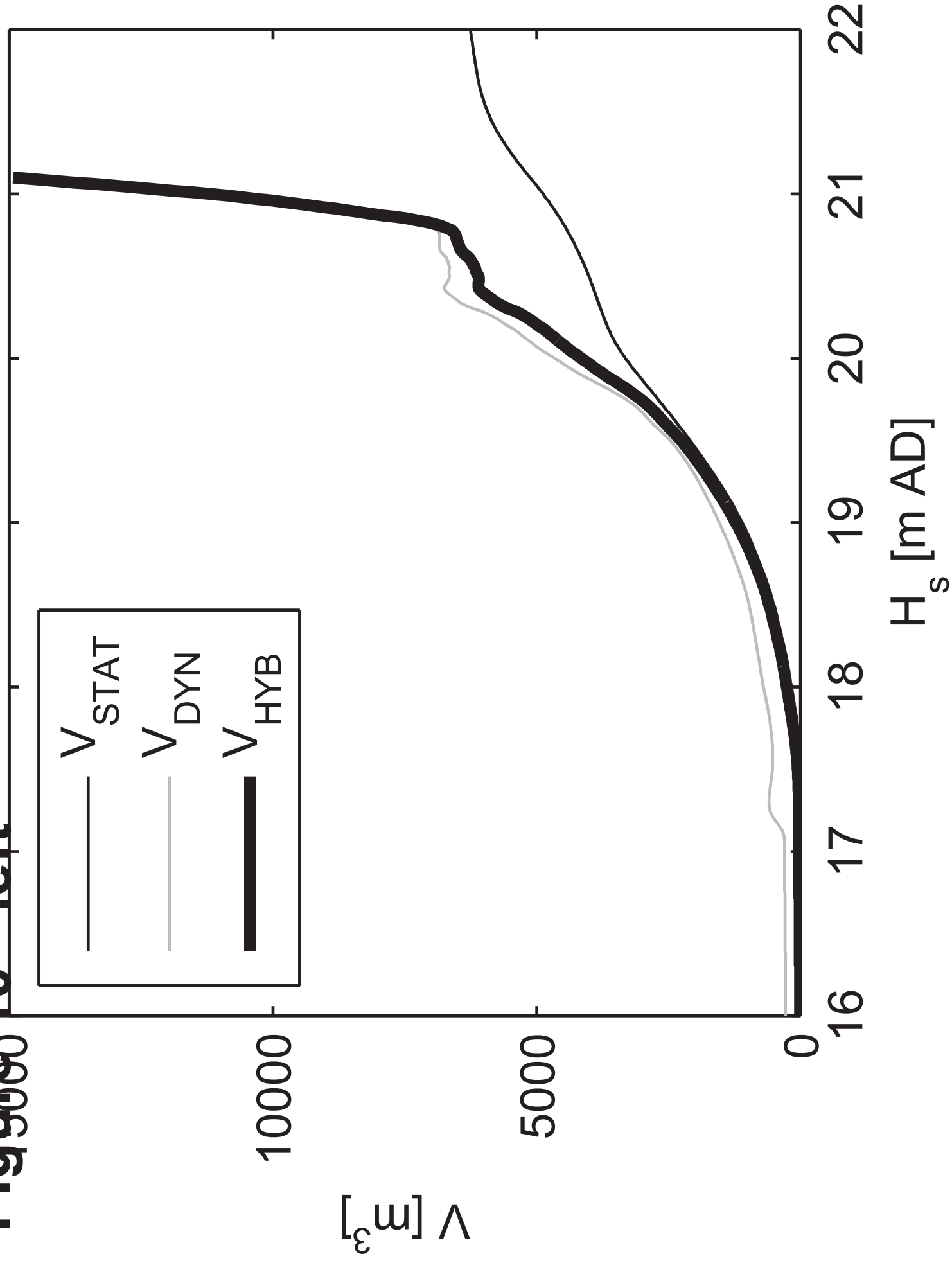


Figure 10 - right

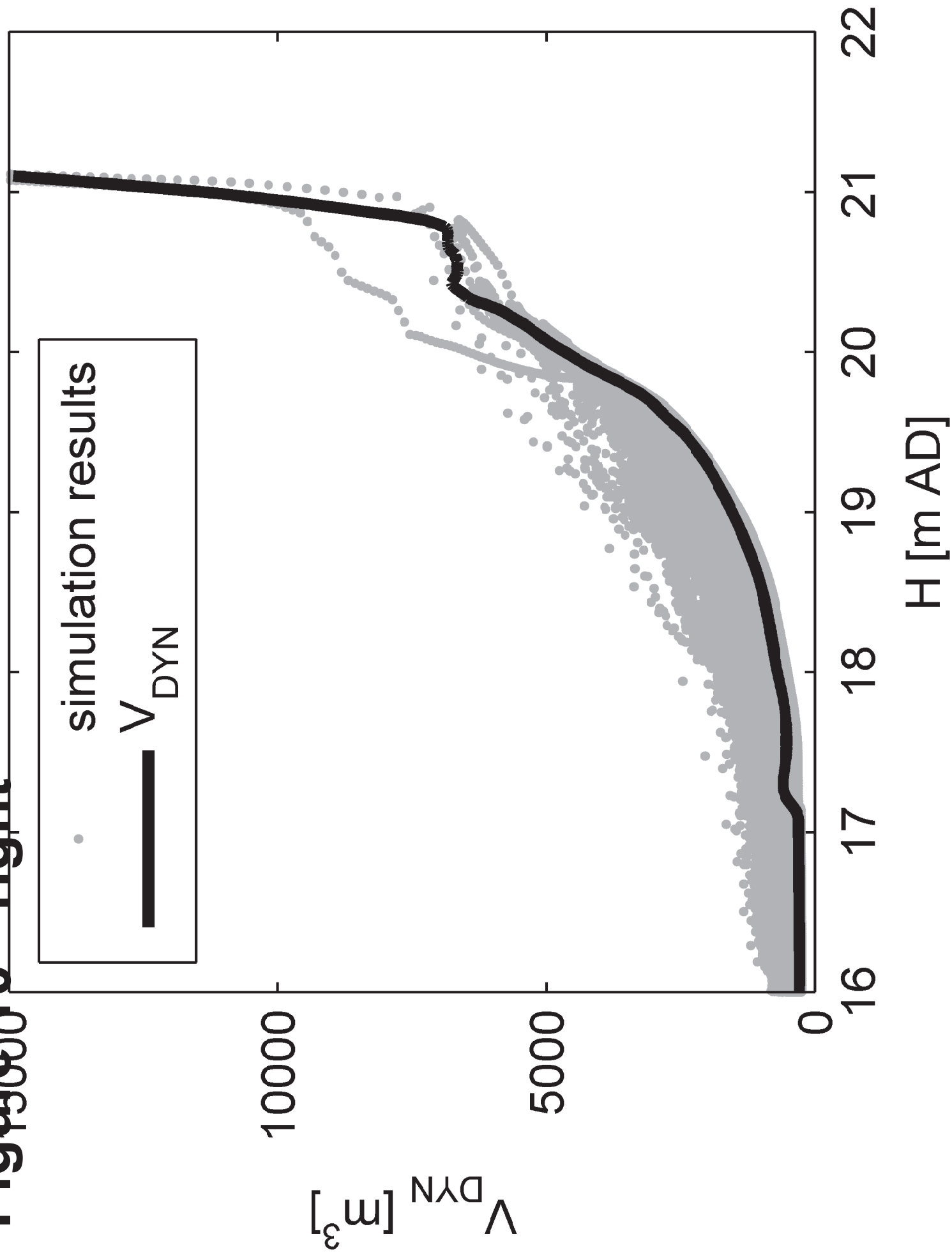


Figure 11

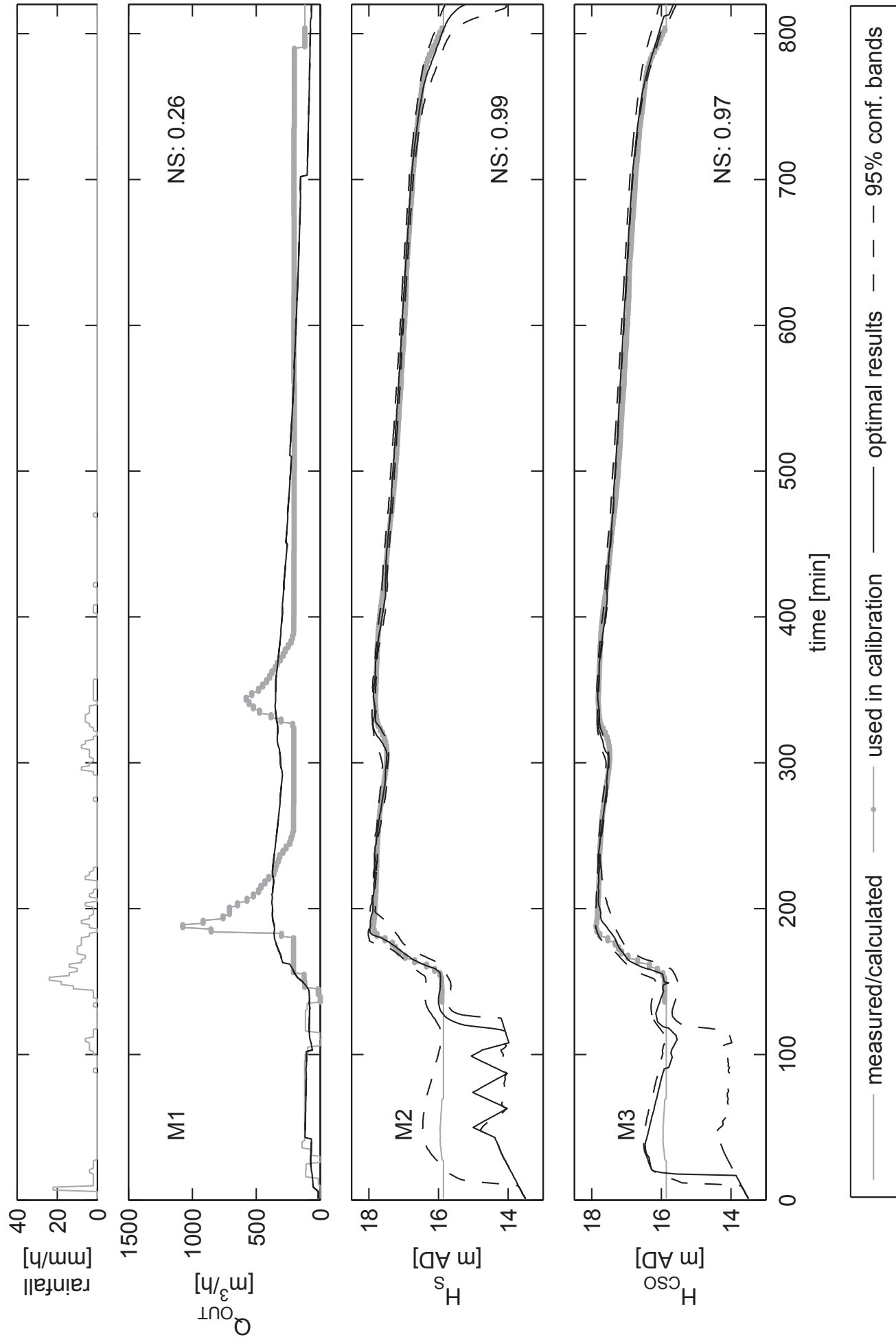
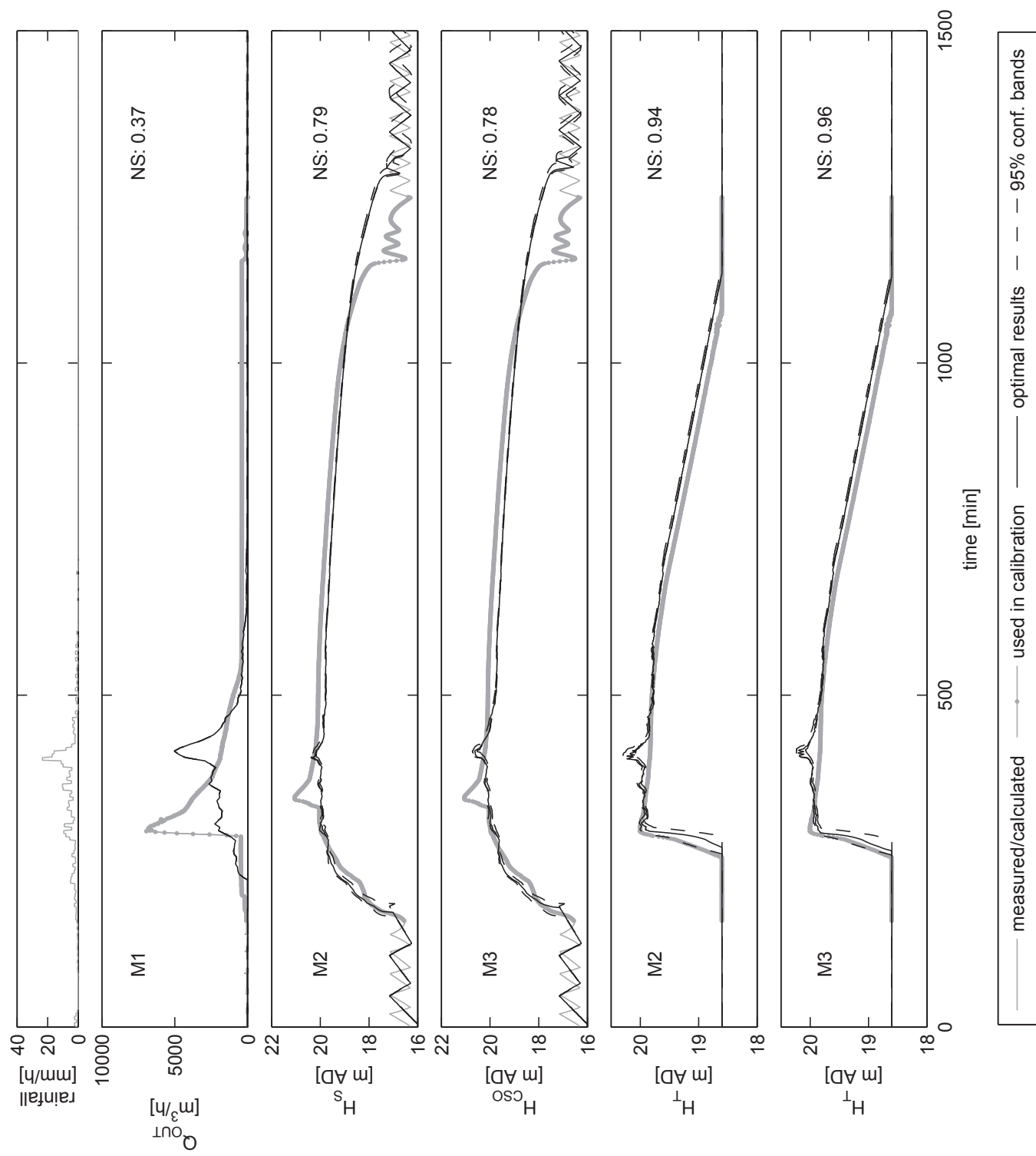


Figure 12



**Figure 13**

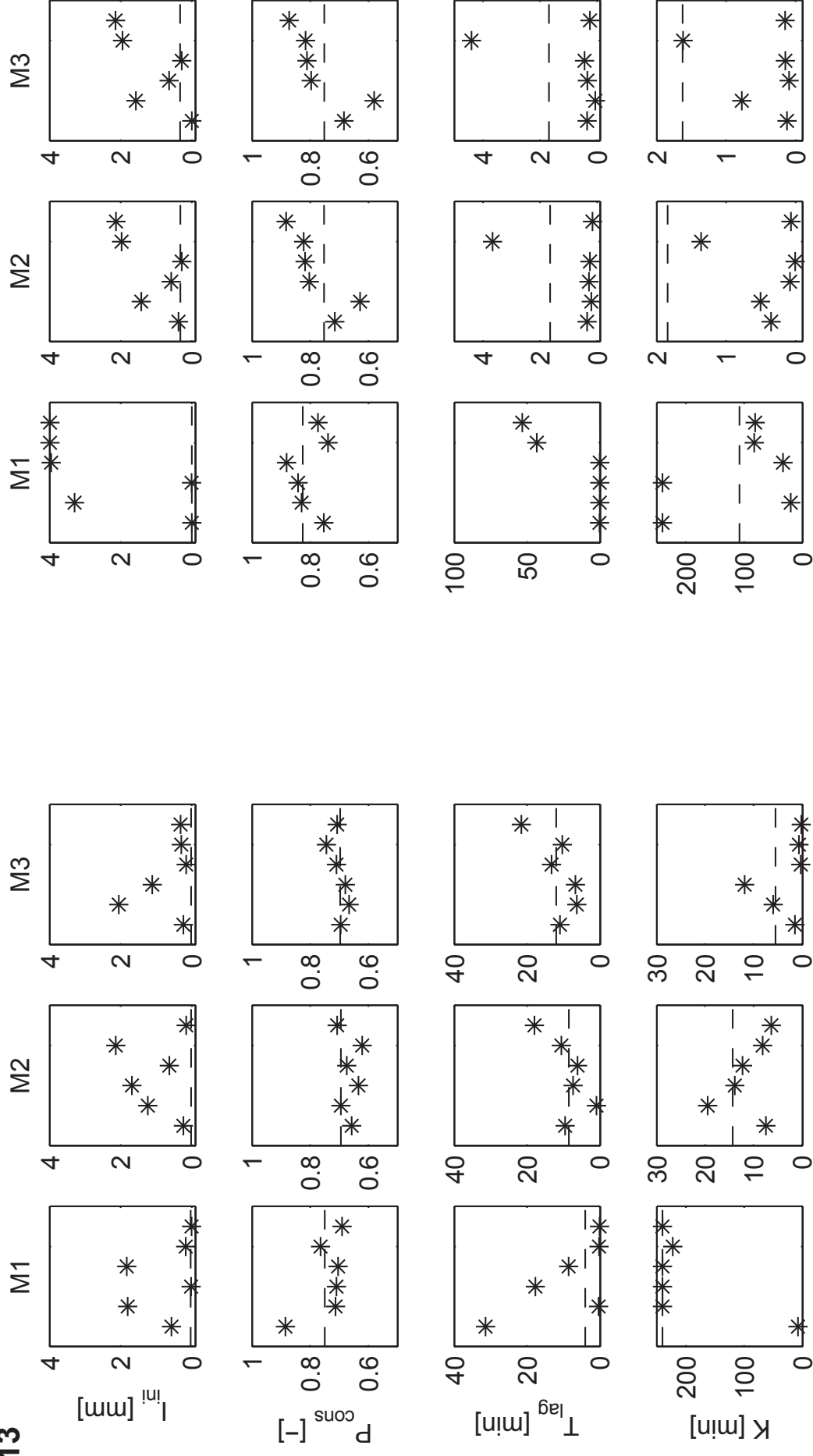




Figure 14

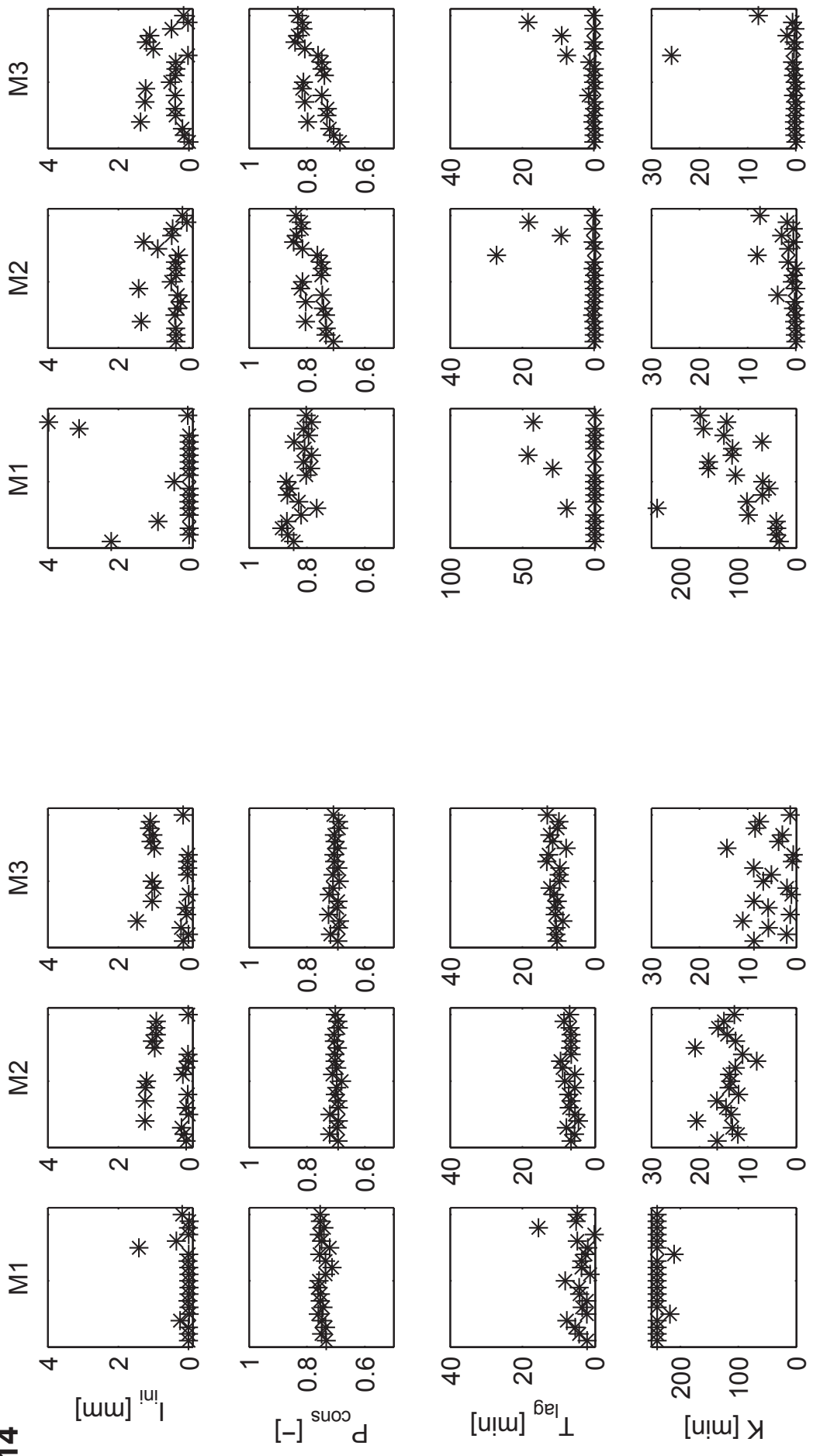


Figure 15

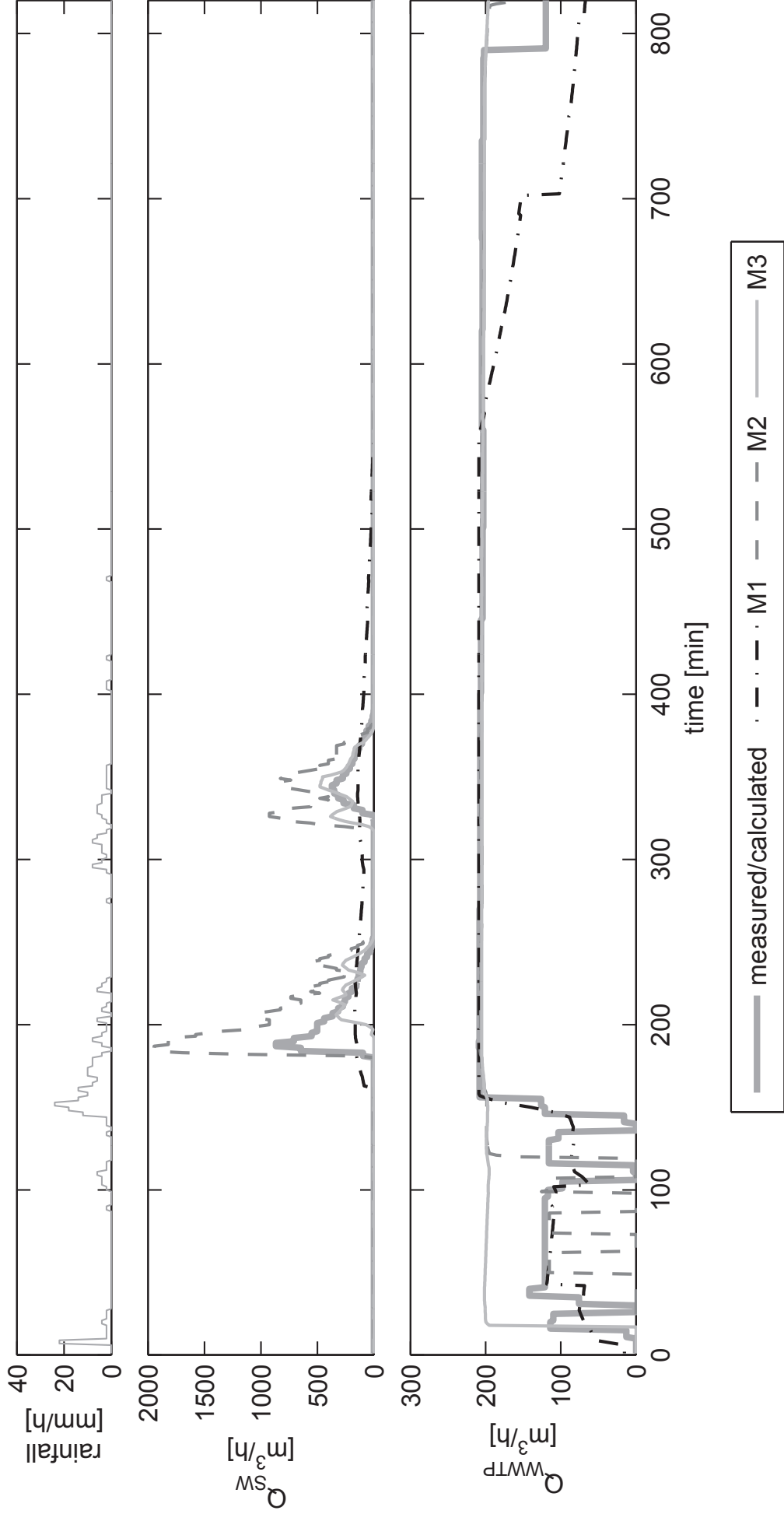
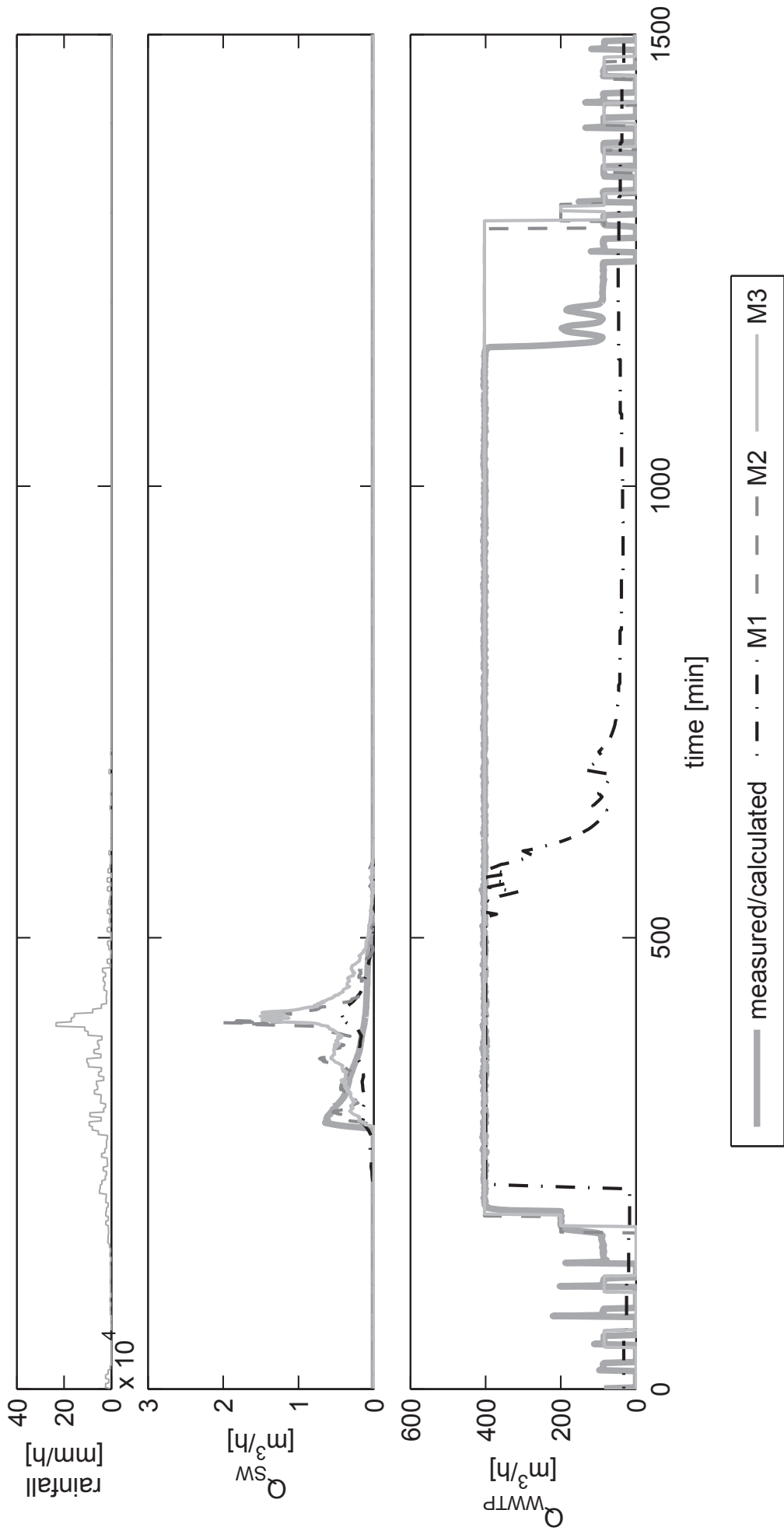


Figure 16



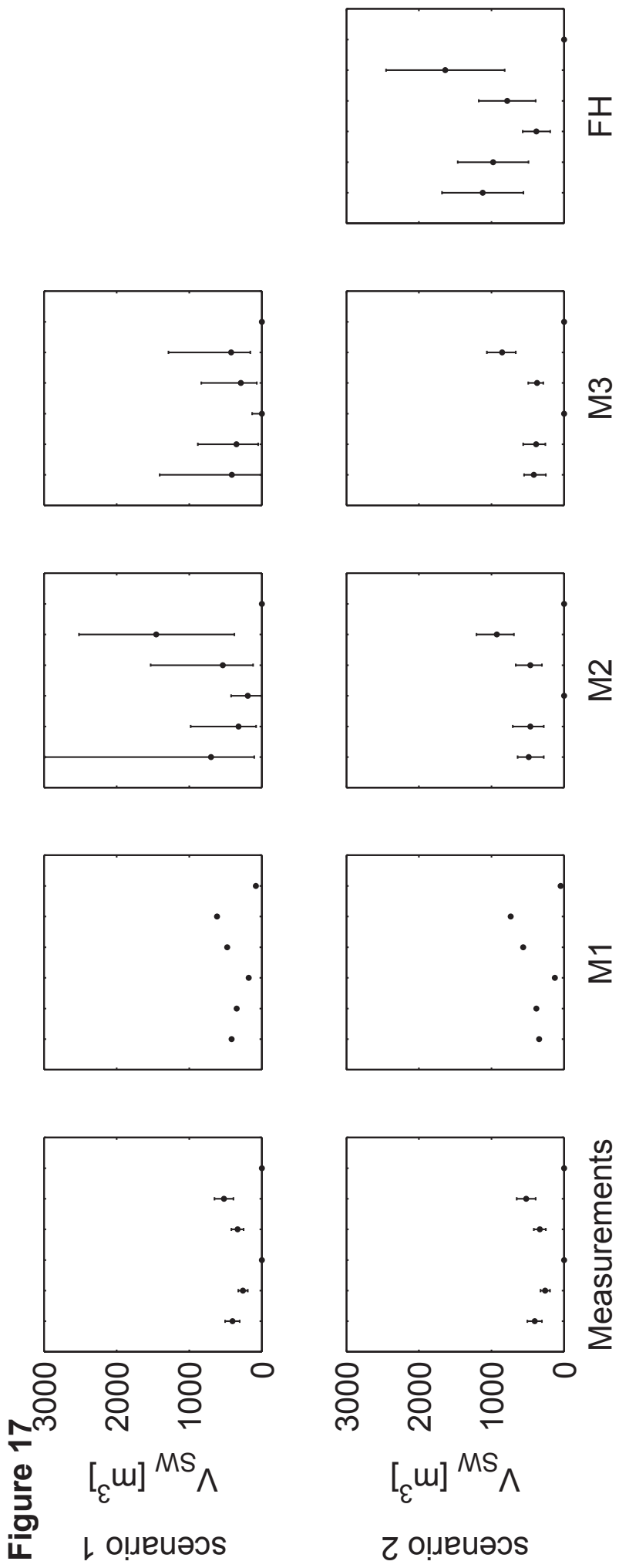
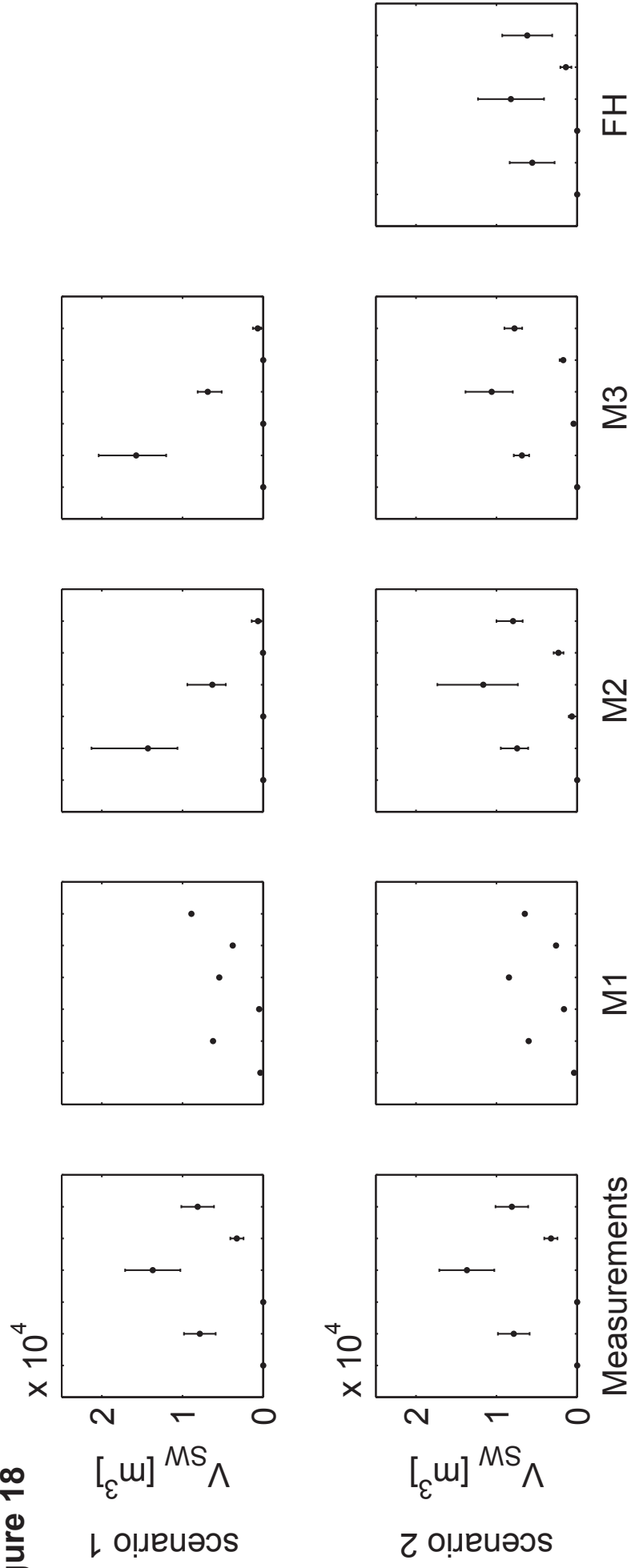


Figure 18



1    **DESIGN AND PERFORMANCE EVALUATION OF A SIMPLIFIED DYNAMIC MODEL FOR**  
2    **COMBINED SEWER OVERFLOWS IN PUMPED SEWER SYSTEMS**

3

4    Petra VAN DAAL-ROMBOUITS<sup>1,2,\*</sup>, Siao SUN<sup>3</sup>, Jeroen LANGEVELD<sup>1,4</sup>, Jean-Luc BERTRAND-  
5    KRAJEWSKI<sup>5</sup>, François CLEMENS<sup>1,6</sup>

6

7    <sup>1</sup> Delft University of Technology, P.O. Box 5048, 2600 GA Delft, the Netherlands

8    <sup>2</sup> Witteveen+Bos, P.O. Box 233, 7400 AE Deventer, the Netherlands

9    <sup>3</sup> Institute of Geographical Sciences and Natural Resource Research, Chinese Academy of Sciences,  
10    Beijing, 100101, People’s Republic of China

11   <sup>4</sup> Partners4UrbanWater, Javastraat 104A, 6524 MJ Nijmegen, the Netherlands

12   <sup>5</sup> University of Lyon, INSA Lyon, DEEP, F-69621 Villeurbanne Cedex, France

13   <sup>6</sup> Deltares, P.O. Box 177, 2600 MH Delft, the Netherlands

14

15   \*Corresponding author’s e-mail: p.m.m.vandaal-rombouts@tudelft.nl

16

17

18    **Abstract**

19    Optimisation or real time control (RTC) studies in wastewater systems increasingly require  
20    rapid simulations of sewer systems in extensive catchments. To reduce the simulation time  
21    calibrated simplified models are applied, with the performance generally based on the  
22    goodness of fit of the calibration. In this research the performance of three simplified and a full  
23    hydrodynamic (FH) model for two catchments are compared based on the correct  
24    determination of CSO event occurrences and of the total discharged volumes to the surface  
25    water. Simplified model M1 consists of a rainfall runoff outflow (RRO) model only. M2  
26    combines the RRO model with a static reservoir model for the sewer behaviour. M3 comprises

27 the RRO model and a dynamic reservoir model. The dynamic reservoir characteristics were  
28 derived from FH model simulations. It was found that M2 and M3 are able to describe the  
29 sewer behaviour of the catchments, contrary to M1. The preferred model structure depends  
30 on the quality of the information (geometrical database and monitoring data) available for the  
31 design and calibration of the model. Finally, calibrated simplified models are shown to be  
32 preferable to uncalibrated FH models when performing optimisation or RTC studies.

33

34

35 **Keywords**

36 calibration, conceptual models, full hydrodynamic models, integrated modelling, monitoring,  
37 urban drainage systems

38

39 **1. Introduction**

40 Optimisation studies in wastewater management are increasingly common (Bach et al., 2014;  
41 Benedetti et al., 2013), requiring model simulations for the wastewater system as a whole, i.e.  
42 the contributing sewer systems, wastewater treatment plants (WWTP) and receiving surface  
43 waters. These model simulations are performed by coupling models for each sub system into  
44 an integrated model. In integrated modelling studies and real time control (RTC) applications  
45 two properties are of main importance: accuracy of the results and the required simulation  
46 time. Accurate results are essential for any modelling study. When working with integrated  
47 models this is especially true since faulty results from one sub model serve as input for the  
48 next sub model. As the simulation time increases with the model size, integrated model  
49 simulations take much time to perform. For example, simulating the full hydrodynamic sewer  
50 model for the Eindhoven case study (4,000 ha) as described in (Langeveld et al., 2013) for a  
51 period of 24 hours takes approximately 45 minutes on a regular laptop (4 cores of 2.8 GHz  
52 each). As optimisation studies generally consist of scenario analysis or the application of RTC,  
53 making evaluation of alternative scenarios beforehand or in real time necessary, the need for  
54 rapid simulation is evident.

55

56 To reduce the simulation time, simplified models, also commonly referred to as conceptual or  
57 surrogate models, are applied. Simplified models consist in many representations, see e.g.  
58 (Coutu et al., 2012; Mannina and Viviani, 2010; Motiee et al., 1997; Vaes and Berlamont, 1999;  
59 Wolfs and Willems, 2014), but all aim to compress the complexity of the real system in only a  
60 few characteristics and/or relationships. To ensure their representativeness, the simplified  
61 models are calibrated against field measurements. The model structure and parameter set  
62 that lead to the best overall fit with the measurements is accepted as the best simplified



63 model. Attempts to find appropriate calibration algorithms are described in e.g. (Krebs et al.,  
64 2014; Mair et al., 2012; Vrugt et al., 2009; Wolfs et al., 2013).

65

66 Previous research, see e.g. (Del Giudice et al., 2015; Dotto et al., 2014; Kleidorfer et al., 2009;  
67 Sun and Bertrand-Krajewski, 2013a, 2012; Vaes et al., 2001), made clear that the model input  
68 can have a major impact on the simplified models performance. When constructing simplified  
69 models for sewer systems in practice, however, usually only a few measurements are available  
70 for model calibration. Sewer systems that are not specifically monitored for research purposes  
71 will likely have water level measurements at the systems edges, at the discharges to the  
72 WWTP and surface water and flow measurements if sewerage is pumped to the WWTP. No  
73 flow measurements are generally available at free flow discharges to the WWTP and at  
74 combined sewer overflow (CSO) locations. Simplified models are therefore, in the majority of  
75 cases, calibrated based on the available water level measurements. The best performing  
76 model is obtained by adjusting model parameters to reproduce the measurements based on  
77 criteria such as Nash-Sutcliffe or root mean squared errors (RMSE).

78

79 The outputs of a (simplified) sewer model applied in integrated modelling are the discharges to  
80 the other sub systems: the WWTP and surface water. Although the quality of the calibration is  
81 a measure for the capability of the simplified sewer model to reproduce observations, it does  
82 not necessarily imply a sufficiently accurate determination of the discharges. Therefore, in the  
83 study presented here, simplified sewer models are calibrated with the established DREAM  
84 algorithm (Vrugt et al., 2008 and 2009), while the performance is evaluated on the correct  
85 determination of the occurrence of CSO events and the best estimation of the total volumes  
86 discharged to the surface water.

87

88 Three simplified models are used in this paper to represent the processes in sewer systems:  
89 i) rainfall runoff outflow (RRO) model, ii) static reservoir model (SR) and iii) dynamic reservoir  
90 model (DR). RRO models simulate the surface runoff generation process and the discharges at  
91 the outlet of small catchments equipped with sloped sewer systems. Among RRO models, (Sun  
92 and Bertrand-Krajewski, 2013b) have demonstrated the effectiveness of the standard linear  
93 reservoir model for such cases. However, the simple linear relation between the discharge and  
94 the storage in the fictitious reservoir of the model is likely not to be effective for looped sewer  
95 systems equipped with pumping stations and CSO structures. Other process descriptions are  
96 needed in order to characterize the flow behaviour in these more complicated systems. In this  
97 study, a standard RRO model is thus complemented with either the SR model or the more  
98 elaborate DR model to represent looped, pumped, systems. For the derivation of the SR  
99 models geometrical information and pumping station settings are taken from a full  
100 hydrodynamic (FH) model, i.e. a 1D model taking into account hydrodynamic processes in the  
101 sewer system. For the DR models additional key relationships between variables are obtained  
102 through FH model simulations. In the development of SR and DR models, simplicity was  
103 constantly balanced against physical representativeness. Simplicity, and by that reproducibility  
104 and applicability in practical RTC situations, was pursued.

105

106 This paper thus presents a comparison of three simplified models: i) a single RRO model, ii) a  
107 combination RRO + SR models and iii) a combination RRO + DR models for the simulation of  
108 CSO events and volumes. Finally, the performances of the simplified and FH models are  
109 compared. This study has been conducted for two catchment areas in the Netherlands: Loenen  
110 and Waalre. Both catchments consist of pumped, combined sewer systems, but differ in size,  
111 structure and average ground level slope.

112

113 **2. Materials and method**

114 **2.1. Catchment areas**

115 Two combined sewer systems have been selected to test the simplified models: Loenen and  
116 Waalre. Loenen is located in the central east of the Netherlands in a mildly sloping area. This  
117 system has a partly looped and partly branched character. It is equipped with one pumping  
118 station and two CSOs. One CSO, referred to as primary, is located downstream in the sewer  
119 system and discharges much more and more often than the upstream, secondary, CSO. At the  
120 location of the pumping station an additional inflow from a small neighbouring sewer system is  
121 incorporated. Sewer system characteristics and layout can be found in table 1 and figure 1  
122 (left).

123

124 Waalre is located in the south of the Netherlands. The sewer system is looped with one  
125 pumping station, a primary CSO equipped with a settling tank and a secondary CSO that rarely  
126 discharges. Additionally Waalre is connected to a neighbouring catchment in the east.

127 Although water can flow both ways, it serves as a discharge for Waalre. Characteristics of the  
128 sewer systems are listed in table 1, while figure 1 (right) displays the sewer system layout.

129 **2.2. Monitoring data**

130 For Loenen monitoring data is available at a one minute interval from June 2001 to January  
131 2002, collected as part of a dedicated research project. Flow measurements are available at  
132 the pumping station and an inflow into the pumping station from a neighbouring catchment.  
133 Level measurements are available in the pumping chamber and at the CSO locations, as  
134 displayed in figure 1 (left). Additionally, two rain gauges were installed in the catchment. Due  
135 to various reasons no continuous data set is available for the measuring period.

136

137 For Waalre monitoring data at the sewer system edges is available at a one minute interval.  
138 Flow is measured at the pumping station. Level measurements are available in the pumping  
139 chamber, inside the settling tank and at the secondary CSO location. The measuring locations  
140 are indicated in figure 1 (right). Rain radar data with pixel sizes of one square kilometre are  
141 available. The radar data is calibrated against rain gauge measurements located approximately  
142 10 km away using a procedure based on conditional merging as described in (De Niet et al.,  
143 2013). The calibrated rain radar data is available only during wet weather days and when the  
144 rain gauges functioned in the period April 2011 to January 2012. All other measurements are  
145 registered permanently. Data validation was performed applying the algorithms described in  
146 (Van Bijnen and Korving, 2008).

147

#### 148 **Dry Weather Flow (DWF)**

149 Daily dry weather flow (DWF) profiles have been derived from the monitoring data for both  
150 catchments. For Waalre it was based on the pump flow measurements in 2011. The mean  
151 hourly pumped discharge at DWF days was used to represent a typical daily DWF profile. DWF  
152 days are defined as having received less than 0.05 mm of precipitation after exponential  
153 smoothing (80% accounted to the current day and 20% to the following day) to prevent false  
154 detection of DWF days due to the absence of rain gauges inside the catchment. Unrealistic  
155 measurements and periods with snowfall have been manually discarded. The DWF profile for  
156 Loenen was previously derived by (Langeveld, 2004) based on the pump flow measurements  
157 using a similar strategy. The resulting profiles can be found in figure 2.

#### 158 **2.3. Full hydrodynamic (FH) models**

159 FH models for both catchments are available in InfoWorks ICM ([www.innovyze.com](http://www.innovyze.com)). The FH  
160 model for Loenen was calibrated by (Langeveld, 2004), following the procedure described by  
161 (Clemens, 2001). The calibration involved a detailed check of the geometrical database and  
162 tuning of several parameters to match measured and modelled water levels at up to ten  
163 locations. As the calibration resulted in very close resemblance between the modelled and  
164 measured water levels (deviations < 5 cm), it was concluded that the geometrical database  
165 was virtually without errors. The FH model for Waalre was validated as described in (Langeveld  
166 et al., 2013). It involved comparison of the measured and modelled water levels as a function  
167 of time at the three monitoring locations. No parameter optimisation was performed. As the  
168 measured and modelled water levels resembled one another in general (based on expert  
169 judgement), it was concluded that no large errors in the geometrical database existed.  
170 Nevertheless, occasional deviations in measured and modelled water levels of up to 50 cm  
171 were present.

172

173 The FH models are applied in this study for three purposes: i) properties of the geometrical  
174 database and pumping station settings are utilized in the design of the SR and DR models,  
175 ii) key relationships between variables are obtained by means of FH model simulations and  
176 applied in the DR model, and iii) the performance of the simplified models is compared to the  
177 performance of the FH models. For all simulations with the FH models for any of the above  
178 purposes, a standard (uncalibrated) parameter set is employed as (Korving and Clemens, 2005)  
179 showed that the portability of event specific parameter sets for FH models is low. The main  
180 distinction between the calibrated FH model for Loenen and validated FH model for Waalre  
181 lies therefore in the trustworthiness of the underlying geometrical database.

182

183 The simulations performed with the FH model for the second purpose, application in the  
184 design of the DR model, are based on ten years (1955-1964) of 15 minute interval rainfall  
185 measurements in De Bilt in the Netherlands. The simulations were executed with a one minute  
186 time step, recording for every time step the volume, water level and flows in all manholes,  
187 conduits, pumps, CSOs etc. The derivation of the required relationships is described in detail in  
188 section 2.4.3.

## 189 **2.4. Model structures**

190 The general structure of the three simplified models tested in this paper is shown in figure 3.  
191 Model M1 includes only a RRO model. Model M2 combines a RRO model and a SR model,  
192 while model M3 combines a RRO model and a DR model. Rainfall, DWF and optional additional  
193 flows are model inputs, while flows to the surface water ( $Q_{SW}$ ) and to the WWTP ( $Q_{WWTP}$ ) are  
194 model outputs. In the following sections, all models are explained in more detail.

### 195 **2.4.1. Rainfall runoff outflow (RRO) model**

196 The standard linear reservoir model is a typical RRO model, see e.g. (Sun and Bertrand-  
197 Krajewski, 2013b). It comprises of a rainfall loss model followed by a linear reservoir. The  
198 rainfall loss model consists of initial ( $I_{ini}$  [mm]) and proportional ( $P_{cons}$  [-]) rainfall losses, i.e.  
199 depression losses and ratio of contributing and total area. The resulting net rainfall ( $I_{net}$  [mm])  
200 occurs with a time lag ( $T_{lag}$  [min]) and feeds the linear reservoir with a reservoir constant ( $K$   
201 [min]). The outflow of the standard linear reservoir ( $Q_{out}$ ) is derived from the inputs using:

202

$$203 \quad Q_{out}(t) = \exp\left(-\frac{\Delta t}{K}\right) Q_{out}(t - \Delta t) + \left[1 - \exp\left(-\frac{\Delta t}{K}\right)\right] I_{net}(t - T_{lag})A, \quad (1)$$

204

205 with A the catchment area [ha]. For more details on the standard linear reservoir model the  
206 reader is referred to (Sun and Bertrand-Krajewski, 2013b).

207

208 To determine the total inflow into the sewer models ( $Q_{in}$  in figure 3) for models M2 and M3,  
209  $Q_{DWF}$  and  $Q_{optional}$  are simply added to  $Q_{out}$ . For model M1,  $Q_{out}$  together with  $Q_{DWF}$  and  $Q_{optional}$   
210 represent both the surface runoff and the subsequent flow routing within the sewer system. It  
211 is split in the two sewer discharges  $Q_{SW}$  and  $Q_{WWTP}$  on the assumption that as much water is  
212 pumped to the WWTP as possible, i.e. all discharges up to the maximum pumping capacity is  
213 accounted to  $Q_{WWTP}$  as illustrated in figure 4 for Loenen. For Waalre,  $Q_{WWTP}$  is determined using  
214 the same method. From the remainder the discharge through the connection to the  
215 neighbouring catchment (determined from FH model simulations as it is not monitored) is  
216 subtracted before accounting it to  $Q_{SW}$ .

#### 217 **2.4.2. Static reservoir (SR) model**

218 The SR model aims to represent processes within the sewer system that the basic RRO model  
219 cannot explicitly simulate. FH model properties of the geometrical database and pumping  
220 station settings are applied in its design. A schematic representation of the SR model for  
221 Loenen is shown in figure 5. It consists of a single basin for the sewer system which is filled by  
222  $Q_{in}$  as described in the previous section. It empties through a pump resulting in  $Q_{WWTP}$ , and a  
223 single CSO resulting in  $Q_{SW}$ .

224

225 Several characteristics or relationships are applied in the SR model, numbered S SR1-SR3 in  
226 figure 5. Their representation and derivation were performed as follows:

227 SR1. Static storage-level curve

228 The static storage-level curve is used to convert the sewer volume ( $V_s$ ) into the water  
229 level in the sewer ( $H_s$ ). It is derived from the geometrical database of the FH model as  
230 the cumulative volume of all manholes, conduits, etc. of the sewer system under each  
231 possible water level.

232 SR2. Discharge through pump

233 The discharge through the pump ( $Q_{s,p}$ ) is calculated through  $H_s$  and the pump  
234 characteristic. The pump characteristic is taken from the FH model.

235 SR3. Discharge through CSO

236 The discharge through the CSO ( $Q_{CSO}$ ) is taken to be only caused by the primary CSO.

237 The discharge is calculated through  $H_s$  and the standard weir equations for frontal  
238 weirs:

239

$$240 \quad Q_{free} = c_1 h^{c_2} \quad (2)$$

241

242 for free outflow, with flow  $Q_{free}$  [ $m^3/s$ ],  $h$  [m] water level above the weir crest,  $c_1$   
243 [ $m^{3-c_2}/s$ ] taken to be 1.36 times the weir width [m] and  $c_2$  [-] taken to be 1.5. Or

244

$$245 \quad Q_{sub} = c_3 h_{DS} \sqrt{2g(h_{US} - h_{DS})} \quad (3)$$

246

247 for submerged outflow, with flow  $Q_{sub}$  [ $m^3/s$ ],  $h_{US}$  and  $h_{DS}$  [m] the upstream and  
248 downstream water level above the weir crest,  $c_3$  [m] taken to be 0.8 times the weir  
249 width [m] and  $g$  the standard acceleration due to gravity [ $9.81 \text{ m/s}^2$ ]. Submerged  
250 outflow is assumed to occur when  $2/3 \cdot h_{US} < h_{DS}$ . For Loenen only free outflow is  
251 assumed.

252



253 A schematic representation of the SR model for Waalre is depicted in figure 6. It consists of a  
254 basin for the sewer system and a basin for the settling tank. The sewer basin is filled by  $Q_{in}$  and  
255 has three discharges: one through the pump resulting in  $Q_{WWTP}$ , one through the connection  
256 with the neighbouring catchment and one through a single CSO to the settling tank. The  
257 discharge through the CSO fills the settling tank that is emptied either through a pump back  
258 into the sewer basin, or through a CSO to the surface water resulting in  $Q_{SW}$ .

259

260 Again several characteristics or relationships have been applied in the model, numbered SR4-  
261 SR10 in figure 6. Their representation and derivation were performed as follows:

262 SR4. Static storage-level curve sewer

263 See SR1, and excluding the settling tank.

264 SR5. Discharge sewer through pump

265 The discharge through the pump ( $Q_{S,p}$ ) is calculated through the water level in the  
266 sewer ( $H_s$ ) and the pump characteristic. The pump characteristic is derived from  
267 analysis of the water level and flow measurements at the pumping station, and (Van  
268 Daal-Rombouts, 2012).

269 SR6. Discharge sewer through connection

270 From simulations with the FH model it was found that water only flows from Waalre to  
271 the neighbouring catchment. The discharge through the connection ( $Q_{CONN}$ ) is  
272 calculated through  $H_s$  and the standard equation for a free outflow over a V-notch  
273 weir,

274

$$275 \quad Q = c_1 \tan(\theta/2) h^{5/2}, \quad (4)$$

276

277 as the connecting sewer is egg shaped. Here  $Q$  is the flow [ $\text{m}^3/\text{s}$ ],  $c_1$  a constant [ $\text{m}^{1/2}/\text{s}$ ]  
278 taken to be 1.4,  $\theta$  the notch angle taken to be  $67^\circ$ , and  $h$  [m] the water level over the  
279 weir crest. Free outflow is assumed at all times and the bottom of the notch is taken to  
280 be the highest invert of the connecting conduit.

281 SR7. Discharge sewer through CSO

282 The discharge through the CSO ( $Q_{\text{CSO}}$ ) is taken to be caused only by the primary CSO  
283 and is calculated through  $H_s$  and equations 2 and 3. Both free and submerged outflow  
284 are allowed (only free outflow is displayed).

285 SR8. Static storage-level curve settling tank

286 The static storage-level curve is used to convert the settling tank volume ( $V_T$ ) into the  
287 water level in the tank ( $H_T$ ). It is derived from the FH model, similar to SR1.

288 SR9. Discharge settling tank through pump

289 The discharge of the settling tank through the pump ( $Q_{T,p}$ ) is based on  $H_T$  and the pump  
290 characteristic. The pump characteristic was taken from the FH model, where the  
291 pumping capacity was adjusted to match the monitoring data.

292 SR10. Discharge settling tank

293 The discharge of the settling tank ( $Q_T$ ) is calculated through  $H_T$  and equation 2.

#### 294 **2.4.3. Dynamic reservoir (DR) model**

295 The DR models for the sewer systems are similar to the SR models, but contain additional  
296 relationships derived from FH model simulations to better account for the dynamic behaviour  
297 of a sewer system. A schematic representation of the DR model for Loenen is shown in figure 7  
298 and can be compared to the SR model in figure 5. Differences are expressed in the storage-  
299 level curve applied (SR1 - DR1) and the water level applied in the CSO discharge (DR2 - no  
300 equivalent in the SR model).

301

302 The characteristics or relationships applied in the DR model are numbered DR1-DR4 in figure 7.

303 Their representation and derivation are explained bellow:

304 DR1. Hybrid storage-level curve

305 A so called hybrid storage-level curve is used to convert the sewer volume ( $V_S$ ) into the  
306 water level in the sewer ( $H_S$ ). The hybrid curve follows the static storage-level curve  
307 (see SR1) for low water levels to correctly model DWF circumstances and pumping  
308 behaviour, and gradually turns to the dynamic storage-level curve for high water levels  
309 (with possibly pressurised flow conditions) to take the dynamic properties of the sewer  
310 system under wet weather flow (WWF) conditions and CSO discharges into account.

311 Figure 8 (left) displays the static, dynamic, and hybrid storage curves for Loenen.

312 The dynamic storage-level curve was derived from simulations performed with the FH  
313 model as described in section 2.3. The resulting water volumes in the entire sewer  
314 system (every minute for 10 years) were grouped in one cm intervals of the  
315 corresponding water level at the pumping station. The grouped volumes were  
316 averaged and smoothed to obtain the dynamic storage-level curve, as displayed in  
317 figure 8 (right). Note that the dynamic storage-level curve converges towards the static  
318 storage-level curve for DWF conditions or low rain intensities as the water level in the  
319 sewer system levels off.

320 DR2. Level at CSO

321  $H_S$  is converted into the water level at the primary CSO location ( $H_{CSO}$ ). The relationship  
322 is based on FH model simulations, where a linear relation is fitted through the  
323 simulated water levels at the pumping station and the CSO location. Only elevated  
324 water levels (WWF conditions) are taken into account.

325 DR3. Discharge through pump

326 See SR2.

327 DR4. Discharge through CSO

328 See SR3, only now  $H_{CSO}$  is applied.

329

330 A schematic representation of the DR model for Waalre is shown in figure 9 and can be  
331 compared to the SR model in figure 6. Differences are expressed in the storage-level curve  
332 applied (DR5-SR4), the water level applied in the CSO discharge (DR6-no equivalent in the SR  
333 model) and the water level applied in and the calculation of the flow through the connection  
334 (DR7-no equivalent in SR model, DR9-SR6).

335

336 The characteristics or relationships applied in the DR for Waalre are numbered DR5-DR13 in  
337 figure 9. Their representation and derivation are explained as follows:

338 DR5. Hybrid storage-level curve sewer

339 A hybrid storage-level curve is used to convert  $V_S$  into  $H_S$ . The derivation follows DR1.

340 The resulting curves for Waalre are displayed in Figure 10: (left) the static, dynamic,  
341 and hybrid storage curves, (right) the derivation of the dynamic storage-level curve  
342 from the FH model simulation results.

343 DR6. Level sewer at CSO

344 Similar to DR2, a relationship has been derived between  $H_{CSO}$  and  $H_S$ . As Waalre is  
345 equipped with the settling tank two linear segments that connect at the highest weir  
346 crest level of the settling tank have been applied. Only elevated water levels (WWF  
347 conditions) are taken into account.

348 DR7. Level sewer at connection

349 Similar to  $H_{CSO}$  in DR6, a relationship between the water level at the connection to the  
350 neighbouring catchment ( $H_{CONN}$ ) and  $H_S$  is derived from the FH model simulations. A

351 linear relation was fitted, taking only elevated water levels (WWF conditions) into  
352 account.

353 DR8. Discharge sewer through pump  
354 See SR5.

355 DR9. Discharge sewer through connection  
356 The discharge of the sewer through the connection to the neighbouring catchment  
357 ( $Q_{\text{CONN}}$ ) is based on  $H_{\text{CONN}}$  and a relationship derived from the FH model simulations.  
358 The simulated water levels at the connection and the corresponding flow through the  
359 connection were fitted with a third order polynomial equation. To prevent unrealistic  
360 (negative) output a maximum value is set for  $H_{\text{CONN}}$ .

361 DR10. Discharge sewer through CSO  
362 See SR7, where  $H_{\text{CSO}}$  is applied in the calculation of the discharge from the sewer.

363 DR11. Static storage-level curve settling tank  
364 See SR8.

365 DR12. Discharge settling tank through pump  
366 See SR9.

367 DR13. Discharge settling tank  
368 See SR10.

## 369 **2.5. Calibration procedure**

### 370 **2.5.1. DREAM algorithm**

371 Calibration, which adjusts model parameters by minimizing the difference between model  
372 outputs and measurements, is an important step before applying simplified models. The  
373 research on calibration methods in the area of rainfall-runoff modelling is comprehensive,  
374 leading to the application of automatic calibration methods instead of traditional manual

375 calibration mainly based on trial and error approaches. In this study an automatic calibration  
376 method (the differential evolution adaptive metropolis (DREAM) method (Vrugt et al., 2008,  
377 2009)) was applied for the calibration of the RRO models. The DREAM method is based on the  
378 Bayesian theorem, which considers model parameters as probabilistic variables revealing the  
379 probabilistic belief on the parameters according to observed model outputs. In DREAM the  
380 probability distribution function of parameters is derived using an iterative approximation  
381 method (the Markov chain Monte Carlo (MCMC) method) coupled with multiple chains in  
382 parallel in order to provide a robust exploration of the search space. In addition to an optimal  
383 model parameter set, DREAM also results in an evaluation of model parameter uncertainty,  
384 which provides important information on model reliability. The effectiveness of DREAM in  
385 water related model calibration has been demonstrated in many previous studies, e.g. (Keating  
386 et al., 2010; Leonhardt et al., 2014).

### 387 **2.5.2. Parameter optimisation**

388 The DREAM algorithm is applied to calibrate the parameters of the RRO model to find the  
389 minimal difference between the simplified model output and the measurements. Table 2  
390 shows the parameters, units and the searching range for the calibration procedure.

391

392 The algorithm minimises the sum of squared errors (SSE) between the model output and  
393 measurements. Water level measurements are applied in the calibration as they are the actual  
394 monitoring data available, containing all information on the sewer systems behaviour. For  
395 Loenen the water level measurement at the primary CSO location is used to calibrate M2 and  
396 M3. For Waalre the water level measurements at the pumping station and inside the settling  
397 tank are applied, by minimising the sum of the SSEs for each model output-measurement  
398 combination. Only periods with elevated water levels are considered in the calibration, as the

399 RRO model parameters are connected to rainfall only. Since water levels do not have  
400 significance in M1, it's calibration is based on the total outflow from the sewer system, i.e. the  
401 sum of the measured pump flow and the calculated outflow at the CSO locations (determined  
402 with the measured water levels and equation 2) for Loenen and Waalre. For Waalre the  
403 outflow through the connection with the neighbouring catchment is added. As this flow is not  
404 monitored, it is based on FH model simulations for the respective rain events.

405

406 The information content on which the models are calibrated is similar, especially for the  
407 elevated water levels relevant for CSO discharges. M2 and M3 are calibrated on measured  
408 water levels at the CSO locations. The discharge to the surface water in M2 and M3 is  
409 calculated using the modelled water level and equation 2. The same equation with the  
410 measured water levels is applied to determine the outflow for the calibration of M1.  
411 Additionally, the pumped outflow supplies information during low intensity rainfall, as  
412 contained in the level measurements at the pumping station (in case of Waalre) or the primary  
413 CSO location (for Loenen) when it is not yet discharging.

414

415 The calibration is performed using 10,000 iterations in DREAM, as it was found from test runs  
416 that the cumulative density functions of the parameters do not change (within the parameter  
417 stability) after several thousand iterations. The last 5,000 iterations are used for further  
418 analysis: the optimal parameter set and model output are derived, and the model is run with  
419 all 5,000 parameter sets to determine the 95% confidence intervals for the water levels and  
420 discharges.

421 **2.5.3. Events**

422 For each catchment six rain events are available for the parameter optimisation, e.g. they led  
423 to a significant rise in water level in the sewer system, with or without discharge to the surface  
424 water, no external influences were known and monitoring data was available and judged  
425 reliable after data validation. The selected events and their characteristics are summarised in  
426 table 3.

427

428 (Korving and Clemens, 2005) showed that the portability of event specific parameter sets for  
429 FH models is low. (Sun and Bertrand-Krajewski, 2012) investigated the impact of calibration  
430 data selection on the model performance of regression models. Given the limited dataset, full  
431 consideration of this aspect is considered beyond the scope of this paper. It is clear, however,  
432 that comparison of the model structures on single event calibration is insufficient. Therefore  
433 three scenarios have been explored:

- 434 1. Calibration of single rain events,
- 435 2. Calibration on all events together,
- 436 3. Calibration on any set of 3 events and verification with the remaining 3 events.

## 437 **2.6. Performance evaluation**

438 The performance of the calibrated simplified model structures should be evaluated on the  
439 capability to correctly represent the sewer systems functioning at the edges of the system. As  
440 argued in the introduction this is not obtained by comparing the best fits between the  
441 measured and modelled water levels but by comparing the discharges from the system, i.e. to  
442 the WWTP and the surface water. As the RRO models are calibrated, i.e. all calibration  
443 parameters are related to rainfall, the focus of the performance evaluation will be on the CSO  
444 discharges to the surface water. As the discharge to the WWTP is also relevant for integrated  
445 studies it will be reported for completeness.



446

447 Common sense dictates that the impact of CSO events depends foremost on the occurrence of  
448 such events, with the absolute discharged flows of secondary consequence. This is supported  
449 by literature stating that impact based RTC can influence the systems performance for small  
450 and moderate events, contrary to large events on which it has no influence (Langeveld et al.,  
451 2013), and that up to a certain point overflow frequency is a good indicator of receiving water  
452 impact (Lau et al., 2002). Therefore the first evaluation criterion for the simplified sewer  
453 models is the correct determination of CSO event occurrences. The second evaluation criterion  
454 is the correct determination of the total discharged volume.

455

456 Based on the monitored water levels at the CSO locations in the sewer systems and settling  
457 tank, for each event and catchment the discharge to the surface water ( $Q_{SW}$ ) is calculated  
458 through application of equation 2. Additionally the total discharge to the WWTP ( $Q_{WWTP}$ ) is  
459 calculated from the pump flow measurements. For each model structure and scenario the  
460 modelled the total discharged volumes ( $V_{SW}$  and  $V_{WWTP}$ ) are determined as the integral of the  
461 model outputs  $Q_{SW}$  and  $Q_{WWTP}$ .

462

463 CSO event occurrences are analysed through false positives (FP) and false negatives (FN). A FP  
464 is defined as a CSO event occurrence ( $V_{SW} > 0$ ) in the model output but not in the  
465 measurements, a FN as a CSO event occurrence in the measurements but not in the model  
466 output. For the comparison of discharged volumes, differences in  $V_{SW}$  (and  $V_{WWTP}$ ) between the  
467 model output and the measurements are calculated and listed for each event and scenario.  
468 Cumulative results for each scenario are determined by taking the root mean squared errors  
469 (RMSE) over all events.

470

471 For comparison purposes the selected rain events have also been simulated using the FH  
472 models. The comparison between simplified models with calibrated inflow parameters and FH  
473 models with uncalibrated inflow parameters is relevant since the FH models simulate the  
474 sewer systems behaviour in greatest detail and hence are deemed to be most accurate (Ferreri  
475 et al., 2010; Meirlaen et al., 2001; Rubinato et al., 2013). This might hold true for calibrated FH  
476 models but not for the much more commonly applied uncalibrated models, as proper  
477 calibration of FH models is very time consuming and requires a very large monitoring data set.  
478  
479 Finally, the simulation time needed by different simplified model structures and the FH model  
480 will be compared.  
481

## 482 **3. Results and discussion**

### 483 **3.1. Calibration**

484 As described in the previous section the performance of the simplified model structures will be  
485 evaluated based upon the correct determination of CSO occurrences and the total discharge to  
486 the surface water. The calibration results, however, provide useful insight into the models  
487 functioning. Therefore, a typical calibration result for each catchment will be presented. Nash-  
488 Sutcliffe efficiency indexes (NS) (Nash and Sutcliffe, 1970) are supplied for easy comparison of  
489 the calibration results. Optimal parameter sets will be given for all events and scenarios.

490

491 The results for the individual calibration of rain events 2001-08-27 (Loenen) and 2011-08-14  
492 (Waalre) for all model structures are displayed in figures 11 and 12 respectively. From top to  
493 bottom the applied rainfall is shown, followed by the model results for M1 (based on the total  
494 sewer outflow), and M2 and M3 (based on the water level in the sewer system). For Waalre  
495 additional water level measurements in the settling tank were applied, the results of which  
496 have been added to the bottom of figure 12. For each model structure the optimal results are  
497 displayed together with their 95% confidence bands.

498

499 Figures 11 and 12 show that M2 and M3 are in general well able to describe the sewer systems  
500 behaviour: the measurements applied in the calibration are closely followed during the filling  
501 of the basins, once they are full and during emptying, resulting in NS values  $> 0.95$  for Loenen  
502 and  $> 0.75$  for Waalre. Small differences occur between these models especially during filling  
503 and in the response to temporal changes in the rainfall. M1 cannot describe the sewer systems  
504 behaviour in detail as it has only the reservoir constant K to account for surface storage and in-

505 sewer storage. The response to rainfall is therefore more smoothed, which is best  
506 demonstrated in figure 11. NS values  $< 0.4$  are found.  
507  
508 For both catchments and all model structures the 95% confidence bands are mostly  $< 1\%$ .  
509 Logically, the influence of the (inflow) calibration parameters on water levels in sewer systems  
510 is most apparent at the onset of a rain event or during temporal changes, resulting in  
511 confidence bands up to 10% for M2 and M3, while they stay  $< 1\%$  for M1.  
512  
513 For all scenarios for Loenen NS values for M2 and M3  $> 0.90$ . For M1, values differ strongly  
514 from -8.52 to 0.44. For Waalre for M2 and M3 in scenario 1, NS values range between 0.61 and  
515 0.96, with one event around zero. In scenario 2 the values drop to 0.5 to 0.6. The NS values for  
516 M1 again differ strongly between events and scenarios from -9.42 to 0.82.  
517  
518 Figure 13 shows the optimal parameter values for Loenen (left) and Waalre (right) for all  
519 model structures. In asterisks the results for scenario 1 (calibration on single rain events) are  
520 given, the line indicates the parameter values for scenario 2 (all events together). Results for  
521 all twenty possible combinations of three calibration events in scenario 3 can be found in  
522 figure 14. The optimal parameter values reflect the results for the water levels and NS values:  
523 the parameters for M2 and M3 show much resemblance within a catchment, while M1  
524 deviates. Especially the difference in K stands out, as the RRO model in M1 has to account for  
525 the surface and in-sewer storage, while in M2 and M3 only for the surface storage. The  
526 optimal parameter values between scenarios 2 (line in figure 13) and 3 (figure 14) are  
527 consistent, indicating that the exact split in a calibration and verification set does not have a  
528 major impact on the outcome.

### 529 **3.2. Performance evaluation**

530 **3.2.1. Model discharge**

531 As the calibration of the simplified models is performed on rainfall related parameters, the  
532 focus of the performance evaluation will be on the discharge to the surface water ( $Q_{SW}$ ) while  
533 the discharge to the WWTP ( $Q_{WWTP}$ ) is included for completeness.

534

535 Optimal  $Q_{SW}$  and  $Q_{WWTP}$  for all model structures for the calibration of the single events of 2001-  
536 08-27 (Loenen) and 2011-08-14 (Waalre) are displayed in figures 15 and 16 as well as the  
537 discharges determined from the measurements. The difference between M1 and M2/M3  
538 observed in the calibration results are also clear from these figures, as  $Q_{SW}$  for M1 tends to be  
539 more smoothed because of the higher value for K.

540 **3.2.2. Determination of CSO events**

541 FPs and FNs for all events for each model structure and scenario, based on the optimal  
542 parameter sets, are given in table 4. For scenarios 1 and 2 the total number is reported, for  
543 scenario 3 the results have been averaged over all combinations and multiplied by two for easy  
544 comparison. Additionally, results for the FH model have been added.

545

546 Based on the FPs and FNs in table 4, M1 can be immediately discarded for these catchments.  
547 For each scenario and catchment two FPs were recorded, the exact number of rain events that  
548 did not lead to a CSO event. This is easily explained since a rain event leading to a significant  
549 rise in water level in a pumped sewer system will likely contain rain intensities higher than the  
550 pumping capacity of the sewer system reserved for WWF (design guideline in the Netherlands:  
551 0.7 mm/h). In M1 all rainfall in excess of this capacity has to be discharged to the surface  
552 water, leading to a CSO event. The calibration algorithm unsuccessfully tries to overcome this

553 inadequacy in the model structure by delaying the rainfall (high  $T_{lag}$ ) and smoothing the  
554 response (high  $K$ ), as can be found from the optimal parameter values in figure 13.  
555  
556 For M2 and M3 the results are less conclusive. Single FPs or FNs occur depending on the  
557 catchment and scenario applied. The floating point values for scenario 3 for Waalre (due to  
558 averaging over all possible combinations) and the optimal parameter values in figure 13  
559 further indicate that the inflow parameters are calibrated differently depending on the  
560 selection of calibration/verification events. Only for M3 for Loenen no FPs or FNs occur in any  
561 scenario signalling that the M3, combining the RRO and DR models, is likely the best  
562 performing model for Loenen.

### 563 **3.2.3. Determination of discharged volumes**

564 The total volumes discharged to the surface water ( $V_{sw}$ ) for each model structure and  
565 scenarios 1 and 2 are displayed in figure 17 for Loenen and 18 for Waalre.  $V_{sw}$  is the integrated  
566 model output  $Q_{sw}$ , for which the optimal values and 95% confidence bands are determined as  
567 described in section 2.5.2. The calculation of the 95% confidence intervals for the  
568 measurements is based on an uncertainty in the standard weir equation of 25%. This  
569 percentage is estimated on previous work by (Van Daal-Rombouts et al., 2014) on scale models  
570 and (Fach et al., 2009) on computational fluid dynamics. Both studies indicate deviations  
571 between the actual (measured or calculated) CSO discharge and the discharge determined  
572 with the standard weir equation of up to 50%. They also indicate that this strongly depends on  
573 the water level over the weir crest leading to under and over estimations of the flow.  
574 Therefore an intermediate value was chosen. For the FH model an uncertainty of 50% was  
575 applied based on the possibility to calibrate FH models up to 5 cm difference in water levels  
576 and equation 2.

577

578 The cumulative results for  $V_{SW}$  and  $V_{WWTP}$ , given in table 5, were determined by taking the  
579 RMSE of the results from the optimal parameter sets over all events. The RMSE for scenario 3  
580 have been averaged over all possible combinations and values for the FH model have been  
581 added.

582

583 The results for  $V_{SW}$  in figures 17 and 18 and table 5 support the preliminary conclusion that M3  
584 outperforms M2 for Loenen. For all scenarios the RMSE and the uncertainty bands for M3 are  
585 smaller than for M2. Despite the inability of M1 to correctly determine CSO event occurrences,  
586 it outperforms M2 based on  $V_{WS}$ . For Waalre the performance of M2 and M3 are similar,  
587 corresponding to the determination of the CSO events. Nevertheless, M2 consistently  
588 performs better than M3. Similar to Loenen, M1 generally performs well based on  $V_{SW}$ . The  
589 difference in the performance of M2 and M3 between the catchments is also reflected in the  
590 optimal parameter values (figure 13). The parameter values for Waalre are close resulting in  
591 similar RMSE values in table 5, while for Loenen there is more variety between the model  
592 structures especially for  $I_{ini}$  and  $K$ .

593

594 These results can be explained by the information available for the simplified model design  
595 and calibration as described in sections 2.2 and 2.3. All information is better known or of  
596 higher quality for Loenen: i) The monitoring data for Loenen was gathered for research  
597 purposes, while the monitoring campaign for Waalre received less dedicated attention. ii) For  
598 Loenen two rain gauges were installed in the catchment itself, while for Waalre no local rain  
599 gauges were available. iii) The geometrical database underlying the FH model for Loenen is  
600 better known than for Waalre. The results for the RMSE of  $V_{SW}$  indicate that the more detailed  
601 model M3, i.e. RRO model for the runoff combined with the DR model for the sewer system, is

602 favoured when high quality information is available (in this case Loenen), while the less  
603 detailed model M2, RRO with SR, suffices when the information is of lower quality (Waalre).

604

605 One main source of uncertainty for Waalre likely stems from the calibrated rain radar input.

606 The rainfall in general seems reasonable with NS values for M2 or M3 > 0.6. In detail the

607 rainfall seems off in intensities and/or timing, an example of which can be found in figure 16.

608 Judging from the rainfall, the models responses in  $Q_{SW}$  are in accordance (main peak in the

609 outflow after main peak in the rainfall). However, in the measurements the main peak in the

610 outflow occurs right at the beginning of the rain event. The other events display a similar

611 mismatch between the rainfall and the outflow. This may also explain the very low values for

612 the parameters  $T_{lag}$  and  $K$ , see figure 13, as the calibration procedure tries to correct the

613 mismatch in the input data.

614

615 For  $V_{WWTP}$  the RMSE values in table 5 show that model M1 consistently performs worse than

616 M2 and M3 for all scenarios and both catchments. M2 and M3 generally perform on a similar

617 level, which is to be expected as the pumping regime in the SR and DR model structures is the

618 same.

619

620 The NS values reported in section 3.1 are based on the calibration parameters for each time

621 step, and the FP/FN in table 4 and RMSE in table 5 on  $V_{SW}$ . Each presents information on the

622 performance of the model structure. NS indicates the quality of the description of the sewer

623 systems behaviour in general, while the others are specific for CSO discharges. The difference

624 between the best performing model structure based on these criteria, especially for Loenen,

625 is striking. Model M2 and M3 have similar NS values > 0.9, but M3 is much more accurate

626 based on FP/FN and RMSE. Simplified sewer models are calibrated on measurements,



627 generally only water levels, but used to determine CSO discharges. These results show that  
628 care should be taken in choosing performance indicators suitable to the purpose of the model,  
629 likely leading to multiple indicators.

#### 630 **3.2.4. Uncalibrated FH models**

631 Finally the performance of the FH models is compared to the performance of the calibrated  
632 simplified models. The comparison is made for scenario 2, calibration for all events together,  
633 since there a single parameter set is derived for each model structure, similar to the single  
634 standard parameter set for the FH model.

635

636 Based on the determination of CSO event occurrences (table 4) the FH model performs at a  
637 similar level as M2 and M3. For Loenen one FP is noted for the FH model, while none for M2  
638 and M3. For Waalre it is reversed.

639

640 Taking the RMSE for  $V_{SW}$  (table 5) into account, the FH model is easily outperformed by both  
641 M2 and M3, while  $V_{WWTP}$  is worse for Loenen and better for Waalre. The results for the  
642 simplified models for  $V_{SW}$  (scenario 3) imply little loss of accuracy when the available data is  
643 split into a calibration and verification set. This suggests that, if a sufficiently large data set  
644 were available, the optimal parameter set should be applicable to other events without much  
645 loss of accuracy.

646

647 The simulation time for the FH models takes 1,000-5,000 times longer than for M2/M3 or  
648 250,000-475,000 times longer than for M1.

649

650 From the perspective of both the simulation time and accuracy of results it is concluded that it  
651 is better to apply simplified calibrated models in optimisation or RTC studies than uncalibrated  
652 FH models.  
653

654 **4. Conclusions and future research**

655 The research described dealt with the design and performance evaluation of a so called  
656 dynamic simplified sewer model for the accurate and rapid calculation of sewer system  
657 discharges for optimisation and RTC studies. The dynamic simplified sewer model (M3)  
658 consists of a calibrated rainfall runoff outflow (RRO) model and a dynamic reservoir (DR) model  
659 for the sewer behaviour. It contains characteristics derived from full hydrodynamic (FH) model  
660 simulations to account for the dynamic properties of the sewer system behaviour.

661

662 The performance of M3 was tested for two combined, pumped catchments and compared  
663 against two other simplified models, M2 (calibrated RRO model with a static reservoir (SR))  
664 and M1 (calibrated RRO model only), and uncalibrated FH models. The performance was not  
665 solely based on the goodness of fit of the calibration but primarily on the correct  
666 determination of CSO event occurrences, and secondly on the correct determination of the  
667 total discharged volumes to the surface water.

668

669 From this research the following conclusions can be drawn:

- 670 – Model M1 simulates > 100,000 times faster than the FH model; models M2/M3  
671 are > 1,000 times faster than the FH model.
- 672 – M1 is unsuitable to correctly predict CSO occurrences for pumped catchments.  
673 The model structure is unable to retain rain intensities higher than the pumping  
674 capacity reserved for WWF, resulting in too many CSO discharges.
- 675 – M2 and M3 are able to describe the behaviour of pumped sewer systems.
- 676 – Performance indicators for the selection of the most appropriate model structure  
677 should be chosen carefully, likely leading to multiple indicators.

678 – In case of detailed and trustworthy information available for the design and  
679 calibration of the model (Loenen), M3 outperforms M2 for all scenarios. If the  
680 available information is of lower quality (Waalre), M2 consistently performs  
681 slightly better indicating that the derivation of the more detailed DR model is not  
682 useful.

683 – For rainfall driven modelling trustworthy and local rain measurements remain  
684 necessary despite the availability of rain radar data, to either apply as direct input  
685 or the correction of radar data.

686 – M2 and M3 outperform the uncalibrated FH models based on the total discharge  
687 to the surface water. In optimisation or RTC studies the application of suitable  
688 calibrated simplified models is preferred over uncalibrated FH models.

689

690 Future research will focus on retrieving more reliable monitoring data (especially rainfall) for  
691 the catchment of Waalre to investigate the impact on the performance of the detailed M3  
692 model. Calibrated simplified sewer models will be derived for the catchments in the case study  
693 area of Eindhoven for application in an integrated model to research the possibilities for  
694 quality based RTC.

695

696 **Acknowledgements**

697 The authors would like to acknowledge Innovyze ([www.innovyze.com](http://www.innovyze.com)) for kindly supplying a  
698 research licence for the use of the software program InfoWorks ICM. Also the authors would  
699 like to thank the Van Gogh Programme for supplying a Travel Grant to cover the travel  
700 expenses for the cooperation between TU Delft and INSA Lyon.

701

702 The research is performed within the Dutch ‘Kennisprogramma Urban Drainage’ (Knowledge  
703 Programme Urban Drainage). The involved parties are: ARCADIS, Deltares, Evides, Gemeente  
704 Almere, Gemeente Arnhem, Gemeente Breda, Gemeente ‘s-Gravenhage, Gemeentewerken  
705 Rotterdam, Gemeente Utrecht, GMB Rioleringsstechniek, Grontmij, KWR Watercycle Research  
706 Institute, Royal HaskoningDHV, Stichting RIONED, STOWA, Tauw, vandervalk + degroot,  
707 Waterboard De Dommel, Waternet and Witteveen+Bos.

708

709 **References**

710 Bach, P.M., Rauch, W., Mikkelsen, P.S., McCarthy, D.T., Deletic, A., 2014. A critical review of  
711 integrated urban water modelling – Urban drainage and beyond. *Environ. Model. Softw.*  
712 54, 88–107.

713 Benedetti, L., Langeveld, J.G., Comeau, A., Corominas, L., Daigger, G., Martin, C., Mikkelsen,  
714 P.S., Vezzaro, L., Weijers, S.R., Vanrolleghem, P.A., 2013. Modelling and monitoring of  
715 integrated urban wastewater systems: review on status and perspectives. *Water Sci.*  
716 *Technol.* 68, 1203–1215.

717 Clemens, F.H.L.R., 2001. Hydrodynamic models in urban drainage: application and calibration.  
718 TU Delft.

719 Coutu, S., Del Giudice, D., Rossi, L., Barry, D.A., 2012. Parsimonious hydrological modeling of

720 urban sewer and river catchments. *J. Hydrol.* 464-465, 477–484.

721 De Niet, A.C., De Jonge, J., Korving, H., Langeveld, J.G., Van Nieuwenhuijzen, A., 2013. Correctie  
722 van neerslagradar op basis van grondstations voor toepassing in stedelijk gebied: het  
723 beste van twee werelden. *H2O online* 1–5.

724 Del Giudice, D., Reichert, P., Bareš, V., Albert, C., Rieckermann, J., 2015. Model bias and  
725 complexity – Understanding the effects of structural deficits and input errors on runoff  
726 predictions. *Environ. Model. Softw.* 64, 205–214.

727 Dotto, C.B.S., Kleidorfer, M., Deletic, A., Rauch, W., McCarthy, D.T., 2014. Impacts of measured  
728 data uncertainty on urban stormwater models. *J. Hydrol.* 508, 28–42.

729 Fach, S., Sitzenfrie, R., Rauch, W., 2009. Determining the spill flow discharge of combined  
730 sewer overflows using rating curves based on computational fluid dynamics instead of  
731 the standard weir equation. *Water Sci. Technol.* 60, 3035–43.

732 Ferreri, G.F., Freni, G., Tomaselli, P., 2010. Ability of Preissmann slot scheme to simulate  
733 smooth pressurisation transient in sewers. *Water Sci. Technol.* 62, 1848–1858.

734 Keating, E.H., Doherty, J., Vrugt, J.A., Kang, Q., 2010. Optimization and uncertainty assessment  
735 of strongly nonlinear groundwater models with high parameter dimensionality. *Water*  
736 *Resour. Res.* 46, 1–18.

737 Kleidorfer, M., Möderl, M., Fach, S., Rauch, W., 2009. Optimization of measurement campaigns  
738 for calibration of a conceptual sewer model. *Water Sci. Technol.* 59, 1523–30.

739 Korving, H., Clemens, F.H.L.R., 2005. Impact of dimension uncertainty and model calibration on  
740 sewer system assessment. *Water Sci. Technol.* 52, 35–42.

741 Krebs, G., Kokkonen, T., Valtanen, M., Setälä, H., Koivusalo, H., 2014. Spatial resolution  
742 considerations for urban hydrological modelling. *J. Hydrol.* 512, 482–497.

743 Langeveld, J.G., 2004. Interactions within wastewater systems. TU Delft.

744 Langeveld, J.G., Benedetti, L., De Klein, J., Nopens, I., Amerlinck, Y., Van Nieuwenhuijzen, A.,  
745 Flameling, T., Van Zanten, O., Weijers, S.R., 2013. Impact-based integrated real-time  
746 control for improvement of the Dommel River water quality. *Urban Water J.* 10, 312–329.

747 Lau, J., Butler, D., Schütze, M., 2002. Is combined sewer overflow spill frequency/volume a  
748 good indicator of receiving water quality impact? *Urban Water* 4, 181–189.

749 Leonhardt, G., Sun, S., Rauch, W., Bertrand-Krajewski, J.-L., 2014. Comparison of two model  
750 based approaches for areal rainfall estimation in urban hydrology. *J. Hydrol.* 511, 880–  
751 890.

752 Mair, M., Kleidorfer, M., Rauch, W., 2012. Performance of auto-calibration algorithms in the  
753 field of urban drainage modelling, in: *Proceedings of UDM9. Belgrade*, pp. 1–10.

754 Mannina, G., Viviani, G., 2010. An urban drainage stormwater quality model: Model  
755 development and uncertainty quantification. *J. Hydrol.* 381, 248–265.

756 Meirlaen, J., Huyghebaert, B., Sforzi, F., Benedetti, L., Vanrolleghem, P.A., 2001. Fast,  
757 simultaneous simulation of the integrated urban wastewater system using mechanistic  
758 surrogate models. *Water Sci. Technol.* 43, 301–309.

759 Motiee, H., Chocat, B., Blanpain, O., 1997. A storage model for the simulation of the hydraulic  
760 behaviour of drainage networks. *Water Sci. Technol.* 36, 57–63.

761 Nash, J.E., Sutcliffe, J.V., 1970. River flow forecasting through conceptual models part I - A  
762 discussion of principles. *J. Hydrol.* 10, 282–290.

763 Rubinato, M., Shucksmith, J., Saul, A.J., Shepherd, W., 2013. Comparison between InfoWorks  
764 hydraulic results and a physical model of an Urban drainage system. *Water Sci. Technol.*  
765 68, 372–379.

766 Sun, S., Bertrand-Krajewski, J.-L., 2012. On calibration data selection: The case of stormwater  
767 quality regression models. *Environ. Model. Softw.* 35, 61–73.

768 Sun, S., Bertrand-Krajewski, J.-L., 2013a. Input variable selection and calibration data selection  
769 for storm water quality regression models. *Water Sci. Technol.* 68, 50–58.

770 Sun, S., Bertrand-Krajewski, J.-L., 2013b. Separately accounting for uncertainties in rainfall and  
771 runoff: Calibration of event based conceptual hydrological models in small urban  
772 catchments using Bayesian method. *Water Resour. Res.* 49, 1–14.

773 Vaes, G., Berlamont, J., 1999. Emission predictions with a multi-linear reservoir model. *Water*  
774 *Sci. Technol.* 39, 9–16.

775 Vaes, G., Willems, P., Berlamont, J., 2001. Rainfall input requirements for hydrological  
776 calculations. *Urban Water* 3, 107–112.

777 Van Bijnen, M., Korving, H., 2008. Application and results of automatic validation of sewer  
778 monitoring data, in: *Proceedings of ICUD11. Edinburgh*, pp. 1–10.

779 Van Daal-Rombouts, P., 2012. Personal communication.

780 Van Daal-Rombouts, P., Tralli, A., Verhaart, F., Langeveld, J.G., Clemens, F.H.L.R., 2014.  
781 Applicability of CFD Modelling in Determining Accurate Weir Discharge-Water Level  
782 Relationships, in: *Proceedings of ICUD13. Sarawak*, pp. 1–8.

783 Vrugt, J.A., Ter Braak, C.J.F., Clark, M.P., Hyman, J.M., Robinson, B.A., 2008. Treatment of input  
784 uncertainty in hydrologic modeling: Doing hydrology backward with Markov chain Monte  
785 Carlo simulation. *Water Resour. Res.* 44, 1–15.

786 Vrugt, J.A., Ter Braak, C.J.F., Gupta, H.V., Robinson, B.A., 2009. Equifinality of formal (DREAM)  
787 and informal (GLUE) Bayesian approaches in hydrologic modeling? *Stoch. Environ. Res.*  
788 *Risk Assess.* 23, 1011–1026.



789 Wolfs, V., Villazon, M.F., Willems, P., 2013. Development of a semi-automated model  
790 identification and calibration tool for conceptual modelling of sewer systems. *Water Sci.*  
791 *Technol.* 68, 167–175.

792 Wolfs, V., Willems, P., 2014. Development of discharge-stage curves affected by hysteresis  
793 using time varying models, model trees and neural networks. *Environ. Model. Softw.* 55,  
794 107–119.

795

796

797 **Table 1.** Sewer system characteristics for Loenen and Waalre.

property	unit	Loenen	Waalre
number of inhabitants	-	2,100	6,200
contributing area	ha	23.4	52.3
average slope ground level	%	0.91	0.14
static storage volume	m <sup>3</sup> - mm	947 - 4.0	2,704 - 5.2
WWF pumping capacity	m <sup>3</sup> /h	209	400
number of CSO structures	-	2	2 (incl. 1 SST)
length of conduits	km	12.3	27.6

798

799 **Table 2.** Calibration parameters with searching range.

parameter	abbreviation	unit	searching range
initial rainfall loss	I <sub>ini</sub>	mm	0 - 4
proportional rainfall loss	P <sub>cons</sub>	-	0 - 1
lag time	T <sub>lag</sub>	min	0 - 120
reservoir constant	K	min	0 - 240

800

801 **Table 3.** Selected rain events with key characteristics.

catchment area	event [dd-mm-yyyyy]	rainfall depth [mm]	max rain intensity [mm/h]	duration [hh:mm]	discharge to surface water [y/n]
Loenen	30-06-2001	9.9	24.8	6:12	y
	18-07-2001	13.9	25.4	14:36	y
	19-07-2001	12.2	34.0	12:15	n
	23-07-2001	12.3	19.4	7:48	y
	27-08-2001	17.0	24.0	7:45	y
	23-10-2001	7.4	6.0	7:39	n
Waalre	29-04-2011	6.5	5.2	6:20	n
	14-08-2011	27.0	23.4	10:35	y
	18-08-2011	12.0	14.9	7:20	n
	22-08-2011	39.2	68.8	23:04	y
	14-12-2011	15.4	11.9	23:31	y
	16-12-2011	33.4	8.5	22:15	y

802

803 **Table 4.** FPs and FNs for all 6 events for each model structure and scenario based on the  
 804 optimal parameter sets. The results for scenario 3 have been averaged over all combinations  
 805 and multiplied by two for easy comparison.

scenario	1: individual		2: all events		3: 3 events calibration, 3 verification			
	events		together		calibration		verification	
catchment / model structure	total FP	total FN	total FP	total FN	mean FP	mean FN	mean FP	mean FN
<b>Loenen</b>								
M1	2	0	2	0	2.0	0.0	2.0	0.0
M2	1	0	0	0	1.0	0.0	1.0	0.0
M3	0	0	0	0	0.0	0.0	0.0	0.0
FH			1	0				
<b>Waalre</b>								
M1	2	0	2	0	2.0	0.0	1.9	0.0
M2	0	1	1	0	0.4	0.2	0.6	0.1
M3	0	1	1	0	0.4	0.2	0.6	0.1
FH			0	0				

806

807

808 **Table 5.** RMSE for  $V_{SW}$  and  $V_{WWTP}$  for all 6 events for each model structure and scenario (1:  
809 individual events, 2: all events together, 3: calibrate and verify on 3 events each) based on the  
810 optimal parameters sets.

catchment / model structure	RMSE [ $m^3$ ]							
	$V_{SW}$				$V_{WWTP}$			
	1	2	3	3	1	2	3	3
			calibra- tion	verifica- tion			calibra- tion	verifica- tion
<b>Loenen</b>								
M1	112	150	147	178	445	242	248	255
M2	416	197	346	364	67	150	135	158
M3	57	145	94	125	124	143	133	132
FH		661				399		
<b>Waalre</b>								
M1	3,470	2,469	2,448	2,157	3,072	2,075	2,307	2,240
M2	5,202	967	2,593	2,212	422	1,331	995	1,330
M3	5,398	1,480	2,788	2,487	556	1,346	1,027	1,354
FH		2,658				619		

811

## Highlights

- 1 • Design of simplified static and dynamic reservoir models for pumped sewer systems.
- 2 • Performance evaluation on CSO event occurrences and total discharged volumes.
- 3 • Static and dynamic models can describe behaviour of pumped sewer systems.
- 4 • Best performing model depends on quality of information for design and calibration.
- 5 • Calibrated simplified models outperform uncalibrated FH models.

1 **Figure 1.** Sewer system layout for Loenen (left) and Waalre (right). Monitoring locations and  
2 locations of pumping stations and CSOs are indicated. Line colour and width indicate pipe  
3 diameter ranges:  $\geq 1500$  mm (thick black),  $\geq 1000$  (black),  $\geq 600$  (thick grey),  $\geq 400$  (grey)  
4 and  $< 400$  mm (light grey).

5

6 **Figure 2.** Daily DWF profiles per person for Loenen and Waalre.

7

8 **Figure 3.** The three simplified models M1-M3 convert the three inputs to two discharges to the  
9 surface water ( $Q_{SW}$ ) and the WWTP ( $Q_{WWTP}$ ). RRO: rainfall runoff outflow, SR: static reservoir,  
10 DR: dynamic reservoir.

11

12 **Figure 4.** The output of the RRO model is split into  $Q_{SW}$  and  $Q_{WWTP}$  based on the maximum  
13 pumping capacity of the catchment ( $209 \text{ m}^3/\text{h}$  for Loenen).

14

15 **Figure 5.** Schematic representation of the SR model for Loenen. Applied characteristics or  
16 relationships as displayed in graphs SR1-SR3 are elaborated upon in the main text.

17

18 **Figure 6.** Schematic representation of the SR model for Waalre. Applied characteristics or  
19 relationships as displayed in graphs SR4-SR10 are elaborated upon in the main text.

20

21 **Figure 7.** Schematic representation of the DR model for Loenen. Applied characteristics or  
22 relationships as displayed in graphs DR1-DR4 are elaborated upon in the main text.

23

24 **Figure 8.** Hybrid storage-level curve (left) and derivation of the dynamic storage-level curve  
25 from the FH model simulation results (right) for Loenen.

26

27 **Figure 9.** Schematic representation of the DR model for Waalre. Applied characteristics or  
28 relationships as displayed in graphs DR5-DR13 are elaborated upon in the main text.

29

30 **Figure 10.** Hybrid storage-level curve (left) and derivation of the dynamic storage-level curve  
31 from the FH model simulation results (right) for Waalre.

32

33 **Figure 11.** Results for the individual calibration of rain event 2001-08-27 for all model  
34 structures for Loenen.

35

36 **Figure 12.** Results for the individual calibration of rain event 2011-08-14 for all model  
37 structures for Waalre.

38

39 **Figure 13.** Optimal parameter values for scenarios 1 (individual calibrated events (asterisks))  
40 and scenario 2 (all events together (line)) for Loenen (left) and Waalre (right). The horizontal  
41 axis presents event numbers. Please note the changing scale for  $T_{lag}$  and  $K$ .

42

43 **Figure 14.** Optimal parameter values for scenario 3 for Loenen (left) and Waalre (right). The  
44 horizontal axis presents the 20 possible combinations to take 3 events from 6. Please note the  
45 changing scale for  $T_{lag}$  and  $K$ .

46

47 **Figure 15.**  $Q_{SW}$  and  $Q_{WWTP}$  for the individually calibrated event of 2001-08-27 for Loenen.

48

49 **Figure 16.**  $Q_{SW}$  and  $Q_{WWTP}$  for the individually calibrated event of 2011-08-14 for Waalre.

50



51 **Figure 17.**  $V_{sw}$  with 95% confidence bands for all events and each model structure for Loenen.  
52 For scenarios 1 (individual events, top) and 2 (all events together, bottom). The horizontal axis  
53 presents event numbers.

54

55 **Figure 18.**  $V_{sw}$  with 95% confidence bands for all events and each model structure for Waalre.  
56 For scenarios 1 (individual events, top) and 2 (all events together, bottom). The horizontal axis  
57 presents event numbers.